NTNU – Trondheim
Norwegian University of
Science and Technology

Effect of Relative Permeability on History Matching a Permian Basin Oil Well

Jørgen Silseth

Petroleum Geoscience and Engineering
Submission date: June 2015
Supervisor: Curtis Hays Whitson, IPT

Norwegian University of Science and Technology
Department of Petroleum Engineering and Applied Geophysics

Preface

This thesis is the final thesis of the five year Master of Science program in petroleum engineering, with specialization in reservoir engineering, at the Norwegian University of Science and Technology (NTNU). The fourth year of the program was spent at the University of Oklahoma, USA as an exchange student. The duration of the thesis was one semester, spring 2015.

First I would like to thank my supervisor on this thesis Dr. Curtis H. Whitson for his advice and feedback. His support and caring together with high expertise on the subject has been a true inspiration and is highly appreciated. I would also like to thank Aleksander Juell at Petrostreamz for his support in shale reservoir modeling and the use of Pipe-It. I thank Petrostreamz for providing me with a license to use Pipe-It, and Coats Engineering for providing a license to SENSOR throughout my master study. A big thanks to family and friends for all the support during this work. A special thanks to all my fellow students and friends at the Department of Petroleum Engineering and Applied Geophysics at NTNU and at the University of Oklahoma for making these five years truly memorable with excellent environment, both social and academic.

Abstract

Production from shale oil and gas has increased significantly the last couple of decades. The industry is constantly developing horizontal well and stimulation technology to increase prouction from these wells. Data acquisition is fairly well established and reliable in conventional reservoirs. This, however, is not the case in unconventional shale reservoirs. In shales the data is usually limited to drilling logs, temperature and pressure measurements and fluid samples. Even the fluid samples can be non-representative. In fact, what you produce at the surface might not the same as what is present in the reservoir [Whitson and Sunjerga, 2012]. Reservoir parameters such as: Matrix permeability, matrix porosity, initial GOR and initial saturations is history matched to best fit observed production rates and pressures. It is important to input the known, tangible data as detailed as possible to reduce error in the well model.

Operators of wells in the United States are obliged to report drilling reports and monthly production rate data to state regulatories. This thesis has compared data acquistion from a subscription based online database, IHS Enerdeq Browser, with data acquired directly from the operator of the well for a well in the Bone Spring Formation, in the Permian Basin. The public available data for this well has proven to be sufficient in order to build a well model. Some reservoir characteristics must be estimated based on neighboring wells, such as: reservoir height, reservoir temperature and reservoir pressure gradient. Simulating a well controlled on monthly average rates instead of daily rates has proven to be sufficient after a couple of months of production.

Relative permeability models are based on simple, analytical relationships in unconventional shale well modeling. The only input, saturation endpoints and curvature, are estimates based on conventional rocks. The curves are then calculated based on Corey Power Law in SENSOR.

This thesis investigated effects of relative permeability on the behavior of the gas-oil ratio, history matching and production forecasting on an oil well located in the Permian Basin, refered to as RHW8. One additional well in the same area has been history matched and production forecasted, refered to as RHW22. The analysis show that GOR is clearly affected by relative permeability of oil and gas. As the oil relative permeability decreases, the producing GOR is increases. When the flowing bottomhole pressure is lowered, a big increase followed by a long transient period (more than a year) is seen on the producing GOR. This proves the importance of numerical modeling of these type of wells, because conventional decline curve analysis will not capture these effects. By history matching the well on relative permeability of oil to gas and matrix permeability it has been shown that three different relative permeability models, n_{og} = 3.5, 4.5 and 5.5, yield equally good history matches for both wells. The production forecast is affected by the relative permeability. Lower relative permeability of oil leads to a higher producing GOR, i.e. lower cumulative oil recovery. However, the effect of this is not significant until after ten years of production. For the RHW8 well the optimal constant flowing bottomhole pressure, in terms of oil production, from time = 0 is 2000 psia for the first 10 years of production. The highest cumulative oil production after 3.5 years is obtained by gradually lowering the FBHP.

Sammendrag

Olje og gass produksjon fra skifer har økt drastisk de siste par tiårene. Teknologien er i stadig utvikling. Det bores stadig lenger og bedre horisontale brønner. Brønnstimulering, hydraulisk frakturering, er også i stadig forbedring. Datainnsamling for konvensjonelle reservoar er forholdsvis enkelt og de innsamlede dataene er detaljerte og pålitelig. Dette er forøvrig ikke like enkelt i ukonvensjonelle tette formasjoner. Eneste data som er tilgjengelig er boredata, samt temperatur og trykk i reservoaret. Denne rapporten sammenligner datainnsamling fra en offentlig database, IHS Enerdeq Browser, med data som operatøren av brønnen har samlet inn for en brønn i Bone Spring formasjonen i New Mexico. De offentlig dataene for denne brønnen har bevist å inneholde nok data til å kunne bygge en brønn modell. Noen reservoar parametre må estimeres basert på nærliggende brønner, som f.eks.: høyden på reservoaret, reservoartemperatur og trykkgradient. Denne oppgaven har også vist at det er tilstrekkelig å simulere en brønn kontrollert av gjennomsnittlig månedlig rate i stedet for daglig rate etter de to første månedene av produksjon.

Relativ permeabilitetskurver er beregnet ved hjelp av *Corey Power Law* i SENSOR. Endepunktene og kurvaturen av kurvene bestemmes basert på estimater innenfor de fysiske rammene for konvensjonelle reservoar. Denne oppgaven har undersøkt hvordan relativ permeabilitet påvirker produserende gass-olje forhold (GOR), historie tilpasning og produksjonsprognoser for en oljebrønn i Bone Spring formasjonen i Perm-bassenget i New Mexico, referert til som RHW8 i denne rapporten. En analyse av historie tilpasning og produksjonsprognose har blitt gjort på en brønn til i samme område, referert til som RHW22 i denne rapporten. Produserende GOR er tydelig påvirket av relativ permeabilitet til olje og gass. Når den relative permeabiliteten til olje minskes øker produserende GOR. Når strømmende bunnhullstrykk (FBHP) senkes sees en umiddelbar økning i produserende GOR med en påfølgende transient på opp til ett år. Dette understreker viktigheten av numerisk simulering av denne type brønner. Tradisjonell *Decline Curve Analysis* vil ikke kunne dekke denne oppførselen. Ved å historietilpasse brønnen som funksjon av relativ permeabilitet av olje og gass samt matriks permeabilitet har denne oppgaven vist at for tre forskellige relativ permeabilitetsmodeller, n_{og} = 3.5, 4.5 og 5.5, kan man få tre like gode historietilpasninger. Produksjonsprognoser for brønnene er også påvirket av relativ permeabilitet. Lavere olje relativ permeabilitet fører til høyere produserende GOR, og

derfor kummulativ oljeproduksjon. Denne effekten kan forøvrig ikke sees før ti år ut i produksjonsprognosen. For RHW8 brønnen er det vist at høyest kummulativ oljeproduksjon er oppnådd med konstant FBHP = 2000 fra tid = 0. Etter 3.5 år er høyest kummulativ oljeproduksjon oppnådd ved å gradvis senke produserende bunnhullstrykk.

Contents

List of Figures

List of Tables

1 Introduction

Onshore shale production has seen a massive growth the last couple of decades. Creating an oil and gas boom in USA. By creating many hydraulic fractures in long, horizontal wells, the surface contact area of the well is increased several orders of magnitude. This is necessary to ensure productivity from wells in ultra-tight formations. In fact, enhanced exploration, drilling and stimulation techniques on onshore shales led to a 35 % increase in estimated reserves onshore US in 2008 compared to 2006 [Mouawad, 2009]. **Fig. 1** shows the main shale plays onshore. Each one of them differs from eachother in both rock and fluid properties.

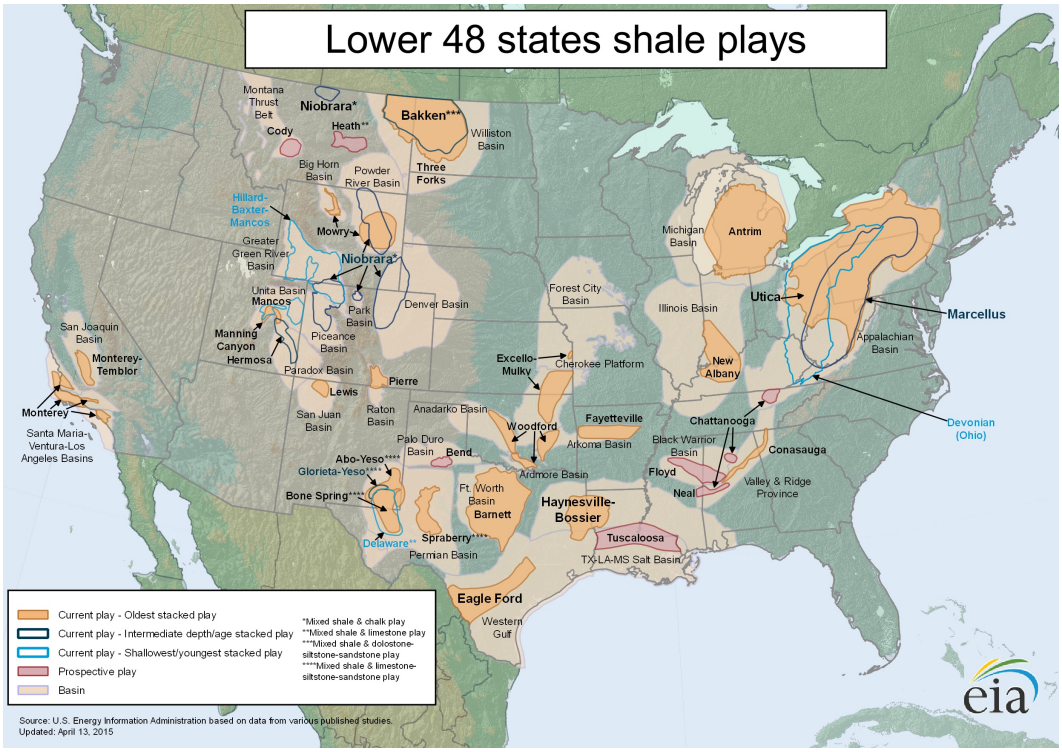

Figure 1: Lower 48 states shale plays onshore US. Retrieved from U.S. Energy Information Administration [2015]

Operators onshore US are obliged to report well data after drilling and completing the well to state regulatories. After start of production the operator is obliged to report production data on a monthly basis to the state regulatories. Well and production data is published by the state regulatories . Each state usually has a open, free of charge, public database for production rates. IHS provides subscription based online access to well and production

data. This data can be used in shale well modeling.

The only reliable data measurements available in shale wells are tangible drilling measurements together with rate data. Data on other parameters, such as reservoir parameters are therefore very limited. Conventional laboratory measurements have proven to be poor and non-representative for shale wells. To limit sources of error in the history matching process it is important to thoroughly search for detailed well data for the well model. Public databases can be an important help to find relevant information of a well before history matching. All the unknown parameters in the well model are either history matching variables, or estimates based on experience from neighboring wells or conventional wells. Relative permeability curves are calculated analytically in shale well reservoir simulators. And solely based on estimates of endpoint saturations and curvature within the range of these values in conventional rocks. Relative permeability can affect both ultimate recovery of oil and gas and the producing gas-oil ratio, R_p. Two wells, RHW8 and RHW22, in the Permian Basin, New Mexico have been studied in this thesis to investigate data acquisition from public databases and the effect of relative permeability on history matching and production forecasting.

This report contains nine chapters. The second chapter covers a technical background relevant for the research in this thesis. The third chapter discusses the data availability and reliability provided by public databases on onshore US shale wells. The fourth and fifth chapter describe the simulation model and well data used in this thesis for the RHW8 well. Chapter six investigates the behavior of Gas-Oil Ratio for the RHW8 well. Chapter seven discusses history matching and production forecasting the RHW8 well with different relative permeability models. The two last chapters conclude this report with conclusions, limitations and further work on the topic. Results of the history matching and production forecasting of the RHW22 well is found in the Appendix. The base case SENSOR datafile, together with a graphical description of the Pipe-It template used in this thesis is also found in the Appendix.

2 Technical Background

2.1 Shale

A shale is defined as a fine-grained sedimentary rock consisting of clay and silt minerals. Organic rich shales are the main source rocks in conventional reservoirs. Recent technology have made it possible to produce oil and gas directly from tight unconventional formations. These formations have very low permeability, which is why they are defined as unconventional reservoirs, or shale plays. The composition of the rock in a shale play can vary significantly from play to play, but also within a play. The reservoir rock does not consists of 100 % shale. A typical unconventional reservoir onshore US is in fact a mix of shale and clay with high organic content, clastic and carbonate minerals. Many of these plays have reasonably high porosity, even though they are tight rocks. This is because of the grain structure in minerals, they are capable of conserving pores during rock compaction.

There are numerous, both big and small, shale plays located onshore US. With Bakken, Niobrara, Marcellus, Haynesville, Eagle Ford and Permian being the biggest ones in terms of growth and production the last couple of years. These plays have contributed almost 90 % of the domestic growth. [U.S. Energy Information Administration, 2014a]. Shale plays can be classified into three groups in terms of production. Dry Gas Plays, Oil Plays and Liquid-Rich Plays.

This thesis has a main focus on Liquid-Rich Shale Plays. A Liquid-Rich Shale Play is defined as a shale play with permeability ranging from 10 to 10,000 nD and more than 20 % of the total revenue is coming from producing liquids [Whitson and Sunjerga, 2012]. Being both in-situ gas and oil plays. As seen in Fig. 1 there is a number of plays onshore US. This thesis is focusing on two wells in the Permian Basin. The Permian is a massive shale play located in Texas and New Mexico. The Permian Basin is one of the biggest plays in the US in terms of growth in drilling activity and production the last couple of years.

2.2 The Permian Basin

The Permian basin is a massive sedimentary basin located in New Mexico and Texas. It has its name because it is one of the world's thickest sedimentary basins from the Permian geologic time period. It is the nations most prolific oil producing area and is the largest petroleum-producing basin in the United States. Six main formations have led to a big increase in oil production in the Permian basin: Spraberry, Wolfcamp, Bone Spring, Delaware, Glorieta and Yeso [U.S. Energy Information Administration, 2014b]. All these formations are classified as shale plays, tight unconventional reservoirs. But none of the formations are identical in geological composition.

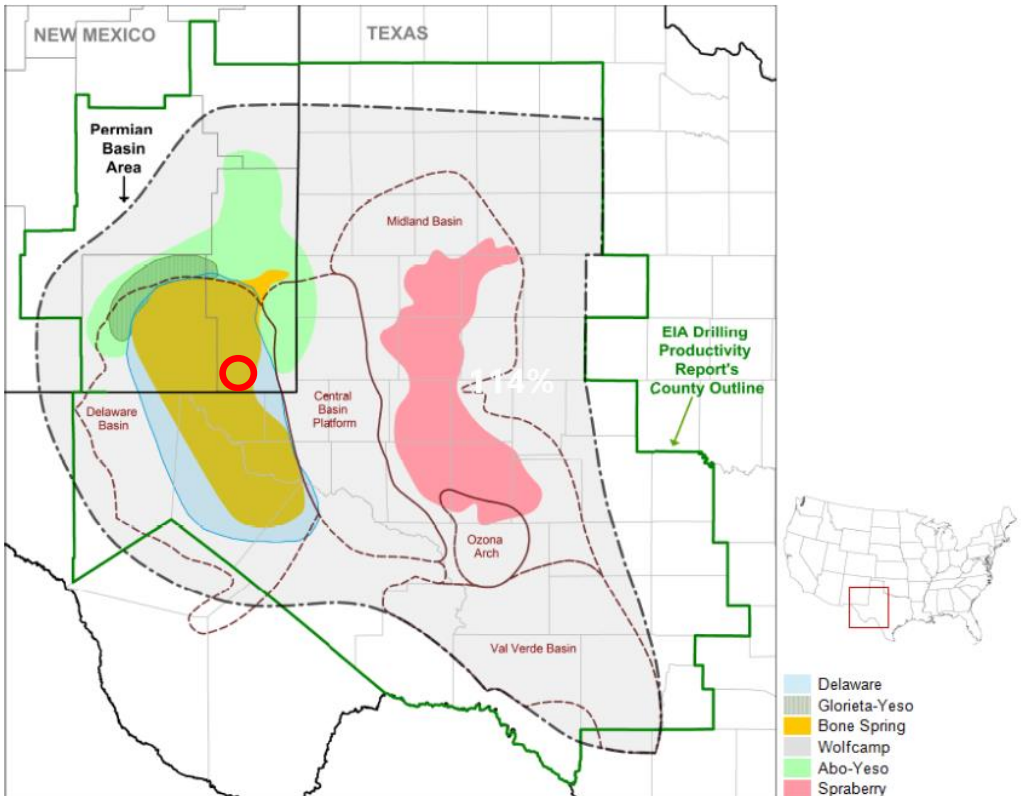

Figure 2: An overview of the plays in the Permian Basin [U.S. Energy Information Administration, 2014b]. The location of the oil wells modeled in this thesis is marked with a red circle.

2.2.1 The Bone Spring Formation

Bone Spring is one of six formations in the Permian Basin. It is located in southeast New Mexico and west Texas. Bone Spring is a thick sediment sequence with interbedded sandstones, carbonates and shale. The depths of the formation range from 6,000 to 13,000 feet, with a thickness of up to 3,500 feet. [Jackson et al., 2014]. There are three main sequences in the formation, named the first, second and third carbonate, and first, second and third sandstone displayed in **Fig. 3**. All with small interbedded shales inbetween. The geological composition in the Bone Spring Formation has big variations locally in each of the sequences as well. Varying in shale content and dolomite cementation.

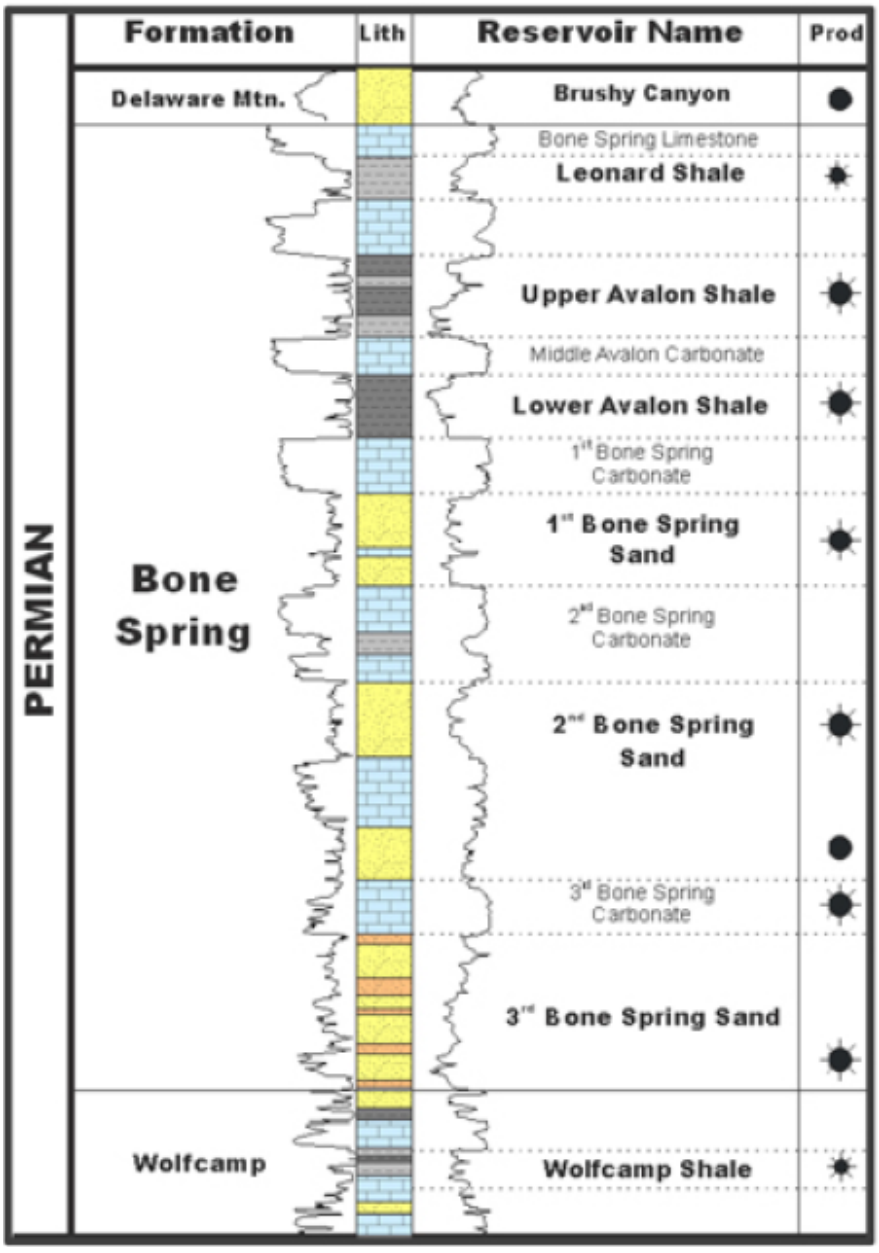

Figure 3: Illustration showing the stratigraphic column of the Bone Spring Formation.Retrieved from Caza Petro [2012].

Vugular, moldic, intergranular, and intercrystalline pores are dominant in the carbonate sequences in the Bone Spring Formation. There are some enhanced permeability parts in the carbonates caused by open, natural fractures. The matrix permeability in the carbonates is very low. The three Bone Spring sandstones consist mainly of siliciclastic turbidites. These turbidites consist of fine-grained sandstones cemented by dolomite and clay minerals, hence the low permeability in the sands as well. Formation tests have shown porosity ranges from 8 to 20 %, and water saturations as high as 35 % to 65 % in the sands [Jackson et al., 2014]. There are no reported substantial natural fracture networks in the Bone Spring sands. Because of the reservoir quality the Bone Spring sands are the main targets in the Bone Spring formation.

The Bone Spring Sandstone formations are not naturally fractured [Carrasco et al., 2014]. A study to achieve more efficient network fractures in the Bone Spring Sandstone was performed by Carrasco et al. [2014]. The results of the study showed that given the relatively ductile formation, the fractures were predicted to be planar fractures. Operators have also reported that about one third or more of the fracture stages took little to no treatment, leading to an inefficient fracture network.

2.3 Rock Properties

The rock properties of the Bone Spring Formation vary within the play, as discussed in the preceding section. This section discusses rock properties in general for unconventional shales including some specific properties of the Bone Spring Formation.

2.3.1 Porosity and pore distribution

Conventional sandstone reservoirs consist mostly of intergranular porosity, void space in-between mineral grains. Unconventional shales are not as simple as conventional sandstones. The pores in shales are on the nanoscale, several orders of magnitude smaller than pores in conventional reservoirs [Curtis et al., 2013]. The porosity distribution varies from play to play, as well as within a play. This is depicted in **Fig. 4**. In the picture the colors depicts different materials. The two lighter gray colors depicts clay and quartz, the dark gray depicts organic matter, the black is organic pores and the white areas depicts other minerals such as pyrite [Curtis et al., 2013].

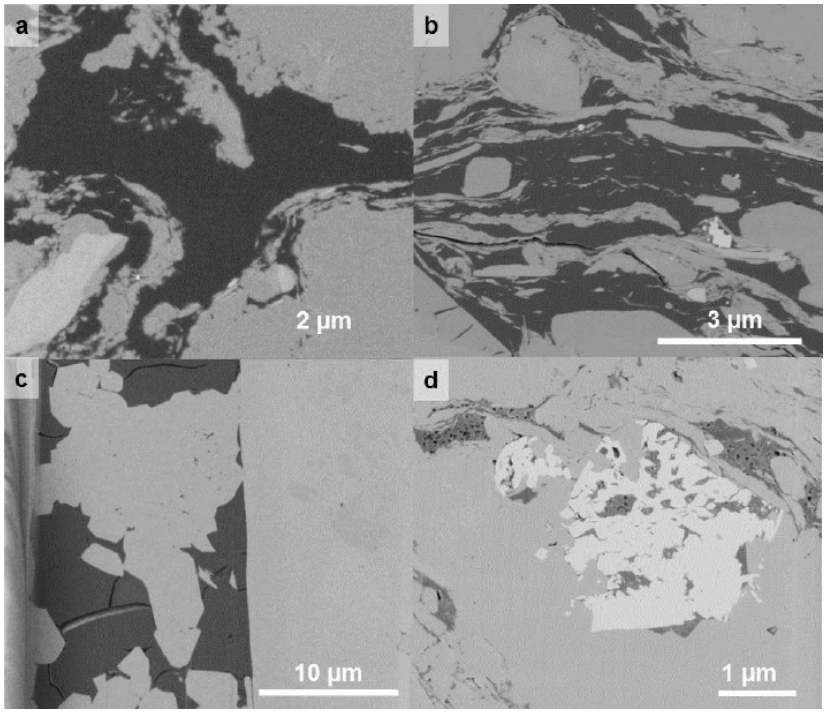

Figure 4: BSE Image of a) Bakken b) Woodford and c) - d) Avalon Shale. Showing the wide variety of mineral content in Shale. [Curtis et al., 2013]

Fig. 4 depicts the diverse structures within shale plays. In a mixed mineral shale the total porosity is a mix of the three porosities listed below:

- Intergranular Porosity - Porosity between grains
- Intragranular Porosity - Porosity within grains
- Organic Porosity - Porosity developed within organic matter

The Bone Spring formation consists of dolomitized sandstone with intersecting clays, both inorganic and organic. This indicates that the Bone Spring Formation has a very complex pore structure with a mix of all of the porosities mentioned above. This leads to a very complex geological model which makes it difficult to correctly address relative permeability and wettability parameters for the simulation model.

2.3.2 Wettability

Wettability describes the preference of a solid to be in contact with one fluid rather than another [Abdallah et al., 2007]. The wettability can change as a function of mineralogy. In shale plays, such as the Bone Spring formation, the wettability will vary between water-wet, oil-wet and mixed-wet throughout the reservoir. The wettability affects the placement of the fluids in the porous media and the relative permeability curves [DiCarlo et al., 1998]. The conventional relationship between wettability and relative permeability might therefore not be applicable for these type of reservoirs.

2.3.3 Permeability

The permeability of a rock is the measure of resistance of fluid flow in the rock matrix. It is determined by the pressure difference necessary to produce a liquid from a rack matrix. The lower the permeability the higher resistance of flow. Relative permeability describes the resistance of flow of a single phase relative to the other phases in a two or more phase reservoir. Relative Permeability is an important input to the simulation model. Relative permeability curves can be estimated through laboratory measurements in conventional reservoirs. Unfortunately, the permeeability in shale plays is generally too low in order to perform valid laboratory measurements on the relative permeability curves. Baker [1988] compares a number of different three-phase relative permeability correlations based on

two-phase data. The results show that the match of analytical and experimental data is often poor and not representative. Analytical relationships such as Corey Law is therefore used in unconventional reservoir simulators.

2.4 Reservoir Fluid Properties

Reservoir fluid properties may vary significantly from reservoir to reservoir. PVT describes the pressure, volume and temperature relationship for a given fluid system. PVT can be described graphically with phase diagrams. For a multicomponent system a phase envelope can be drawn. Inside the envelope both liquid and vapor phases coexist. The borderlines of the envelope is bubblepoint line, where the first bubbles of gas are coming out of the liquid and dewpoint line, where the first drops of liquids are coming out of the gas. Proper PVT treatment in unconventional reservoirs is important to provide improved short- and long-term oil and gas production forecasts, and define the initial oil and gas in place [Whitson and Sunjerga, 2012].

Solution Gas-Oil Ratio

The gas-oil ratio(GOR) is an important relationship to determine the ratio of gas to oil produced at the surface. When a reservoir mixture produces both surface gas and oil, the GOR, R_{go} defines the ratio of standard gas volume to standard oil volume [Whitson and Brule, 2000].

$$R = \frac{(V_g)_{sc}}{(V_o)_{sc}} = \frac{V_{\bar{g}}}{V_{\bar{o}}} \tag{1}$$

in units of scf/STB. GOR can be defined as both producing GOR, R_p and solution GOR, R_s. R_s is the volume of gas at standard condition which is liberated from a single phase liquid at elevated pressure and temperature, divided by the resulting stock tank oil volume, in scf/STB. R_s is constant at pressures above the bubblepoint and decreases as gas is liberated at pressures below bubblepoint [Whitson and Brule, 2000]. R_p is the instantaneous ratio of the surface gas volume produced divided by the stock tank oil volume produced, in units scf/STB.

Conventional reservoirs typically initially produce with R_p more or less equal to R_s. This might not be the case for liquid-rich reservoirs due to the low permeabilities that lead to large drawdowns close to the fracture, which yields a liquid drop-out in the reservoir. [Whitson and Sunjerga, 2012]. The produced fluid can therefore be different from the in-situ fluid. It is therefore important to distinguish between producing and solution Gas-Oil ratio.

Solution Oil-Gas Ratio

For reservoirs producing at high Gas-Oil ratios, typically gas condensate systems, it can be more convenient to use the Oil-Gas ratio (OGR), the inverse of the Gas-Oil ratio. The solution oil-gas ratio is defined as:

$$r = 1/R = \frac{V_{\bar{o}}}{V_{\bar{g}}} \tag{2}$$

Whitson and Sunjerga [2012] discusses the oil-gas ratio as a function of flowing bottom-hole pressure. They show that it is a strong function of FBHP in liquid-rich reservoirs. the r_p remains more or less constant for extended periods of time for all LRS wells if the bottomhole pressure is approximately constant. Producing Oil-Gas ratios for oil reservoirs will lie somewhere between $r_p = r_s(p_{wf})$ and some smaller fraction of the initial solution OGR, r_i

Black-Oil PVT Formulations

Black-Oil (BO) formulation is a simplified PVT formulation. It is needed to practically relate surface volumes to reservoir volumes and vice versa [Whitson and Brule, 2000]. Black-oil tables are generated by using a modified equation of state (EOS). In this thesis the Soawe-Redlich-Kwong (SRK) EOS is used. Typically the $r_p(p_{wf})$ and $R_p(p_{wf})$ are the most important for LRS wells. **Fig. 5** depicts the relationship of these for the well modeled in this thesis.

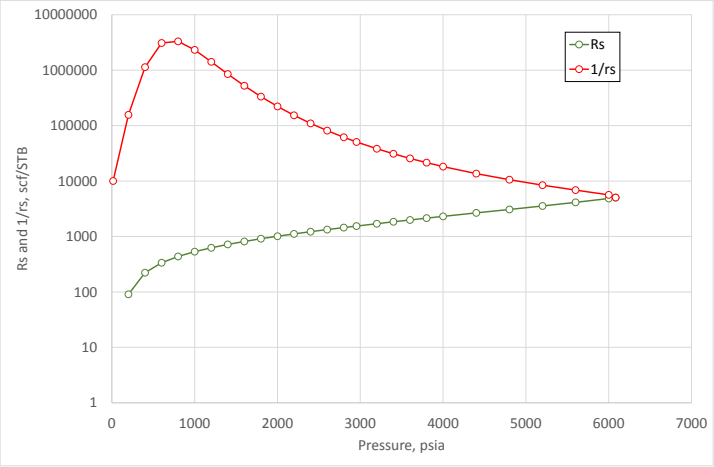

Figure 5: Relationship of Rs and $1/\text{rs}$ as a function of pressure for the Permian Basin Oil Well modeled in this thesis.

2.5 Fluid Flow in Unconventional Tight Reservoirs

In conventional reservoirs the fluid flow is usually radially towards the wellbore. In unconventional tight reservoirs conventional radial flow is not seen. Pseudo-Radial flow can be seen in unconventional reservoirs when the depletion area is big enough compared to the well and hydraulic fracture so that it can be seen as a point source. This will usually not happen in the lifetime of tight shale wells. Assuming planar fractures extending outwards from the well, most of the flow will be linear and perpendicular to the hydraulic fracture, depicted in **Fig. 6**.

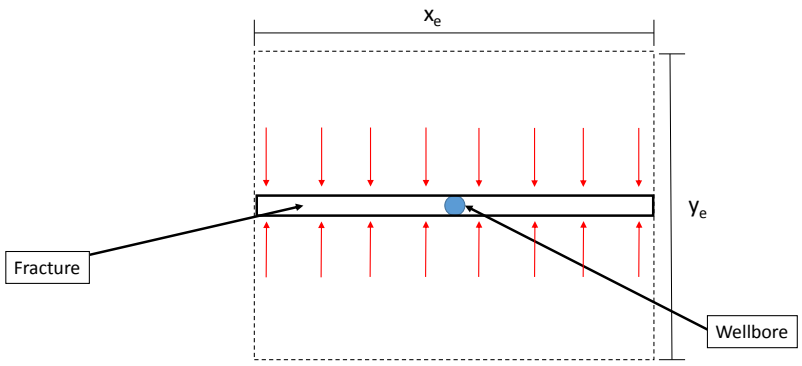

Figure 6: Illustration of linear flow towards the planar hydraulic fracture. Fluid flow is depicted as red arrows. The dashed lines illustrate the boundaries of the model.

There is a number of analytical solutions to the diffusivity equation to describe linear and pseudo-radial flow in tight formations. Wattenbarger et al. [1998] derived equations based on the diffusivity equations for one-dimensional flow. These equations describe the linear flow from matrix towards the hydraulic fracture. The diffusivity equation is solved by defining two inner boundary conditions, constant rate and constant flowing bottomhole pressure, and closed reservoir outer boundary condition. Wattenbarger et al. [1998] derived both short and long term approximations, for both constant pressure and constant rate solution.

The short term approximations are given in **Eqs. 3 and 4** for constant rate and constant pressure respectively.

$$p_{wD} = \sqrt{\pi t_{D_{x_f}}} \tag{3}$$

$$\frac{1}{q_D} = \frac{\pi}{2}\sqrt{\pi t_{D_{x_f}}} \tag{4}$$

The long term approximations are given in **Eqs. 5 and 6**

$$p_{wD} = \frac{\pi}{2}\left(\frac{x_f}{y_e}\right) t_{D_{x_f}} + \frac{\pi}{6}\left(\frac{y_e}{x_f}\right) \tag{5}$$

$$\frac{1}{q_D} = \frac{\pi}{4}\left(\frac{y_e}{x_f}\right) exp\left[\frac{\pi^2}{4}\left(\frac{x_f}{y_e}\right)^2 t_{D_{x_f}}\right] \tag{6}$$

In the long term approximations it is assumed that the fracture extends all the way to the drainage boundary ($x_f = x_e$). In order to have only linear fluid flow. Where the dimensionless variables are defined by:

$$p_{wD} = \frac{kh(p_i - p_{wf})}{141.2qB\mu} \tag{7}$$

$$\frac{1}{q_D} = \frac{kh(p_i - p_{wf})}{141.2qB\mu} \tag{8}$$

$$t_{D_{x_f}} = \frac{0.00633kt}{\phi\mu c_t x_f^2} \tag{9}$$

The short-term solutions are applicable for infinite reservoir boundary. Closed reservoir solutions are approximated by the long-term solutions. [Wattenbarger et al., 1998].

2.6 Hydraulic Fracturing

Hydraulic fracturing is the well stimulation technique that have made production from shales economically feasible. There is a number of different fracking techniques available in the industry. All techniques are in general similar. The long horizontal wells are perforated in clusters. Each cluster is then isolated by packers and the stimulation job can start. Large amount of frack water is then pumped at high pressures into one cluster at the time. The water also contains some chemicals and large amounts of proppants. The pressure in the well must exceed the fracturing pressure of the formation to create fractures. The fracturing pressure of the formation for a horizontal wells are given in equation 10. [Fjaer et al., 2008]

$$p_w^{frac} = 3\sigma_H - \sigma_v - p_f + T_0 \tag{10}$$

Where p_w^{frac} is the fracture pressure (psia), σ_H the largest horziontal stress (psia), σ_v the vertical stress (psia), p_f the pore pressure (psia) and T_0 the tensilestrength of the formation (psia). The in-situ stresses are key parameters. The in-situ stresses determine both the fracture pressure and the fracture orientation. The fractures will open perpendicular to the least principal stress (σ_h). In a normal tectonic situation the largest principal stress is the vertical stress. Horizontal wells should therefore be drilled along the direction of the least horizontal stress to create large vertical fractures perpendicular to the wellbore. The proppants in the frack water are used to keep the fracture open. Different additives increase the fracture propagation. The stiumulation job can be initiated by pumping acid before water in wells with high carbonate content. This is to dissolve carbonate cementation to ensure a better fracking job.

3 Public Data Acquisition

Well and production data is reported by the operator of the well on a monthly basis to state regulatories. Monthly production data together with well and drilling data is published in databases provided by the state regulatories, such as the Texas Railroad Commission, Oklahoma Corporate Commission and Go-Tech by New Mexico Tech University. These data sets are open to everyone and are free of charge. The data provided in these databases is not sufficient in order to build a well model. IHS is a global provider of energy information [IHS, 2014]. The IHS Enerdeq Browser provides subscription-based online access to US well and production data [IHS, 2014]. The IHS Enerdeq Browser provides significantly more well data compared to the public state regulatory databases. IHS Enerdeq Browser is therefore used in this thesis to investigate if it is possible to build reliable well models based solely on public data.

3.1 Data Availability - IHS Enerdeq Browser

A detailed investigation of the available data in the Enerdeq Browser is performed in this chapter. **Tab. 1** gives an example of the data needed to build a model, using Pipe-It and SENSOR, and the availability of these data in the Enerdeq Browser.

Table 1: Data Availability from IHS Enerdeq Browser

Parameter -	Available Y/N	Comments -
Frac Half Length	No	History Matched
Permeability Rock	No	History Matched
Porosity Rock	No	History Matched
GORi	Yes	Early monthly GORs, might not be reliable
m_{dep}	No	History Matched
n	No	History Matched
S_{wc}	No	History Matched
S_{wi}	No	History Matched
Initial Res. Pressure	No	-
Thickness Reservoir	No	-
Vertical Depth	Yes	Found in Well Report
Well Spacing	Yes	Available in Scout Ticket
Hor. Well Length	Yes	Found in Well Report
Number of Fracs	Yes	Found in Scout Ticket
Tubing Diameters	Yes	Found in Well Report
Rates	Yes	Found in Production Data, reported Monthly
p_{wf}	For some wells	Producing Tubing Pressures
Fluid Data	For some wells	Oil density and Gas gravity only

Producing Gas-Oil Ratio is reported on a monthly basis. Public data might not be accurate on the early production producing GOR because of the big variations seen in producing GOR in the early production. The unreliable early GOR measurements can affect the initial fluid model and also cause some errors when history matching the well early in the production. Relative Permeability models are not available for any shale reservoirs and must be estimated. Reservoir pressure and thickness can be estimated based on neighboring wells. The reservoir thickness is important to correctly calculate fracture area in the model and to correctly calculate OOIP and OGIP. The reservoir thickness can be estimated based on the geological stratigraphy of the target formation if no neighbor well data is available.

3.2 Data Reliability

The well data obtained from the Enerdeq Browser is reported after startup followed by monthly production reports. Data from a well in the Bone Spring Formation was acquired directly from the operator of the well. The public data has been compared to data acquired from the operator one the Bone Spring well. A summary of the comparison is depicted in **Tab. 2**.

Table 2: Comparison of data from IHS and Operator

Parameter -	Value IHS	Value Operator	Unit -
GORi	~2600	~1900	scf/bbl
Vertical Depth	~9370	9370	ft
Well Spacing	160	160	acres
Hor. Well Length	3906	3876	ft
Number of Fracs	20	20	-
Tubing Diameter	2 7/8	2 7/8	in
Gas gravity	0.791	0.791	-
Oil Gravity	47.9	47.9	°API

The comparison of the RHW8 Well data shows that the public well data for this particular well is accurate and reliable compared to the data acquired directly from the operator of the well. The difference in initial Gas-Oil Ratio might be a result of two inaccuracies. Firstly, it is difficult to measure initial GOR for a liquid-rich shale well [Whitson and Sunjerga, 2012]. Secondly, the initial GOR value obtained from public data is either calculated from oil and gas rate the first month of the production, or reported in the data set. Unfortunately, it is impossible to know when and how the reported GOR in the data set is measured. The difference in Vertical Depth can be related to the reporting. The vertical depth of the well is varying slightly along the horizontal section of the well. The vertical depth to be used in the model is therefore an average value of the measured depths in the drilling report. The origin of the vertical depth from the operator is unknown.
The oil-gas-water rates obtained from the operator of the well and IHS Enerdeq Browser were compared to investigate the reliability. The comparison of rates is depicted in **Figs. 7 - 10**.

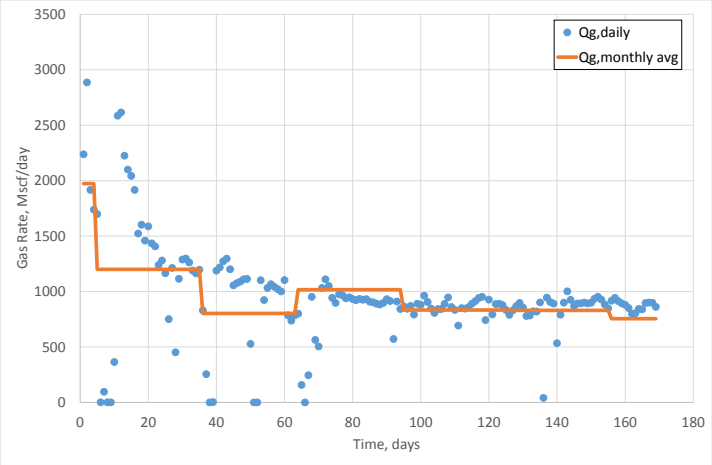

Figure 7: Comparison of measured Gas Rates from operator and public database. Operator data is daily measured data, depicted with blue dots. Public data is average monthly production.

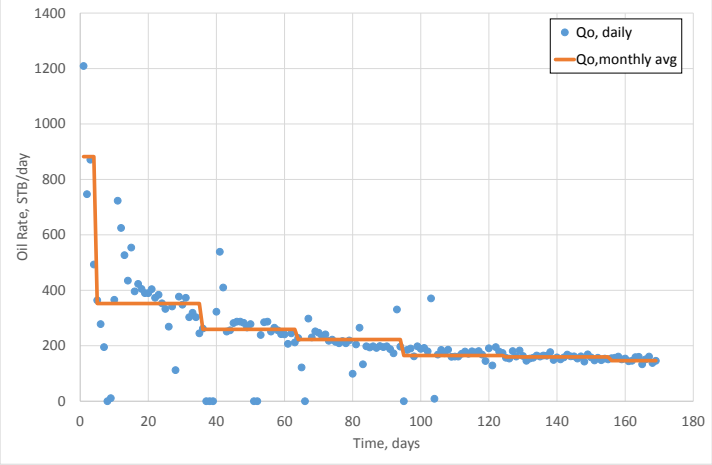

Figure 8: Comparison of measured Oil Rates from operator and public database. Operator data is daily measured data, depicted with blue dots. Public data is average monthly production.

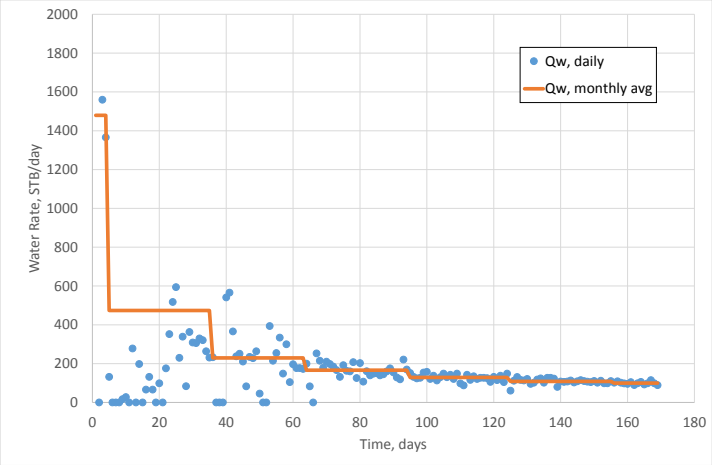

Figure 9: Comparison of measured Water Rates from operator and public database. Operator data is daily measured data, depicted with blue dots. Public data is average monthly production.

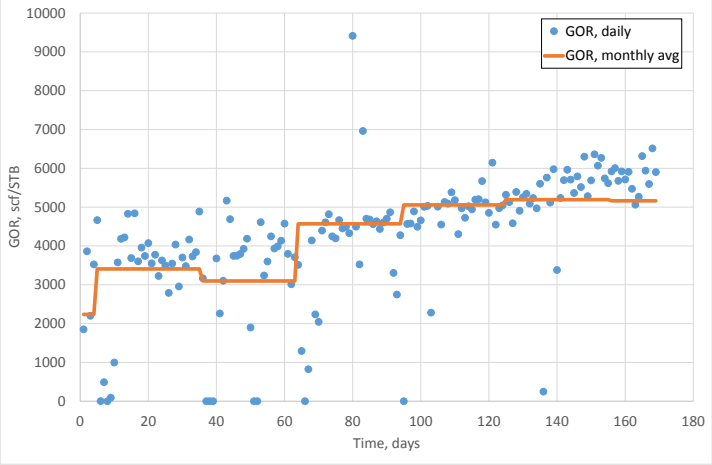

Figure 10: Comparison of calculated Gas-Oil Ratio from operator and public database. Operator data is calculated based on daily measured data, depicted with blue dots. Public data GOR is calculated from average monthly production.

The rate comparison of the first 170 days of production shows that monthly reported production data is not representable for the big changes in rates the first 30-40 days of production. The rates do not differ significantly from eachother after 40 days of production. The available reservoir and well data in the public databases have proven to be accurate. Additional reservoir properties, such as thickness and reservoir pressure, must be estimated based on neighboring wells or experience in the reservoir. IHS Enerdeq Browser provides monthly production data which is representing the well behavior after a couple of months of production. A reliable well model for the two Permian Basin oil wells in this thesis can be created by combining the public data together with some estimates based on experience and general knowledge of the area.

4 Simulation Model Description

All work in this thesis is done with the integrated modeling software Pipe-It . Pipe-It allows the user to graphically and computionally integrate models by connecting an unlimited number of applications together and run them sequentially and in parallel [Petrostreamz, 2014]. This allows the user to connect input and output together from the different applications simultaneously in the same program. This feature allows an integrated optimization across platforms. All the modeling in this thesis is performed by using a Pipe-It template developed by Aleksander Juell at Petrostreamz. The template is designed to handle shale well modeling, including history matching and production forecasting of liquid-rich shales.

4.1 SENSOR Reservoir Simulator

All simulations performed in this thesis is done by using a commercial numerical reservoir simulator, SENSOR Inc. [2015]. SENSOR has proven to provide stable, accurate and reliable simulation results on black-oil simulations on shale wells. It is therefore the preferred simulator in this thesis. Other commercial reservoir simulators could also have been used in this thesis.

4.2 Pipe-It

Petrostreamz's unique IAM software Pipe-It is used in this thesis. It allows the user to chain together an unlimited number of applications to be run sequentially or parallell. Pipe-It enables third party softwares with a graphical interface. It gives a good overview of the different modules of a simulation data-file generated for reservoir simulators such as SENSOR. Pipe-Its Optimization interface enables the user to define any number in the datafile as a variable. For shale wells this is a very beneficial feature as it allows the user to define history matching variables thorugh the optimizer, set an objective, and minimize SSQs with the built-in solvers. The history matching process is therefore more or less automated by using these features in Pipe-It.

4.3 Grid Dimensions

The gridding of the half-fracture model is a built-in utility in the Pipe-It software. It uses a combination of linear and logarithmic gridding. The size of a logarithmic gridcell is calculated with Equation 11

$$r_i = r_{i-1}\left(\frac{L}{w_f}\right)^{\frac{2}{N}} \tag{11}$$

where w_f is the fracture width, L is the distance between two fractures, N is the number of grid cells between two fractures, r_i is the distance from the center of the fracture to the edge of cell *i*. And $r_0 = 0.5w_f$.
In this thesis a logarithmic gridding from the fracture and to the x-extent of the model is used [Petrostreamz, 2012]. There are two options on the gridding in y-direction in the grid-utility in Pipe-It. One with linear gridding from wellbore to fracture tip and logarithmic gridding from fracture tip to the y-extent of the model, as seen in **Fig. 11**. And one with logarithmic gridding both from wellbore to fracture tip and from fracture tip to the y-extent of the model, as seen **Fig. 12**.

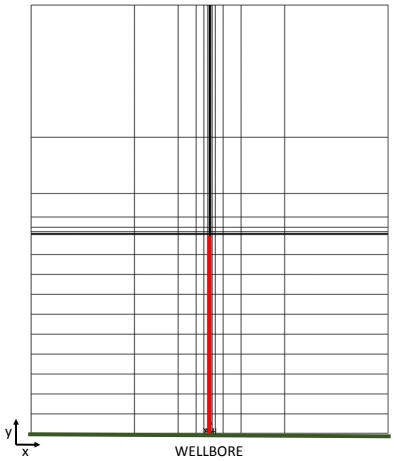

Figure 11: Half-Fracture model of GRID22 in Pipe-It, fracture in red and wellbore is green. Logarithmic gridding along wellbore and from fracture tip and out to the y-extent of the model. Linear gridding from wellbore to fracture tip.

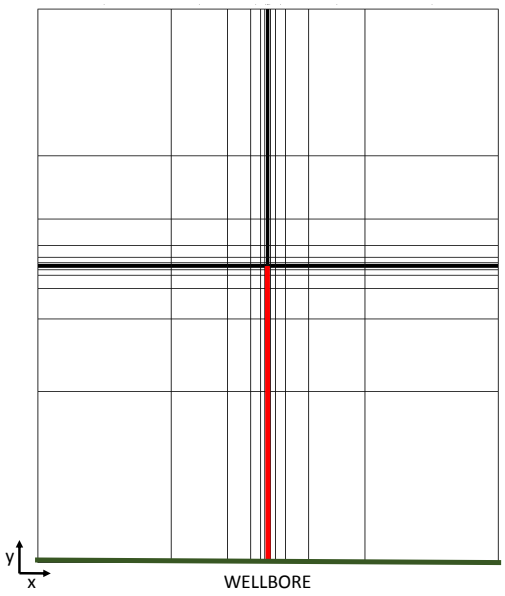

Figure 12: Half-Fracture model of GRID23 in Pipe-It, fracture in red and wellbore is green. Logarithmic gridding along wellbore, from wellbore and out to the fracture tip and from fracture tip to the y-extent of the model.

Both grid-models depicted above have an equal number of gridcells in both x and y direction. In LRSR the gridding is particular important. This is because of the highly localized flow occuring close to the fracture, and erratic oscillations in GOR is observed if the grid is too coarse [Juell and Whitson, 2013]. To be sure the model have sufficient amount of gridcells the OGR behavior can be investigated. When the model is fully converging there should be no oscillations in the OGR. This was performed for the base-case well model in this thesis. The OGR behavior is depicted in **Figs. 13 and 14**.

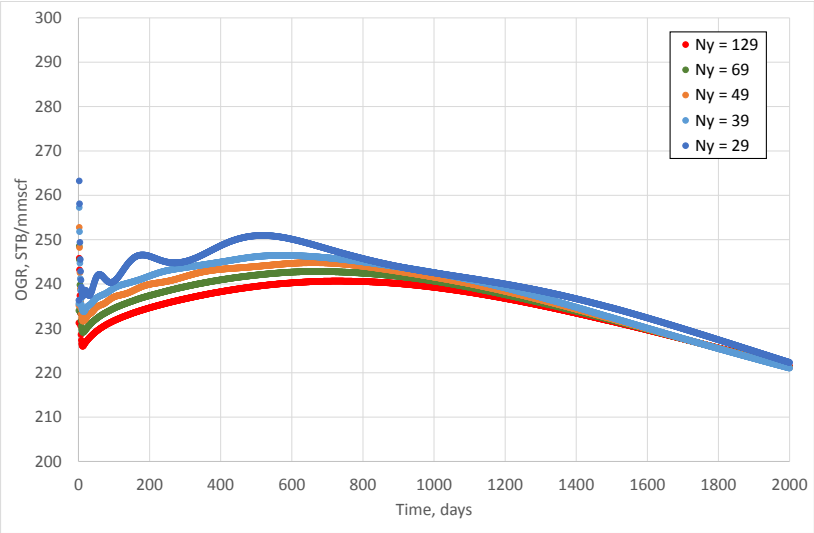

Figure 13: Producing oil-gas ratio behavior for the base case model. The model is based on GRID22 in Pipe-It. Number of gridcells perpendicular to the wellbore is varied.

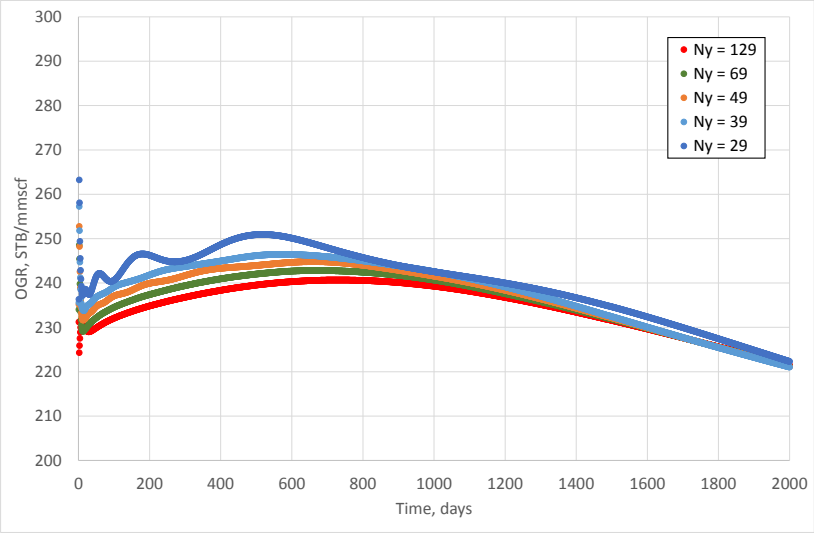

Figure 14: Producing oil-gas ratio behavior for the base case model. The model is based on GRID23 in Pipe-It. Number of gridcells perpendicular to the wellbore is varied.

Due to runtime of the model it is desired to minimize the number of gridcells, but sufficient number of cells to have convergence. Producing GOR is plotted for both grid-types with changing number of gridcells in the y-direction. Both models are identical in terms of GOR oscillations, as seen in Figs. 13 and 14. The models are converging for more than 49 gridcells perpendicular to the wellbore. Linear flow will dominate from fracture along the wellbore during the modeling time of this well. Linear grid from wellbore to fracture tip and logarithmic gridding from fracture tip to the y-extent of the well is therefore chosen in this thesis.

4.4 Relative Permeability

It is difficult to measure relative permeability in shale, as discussed in the preceding chapter. Simple analytical models, such as the Corey Power Law, is applicable to use for this type of simulation model. In analytical models endpoint saturations and curvature are the only properties necessary. These values are assumed and/or estimated based on experience in the area. In SENSOR there is a default built-in function to create analytical relative permeability curves, *KRANALYTICAL* [Coats Engineering Inc., 2015]. This has been used in this thesis. The *KRANALYTICAL* keyword requires a limited number of unknown, estimated parameters. SENSOR creates the curves ready to be used in the simulation model. The curves are created based on the Corey Power Law, given by Equations 12 - 15 [Coats Engineering Inc., 2015]

$$k_{rw} = k_{rwro} \cdot \left[\frac{S_w - S_{wc}}{1 - S_{orw} - S_{wc}} \right]^{n_w} \tag{12}$$

$$k_{row} = k_{rocw} \cdot \left[\frac{1 - S_{orw} - S_w}{1 - S_{orw} - S_{wc}} \right]^{n_{ow}} \tag{13}$$

$$k_{rog} = k_{rocw} \cdot \left[\frac{1 - S_{org} - S_{wc} - S_g}{1 - S_{org} - S_{wc}} \right]^{n_{og}} \tag{14}$$

$$k_{rg} = k_{rgro} \cdot \left[\frac{S_g - S_{gc}}{1 - S_{org} - S_{wc} - S_{gc}} \right]^{n_g} \tag{15}$$

Where

k_{rw} = Water relative permeability

k_{rog} = Oil relative permeability to gas

k_{rog} = Oil relative permeabilty to water

k_{rg} = Gas relative permeability

S_{wc} = Connate water saturation, fraction

S_{orw} = Residual oil saturation to water

S_{org} = Residual oil saturation to gas

S_{gc} = Critical gas saturation

k_{rwro} = Relative permeability of water at $S_w = 1 - S_{orw}, S_g = 0$

k_{rgro} = Relative permeability of gas at $S_w = S_{wc}, S_o = S_{org}$

k_{rocw} = Relative permeability of oil at $S_w = S_{wc}, S_g = 0$

n_w, n_{ow}, n_g and n_{og} = exponents for creating the analytical k_r curves

It is very difficult to correctly decide on the relative permeability parameters due to the little to no data available on shales. A lot more data is available for conventional rocks. Using relative permeability parameters within the range of conventional rocks is used in shale well modeling. The range of the parameters is given in **Tab. 3**.

Table 3: Physical Range of Conventional Relative Permeability Parameters

Parameter	Min Value	Max Value
S_{wc}	0.1	0.4
S_{orw}	0.1	0.4
S_{org}	0.1	0.3
S_{gc}	0.02	0.2
n_g	2.5	4
n_w	2.5	4
n_{ow}	2.5	4
n_{og}	3.5	4

Table 4: Analytical Relative Permeability Input Parameters

Parameter	Value
S_{wc}	0.15
S_{orw}	0.1
S_{org}	0.2
S_{gc}	0.1
n_g	2
n_w	2.5
n_{ow}	2.5
n_{og}	3.5

Tab. 4 depicts a general relative permeability model that can be used in LRSR well modeling. The corresponding Oil-Gas and Oil-Water curves are depicted in **Figs. 15 and 17** respectively. **Figs. 16 and 18** shows the same relative permeability curves, plotted on a log scale to depict permeabilities at gas and water saturations near critical values. **Figs. 19 and 20** shows Oil-Gas Relative Permeability curves for different oil-gas exponents, n_{og}

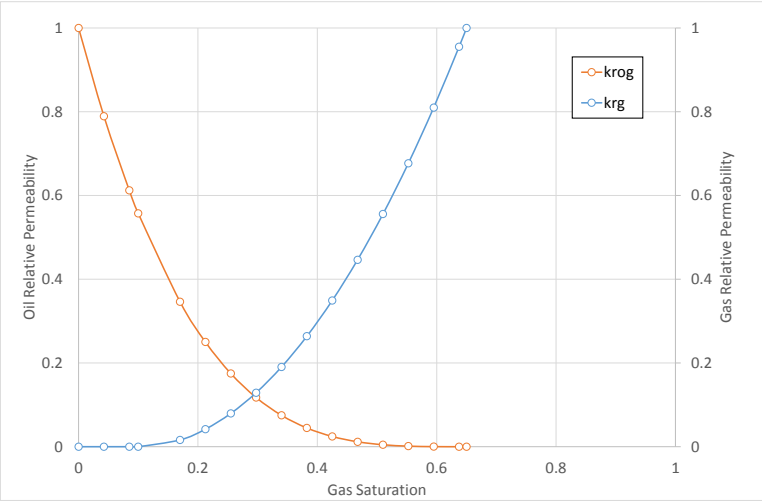

Figure 15: Oil and Gas relative permeability curves plotted with linear scale

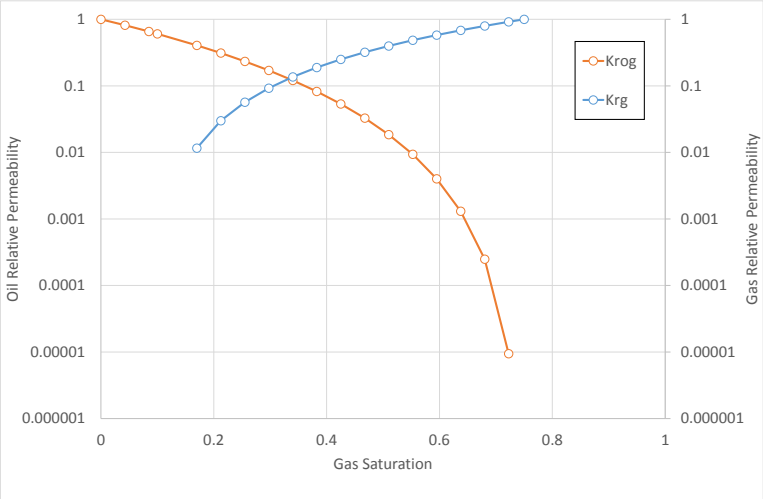

Figure 16: Oil and Gas relative permeability curves plotted with logarithmic scale

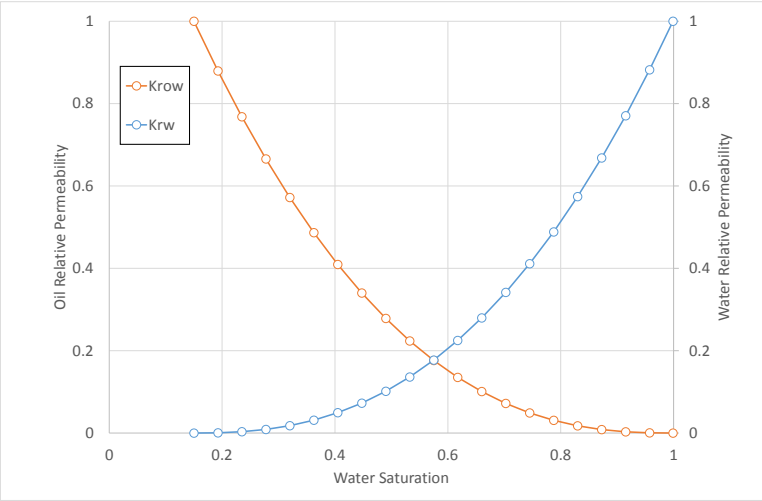

Figure 17: Oil and Water relative permeability curves plotted with linear scale

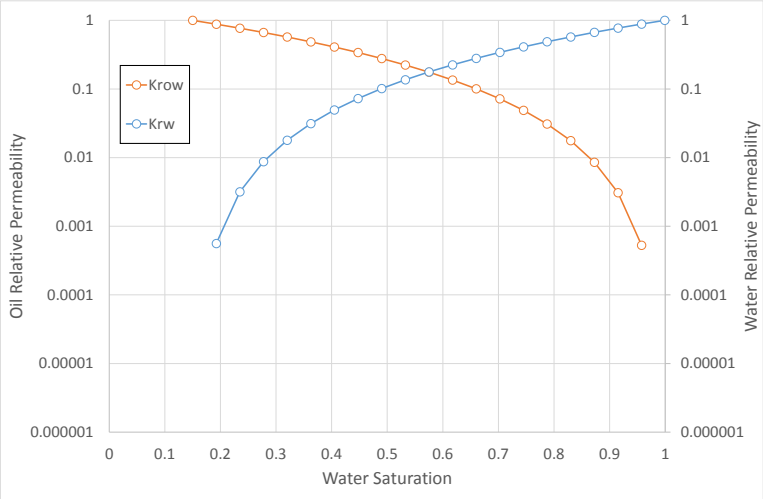

Figure 18: Oil and Water relative permeability curves plotted with logarithmic scale

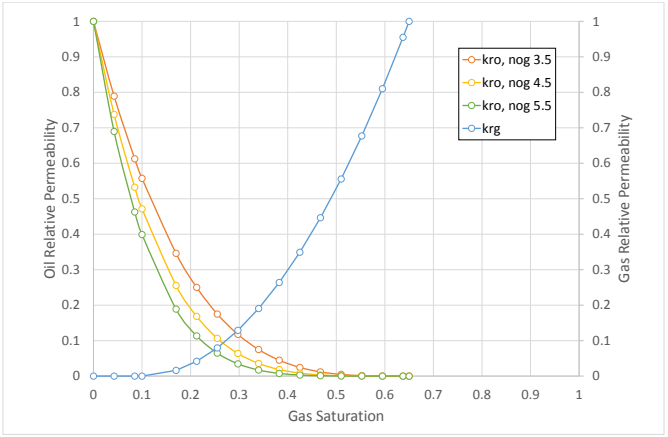

Figure 19: Oil and Gas Relative permeability curves with linear scale. n_{og} is varied.

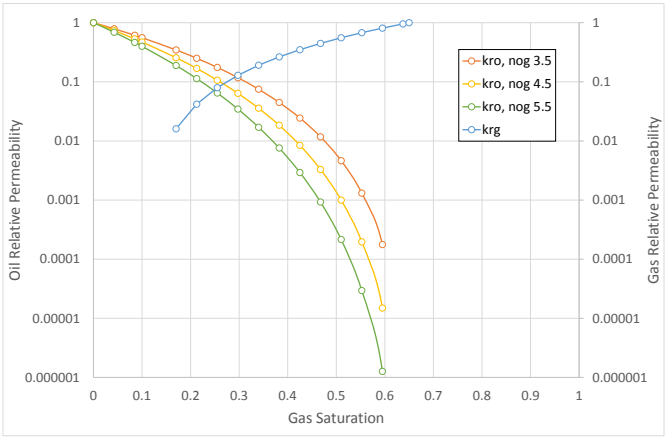

Figure 20: Oil and Gas Relative permeability curves with logarithmic scale. n_{og} is varied.

Figs. 19 and 20 shows how the relative permeability is altered by changing the saturation exponent, n_{og}. A higher n_{og} decreases the relative permeability of the oil relative to the gas. This can be described as an initial oil model where gas is coming out of solution as the pressure is lowered. The small gas molecules will then flow easier in the nanoscale porethroats compared to the bigger oil molecules. The relative permeability exponents of gas, water and water to oil, n_g, n_w and n_{ow} has been kept constant in this thesis.

4.5 History Matching and Production Forecasting using Pipe-It

There are many uncertain parameters in shale well modeling. These are decided by history matching. Assigning correct value to these parameters is important, because it can have a big influence on the production forecast. The most common history matching parameters are displayed in below. In addition to these main parameters it is decided to investigate history matching as a function of initial gas saturation and relative permeability model in this thesis.

- Fracture Half-Length x_f
- Matrix Permeability k_m
- Matrix Porosity ϕ
- Initial Gas-Oil Ratio GOR_i
- Stress dependent permeability exponent in fractures m_{dep}

Pipe-It [Petrostreamz, 2014] provides an efficient algorithm for history matching half-fracture shale well models. History matching a FD model to observed pressure and rate data is preferably performed with bottomhole pressure control, measured or calculated from surface pressures. This is because of the strong correlation between producing GOR and producing bottomhole pressure (FBHP) [Juell and Whitson, 2013]. The performance of the well is then matched to the observed data by minimizing the calculated sum of squares (SSQ). SSQ of a specific rate or pressure is given in Eq. 16.

$$\sum SSQ_q = \sum_{i=1}^{n} w_{q,i}\left(\frac{q_{obs,i} - q_{model,i}}{q_{ref}}\right)^2 \tag{16}$$

where q_{obs} is measured rate, q_{model} is calculated rate from the simulation and q_{ref} is a reference rate, usually the average of q_{obs}.

The individual SSQs are then summed to a total SSQ for the well shown in 17. Visual inspection of the rate performance is necessary to find reasonable weighting factors for all individual points. This is often a trial and error process.

$$\sum SSQ_{total} = \sum \left(W_{oil} \cdot SSQ_{q_{oil}} + W_{gas} \cdot SSQ_{q_{gas}} + W_{water} \cdot SSQ_{q_{water}} + W_{pwf} \cdot SSQ_{pwf} \right) \quad (17)$$

Again a set of weighting factors must be decided. The total SSQ is then minimized to get the best history match.

Production forecasting of the well is performed after obtaining reservoir and well parameters through the history match. It is important to perform forecasting to predict the economics of the given well. Numerous production strategies can be simulated to obtain an optimized drawdown strategy. The forecasting is usually run on constant flowing bottomhole pressure. Production limitations on the surface due to the facilities must be taken into account. There is a number of different constraints that might be important. Such as: Transportation, Production Processing, Pipelines and so on. The different production strategies is then compared and the best solution is found in order to make the well as profitable as possible. Pipe-It provides an optimization feature in order to optimize well and production design in terms of economics. This feature has not been used in this thesis.

5 RHW8 Well Model

The RHW8 well is located in the Bone Spring Formation in Southeast New Mexico. The location of the well is depicted with a red circle in Fig. 2. This well is an oil well with an initial GOR of about 2400 sct/STB. The GOR of the well is strictly increasing with time as seen in **Fig. 21**. The well model is built based on the values obtained in the public database together with daily rate data for the first 186 days of production. Reservoir thickness, pressure and temperature was based on neighboring wells. No flowing bottomhole pressures was obtained for this well.

5.1 Reservoir and Well Data

The well and reservoir data for this well is based on well information found in the IHS Enerdeq Browser [IHS, 2014]. The Bone Spring formation consists of a mix of sand, limestone and shale minerals. It has been decided to model this well with a planar fracture because of the composition of the nature of the Bone Spring Formation. Reservoir data such as fracture half length, matrix permeability, matrix porosity, $m_{dep_{fracs}}$, relative permeability curves and initial gas saturation are history matching variables. Reservoir and Well Data has been put together into a base case well model for the RHW8 Well. Parameters are depicted in **Tab. 5**. Fracture Half Length, Matrix Porosity, initial GOR and m_{dep} was history matched to give a reasonably good match with an oil-gas relativity exponent, $n_{og} = 4.5$. x_f, ϕ, GOR_i and m_{dep} was kept constant for the rest of the modeling performed in this thesis.

Table 5: Reservoir and Well Input Data - Base Case

Parameter	Value	Unit	Comment
x_f	400	feet	History Matching variable
k_m	730	nd	History Matching variable
ϕ	0.05	-	History Matching variable
GOR_i	2400	scf/STB	History Matching variable
$m_{dep_{fracs}}$	0.5	-	History Matching variable
n_g	2	-	Assumed
n_w	2.5	-	Assumed
n_{og}	4.5	-	Assumed
n_{ow}	2.5	-	Assumed
S_{wc}	0.15	-	History matching variable
S_{wi}	0.35	-	History matching variable
S_{gi}	0.08	-	History matching variable
S_{org}	0.127	-	History matching variable
S_{orw}	0.1	-	Assumed
P_{res_i}	3930	psia	Assumed based on the area
Reservoir Height	200	feet	Assumed based on the area
Vertical Depth	8932	feet	Found in Enerdeq Browser
Well Spacing	160	acres	Found in Enerdeq Browser
Lateral Well Length	4051	feet	Found in Enerdeq Browser
Number of Fracs	20	-	Found in Enerdeq Browser
Frac Width Physical	0.01	feet	Assumed
Frac Porosity	0.25	-	Assumed
Frac Width Model	0.08333	feet	Assumed
C_f	1000	md-feet	Assuming Infinite-Acting Fracture
Tubing Diameter	4.5	inch	Found in Enerdeq Browser
Lateral Wellbore Diameter	2.875	inch	Found in Enerdeq Browser

Where, x_f is fracture half length, k_m is matrix permeability, ϕ is matrix porosity, GOR_i is initial GOR, $m_{dep_{fracs}}$ is the stress dependent permeability exponent in fractures, n_g, n_w, n_{og} and n_{ow} is relative permeability exponents, p_{res_i} is initial reservoir pressure and C_f is fracture conductivity.

5.2 Production Data RHW8

Production performance plots of the RHW8 well is plotted below. The data is a combination of daily production data from the operator for the first 186 days, followed by monthly production rates from the Enerdeq Browser.

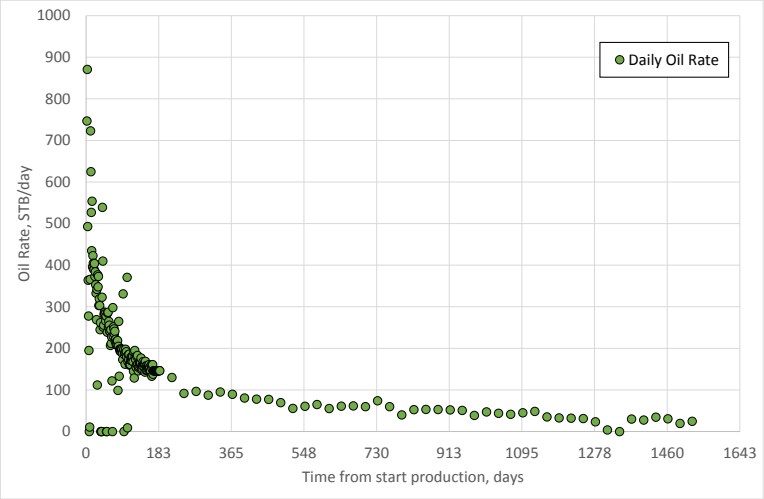

Figure 21: Measured Oil Production Rate for the RHW8 well. Daily data from operator for the first 168 days.

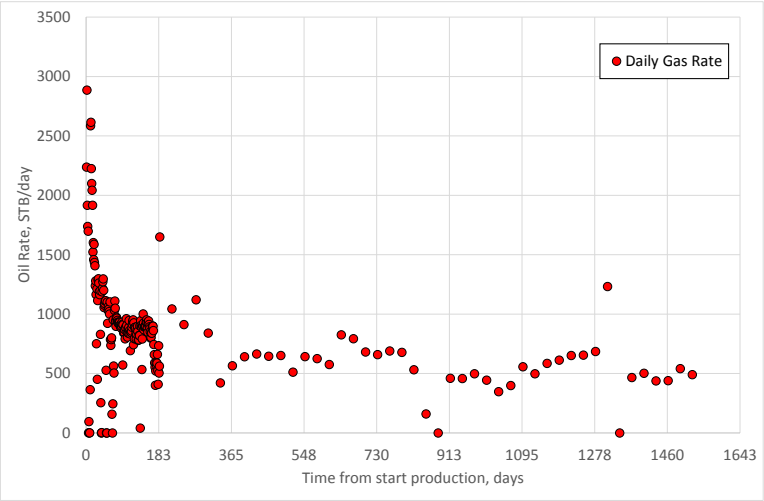

Figure 22: Measured Gas Production Rate for the RHW8 well. Daily data from operator for the first 168 days.

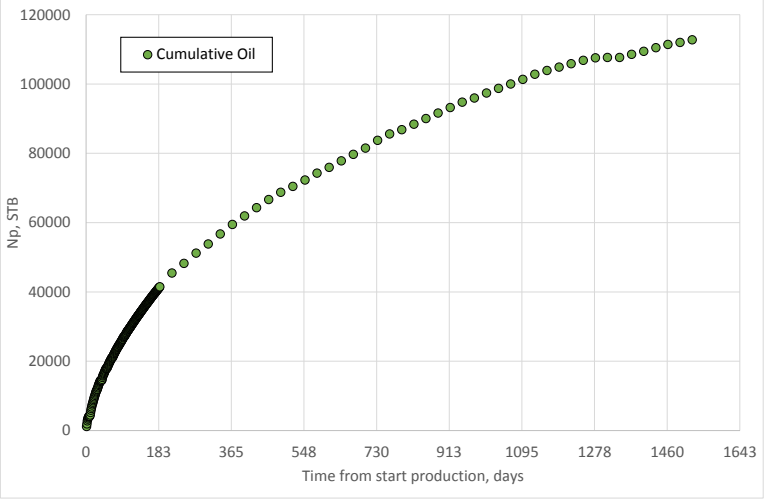

Figure 23: Measured Cummulative Oil Production for the RHW8 well. Daily data from operator for the first 168 days.

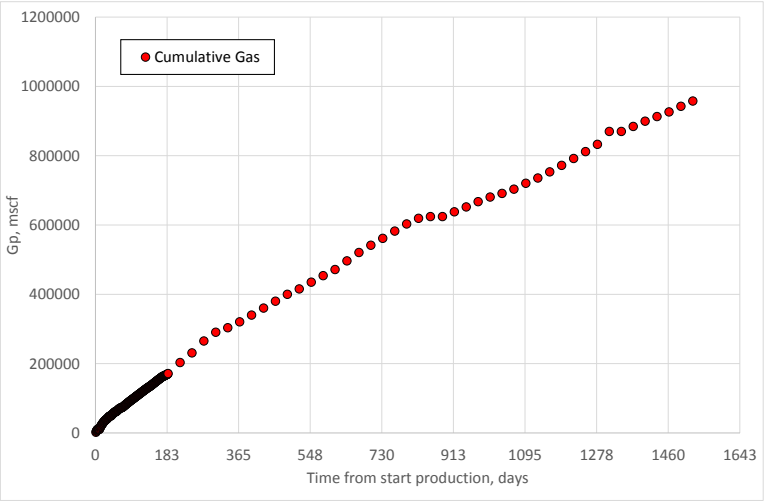

Figure 24: Measured Cummulative Gas Production for the RHW8 well. Daily data from operator for the first 168 days.

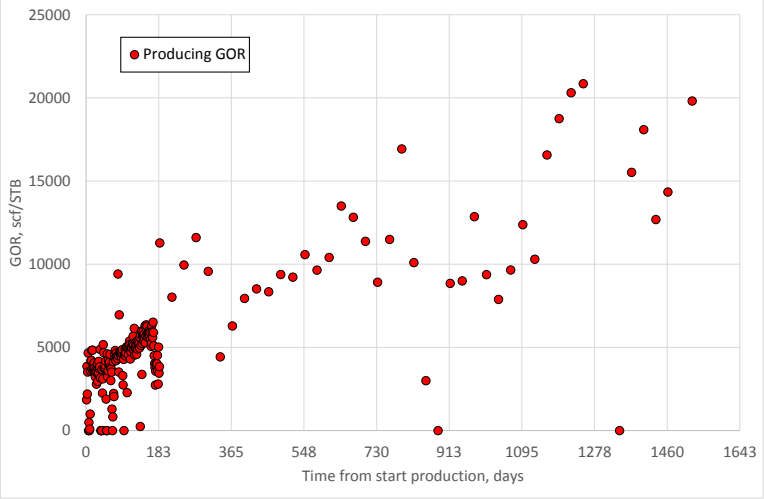

Figure 25: Producing gas-oil ratio behavior for the RHW8 well. Calculated based on measured oil and gas rates.

The model will be run on gas rate control in the history match. The effect of controlling the well on average monthly production data versus controlling it on daily production data must therefore be investigated. Two simulation cases were run in order to investigate the effect of using monthly average public data compared to daily operator data. The model is the same as the Base Case Model in Tab. 5. The well is controlled on gas rate in both cases, as plotted in **Fig. 26**. For the public data the reported monthly production is divided by number of days in a month (30.4), and set to produce the calculated average rate for 30.4 days, except the first four days from start of production. The well started producing the first days of December, the measured rates of December are therefore based on four days only. **Figs. 26 - 29** depict the difference in oil and gas rates, producing GOR and flowing bottomhole pressure.

5.3 Gas Rate Controlled Well - Daily vs Monthly Data

The measured gas rates are used to control the well in the simulations. The rates differ significantly from eachother the first 60 days of production. After 60 days the two tend to follow the same trend. The total cumulative gas production is kept the same for both datasets.

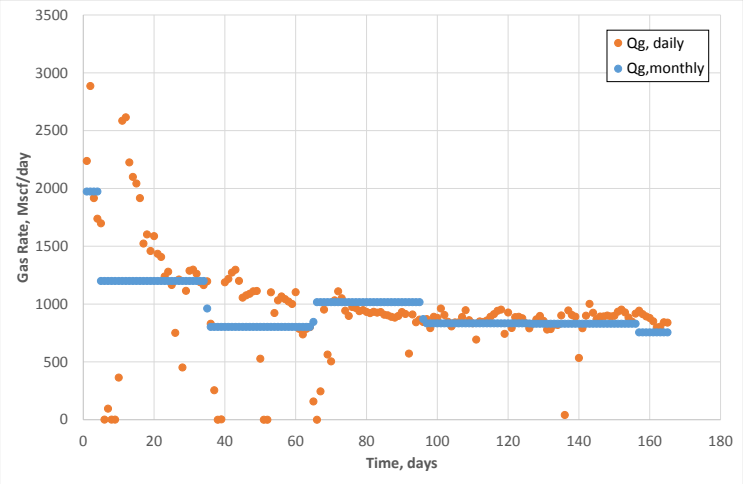

Figure 26: Measured Gas Rates from operator and IHS Enerdeq Browser. The gas rates are used to simulate well on gas rate control.

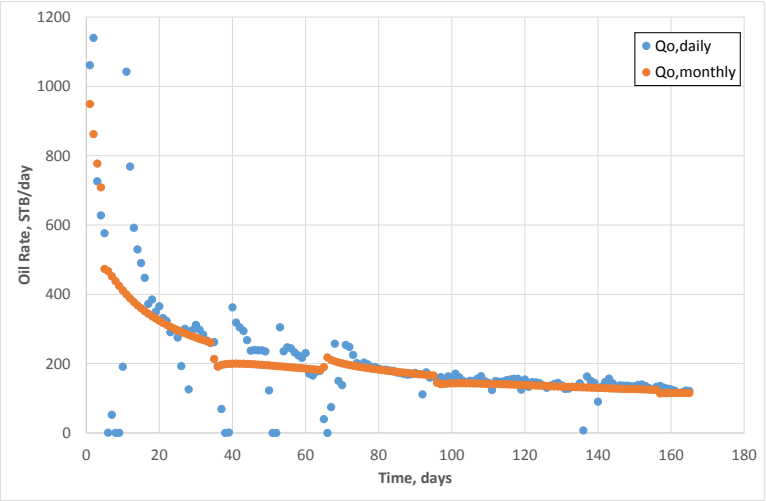

Figure 27: Comparison of calculated Oil rates based on gas rate control simulation of daily and monthly data.

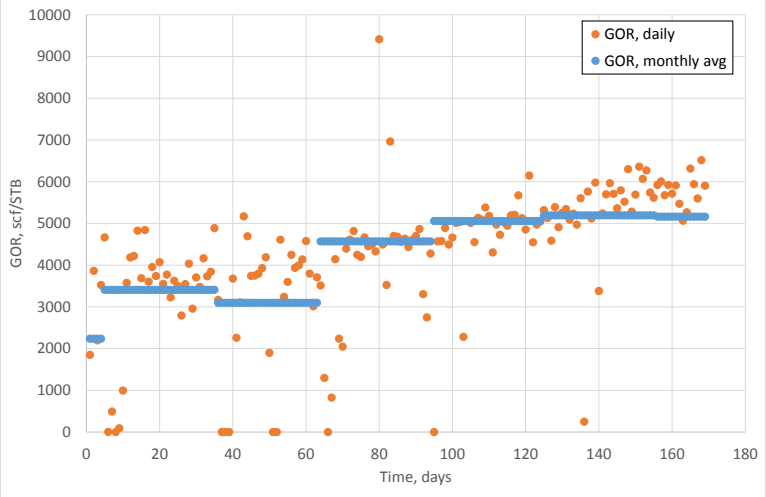

Figure 28: Comparison of calculated Producing Gas-Oil Ratio based on gas rate control simulation of daily and monthly data.

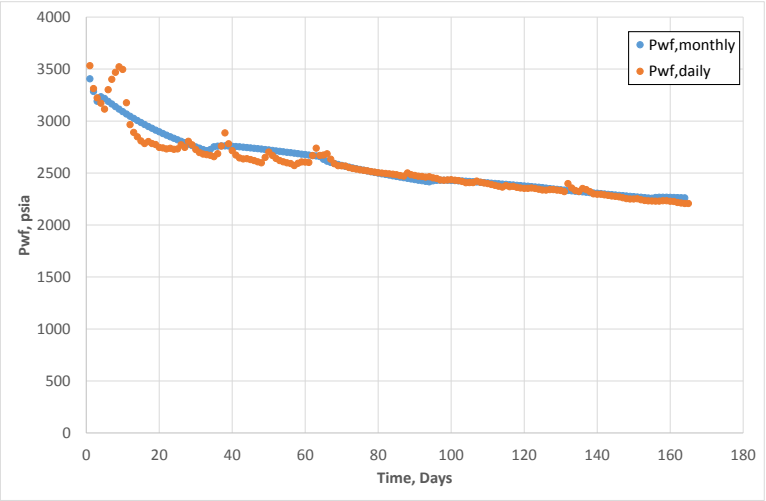

Figure 29: Comparison of calculated flowing bottomhole pressures based on gas rate control simulation of daily and monthly data..

Calculated oil rate, producing GOR and producing FBHP is plotted in Figs. 27 - 29. The simulations show that even though the gas rates differ in the first months the calculated rates and pressures give reasonable match. There is some difference in the first two months, but from 60 days the two simulations yield very similar rate, pressure and GOR. This indicates that if daily measured rates are unavailable, monthly measured rates can give a representative well behavoir in the simulation model. Daily measured rates should be used if available, especially for early production times.

6 Producing Gas-Oil Ratio

This chapter investigates the effects of flowing bottomhole pressure and the relative permeability model on the producing gas-oil ratio. The model used in this chapter is the base case model for the RHW8 well described in Tab. 5, unless else is mentioned.

6.1 Effect of Flowing Bottomhole Pressure on Producing Gas-Oil Ratio

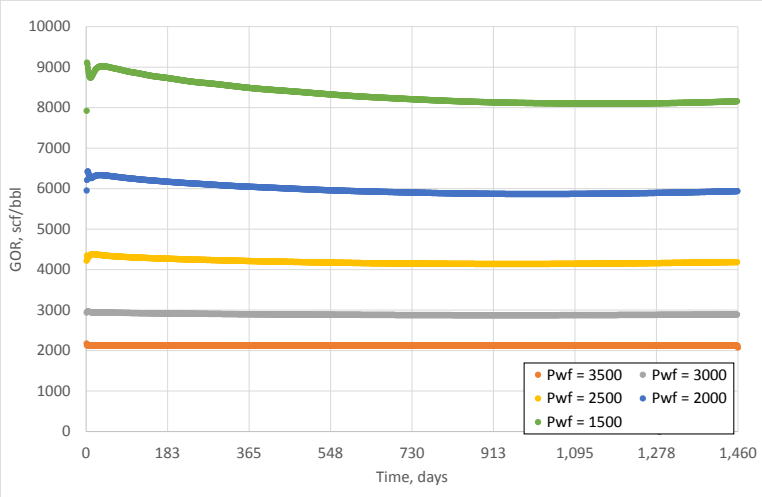

Figure 30: GOR as a function of time with constant flowing bottomhole pressure ranging from 1500 - 3500 psia. Each line represents a separate simulation with constant flowing bottomhole pressure from time = 0.

Each simulation in **Fig. 30** is simulated with a constant FBHP from time = 0. Fig 30 shows the strong relationship between flowing bottomhole pressure and producing GOR. Each of the simulations show a constant producing GOR for constant FBHP throughout the simulation period of four years. By producing at a pressure close to the initial reservoir pressure the producing GOR is approximately equal initial GOR. By lowering the FBHP the producing GOR increases.

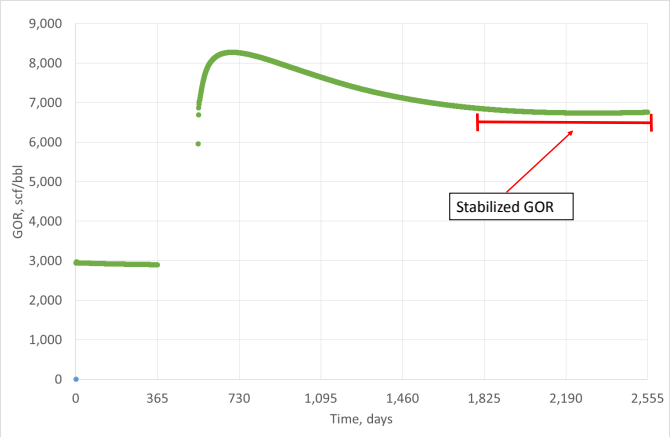

Figure 31: GOR as a function of time with constant flowing bottomhole pressure. $P_{wf} = 3000psia$, followed by a shut-in, then $P_{wf} = 2000psia$. The figure illustrates GOR behavior as a function of flowing bottomhole pressure. Definition of Stabilized GOR for this thesis is depicted.

The producing GOR is constant for constant flowing bottomhole pressure. **Fig. 31** is simulating the effect of production shut-in on the producing GOR. The model is simulated at a constant flowing bottomhole pressure of 3000 psia followed by a short shut-in and then producing at a flowing bottomhole pressure of 1500 psia. After the shut-in the model shows a long transient of up to two-three years before the producing GOR stabilizes at a value a little higher compared to if the well was producing on the same FBHP from time=0 as shown in Fig. 30. The GOR behavior of this well as a function of lowering FBHP was also investigated and depicted below.

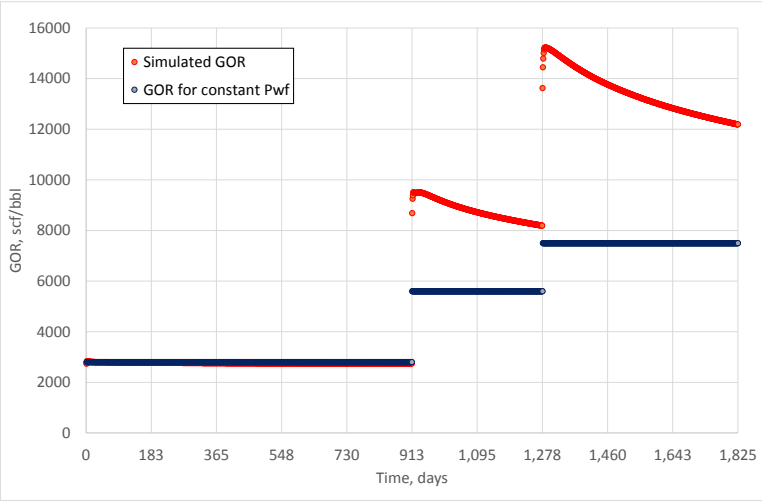

Figure 32: Comparison of numerically simulated GOR and GOR based on constant flowing bottomhole pressure from time = 0. p_{wf} = 3000 psia the first 2.5 years, followed by p_{wf} = 2000 for one year, followed by p_{wf} = 1500 for the last 1.5 years.

Fig. 32 shows the big spikes with long transients (more than a year) before the well produces at the expected $R_p(p_{wf})$. These transients in GOR will only be seen with a numerical simulation, and not with analytical solutions such as decline curve analysis (DCA).

6.2 Effect of Relative Permeability on Producing Gas-Oil Ratio

The choice of relative permeability model will affect the producing GOR. The relationship between stabilized producing GOR and relative permeability model is depicted in **Fig. 33 and 34**. Each point is a separate simulation with constant FBHP from time = 0. The plotted GOR is the stabilized GOR. In Fig. 33 n_{og} = 3.5 for all simulations. In Fig. 34 S_{org} = 0.2 for all simulations.

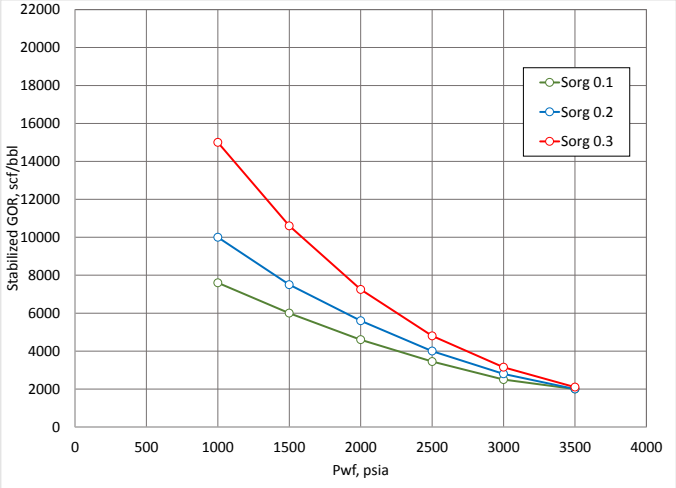

Figure 33: Stabilized GOR as a function of flowing bottomhole pressure, S_{org} ranging from 0.1 to 0.3, n_{og} = 3.5. Each symbol represents a simulation run with constant flowing bottomhole pressure from time = 0.

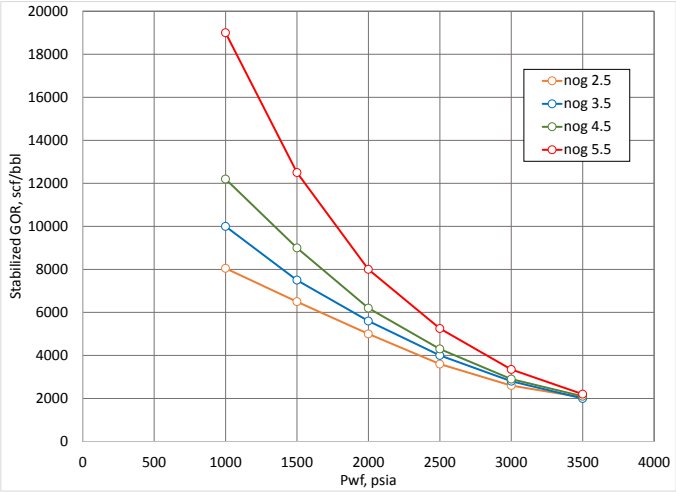

Figure 34: Stabilized GOR as a function of flowing bottomhole pressure, n_{og} ranging from 2.5 to 6.5, $S_{org} = 0.2$. Each symbol represents a simulation with run constant flowing bottomhole pressure from time = 0.

Figs. 33 and 34 shows that the producing GOR is a strong function of oil-gas relative permeability. When the oil relative permeability in the reservoir is lowered the producing GOR is increasing. The results also depicts the strong relationship between R_p and p_{wf}. GOR is monotonically increasing for decreasing FBHP.

7 Effect of Relative Permeability on Well Modeling

The relative permeability curves that are used in shale well modeling are analytical with values assumed based on range of conventional rocks, as discussed in the preceding chapters. Numerous different relative permeability curves can be created for these liquid-rich shale wells based on the estimates. The RHW8 well has been history matched and forecasted with three different relative permeability models in this chapter. Matrix permeability, k_m and residual oil saturation to gas, S_{org} was the history matching parameters. Three different values of n_{og}, the oil-gas exponent, were used to create three different relative permeability models.

7.1 History Matching RHW8 Well

Figs. 35 - 52 shows the best history match for three different relative permeability models. In each case x_f, matrix porosity, GOR_i and m_{dep} were kept constant equal to the initial reasonable history match. For each of the three different values of the gas-oil exponent, n_{og}, S_{org} and matrix permeability were set to be the history matching parameters.

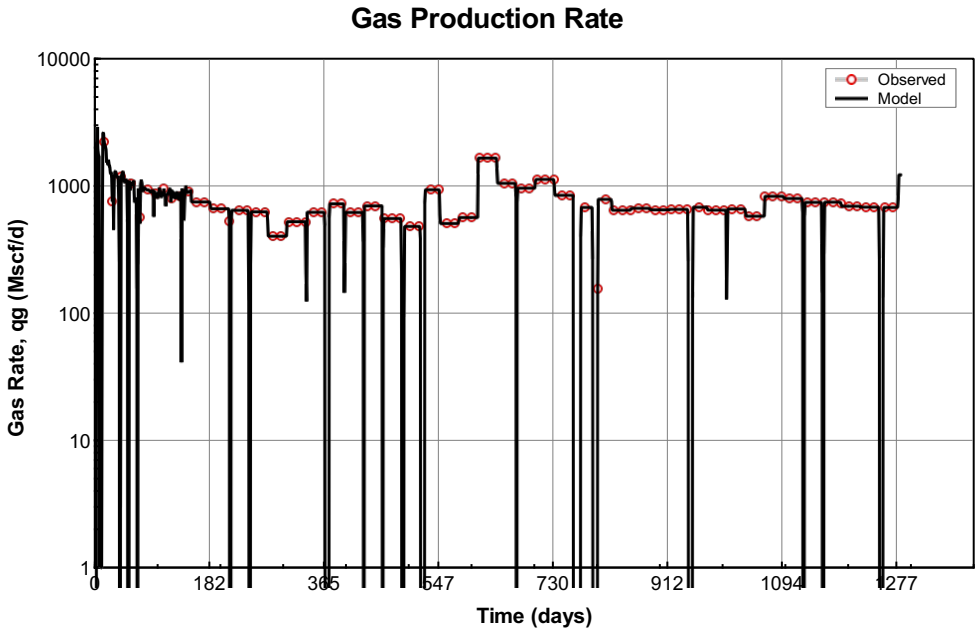

Figure 35: Measured Gas Rates. Well is run on gas rate control throughout the history match.

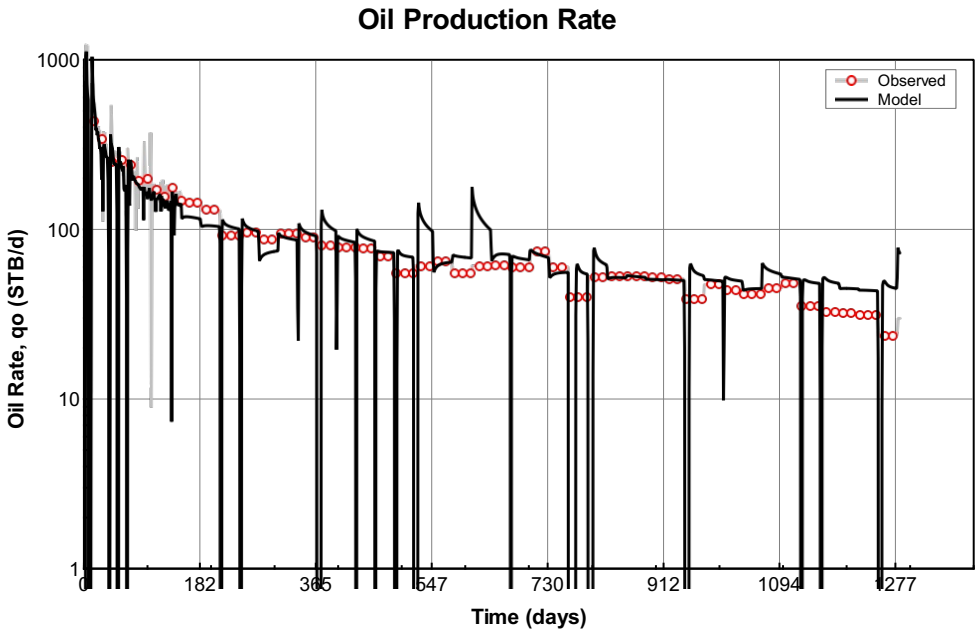

Figure 36: Calculated Oil Production Rates for the best history match with $n_{og} = 3.5$.

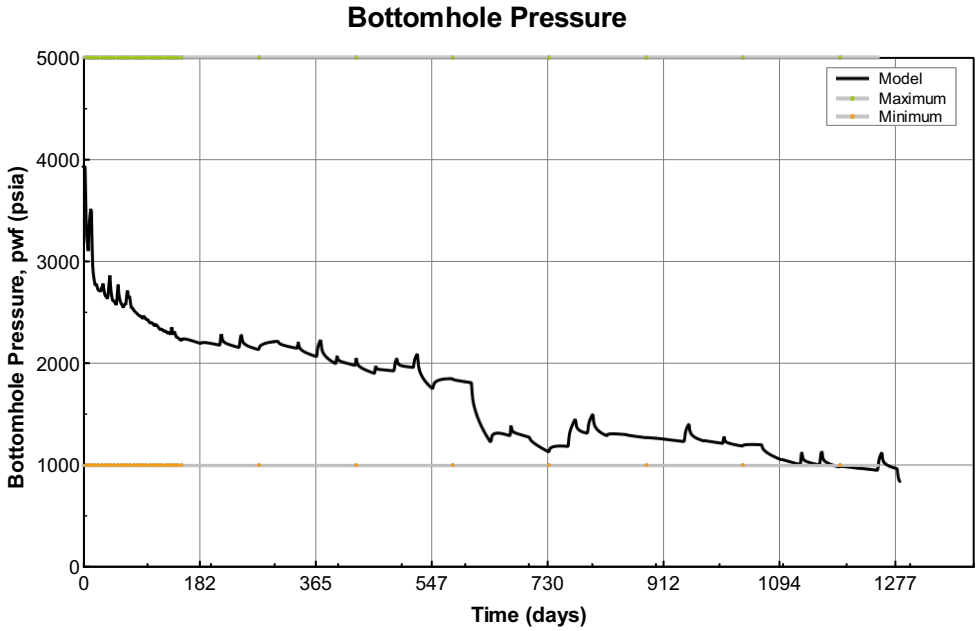

Figure 37: Calculated Flowing Bottomhole pressures for the best history match with $n_{og} = 3.5$.

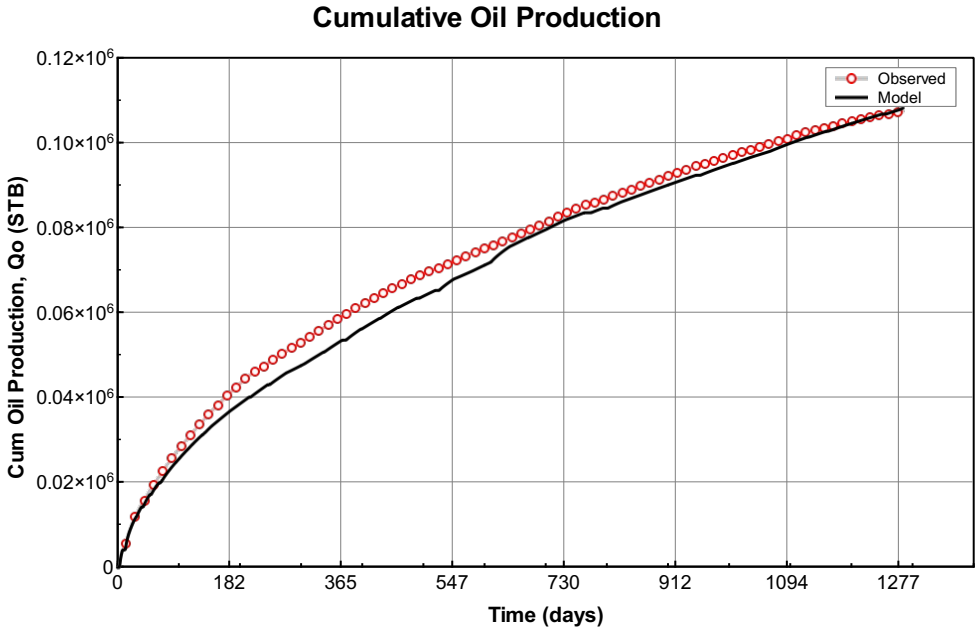

Figure 38: Calculated Cumulative Oil Production for the best history match with n_{og} = 3.5.

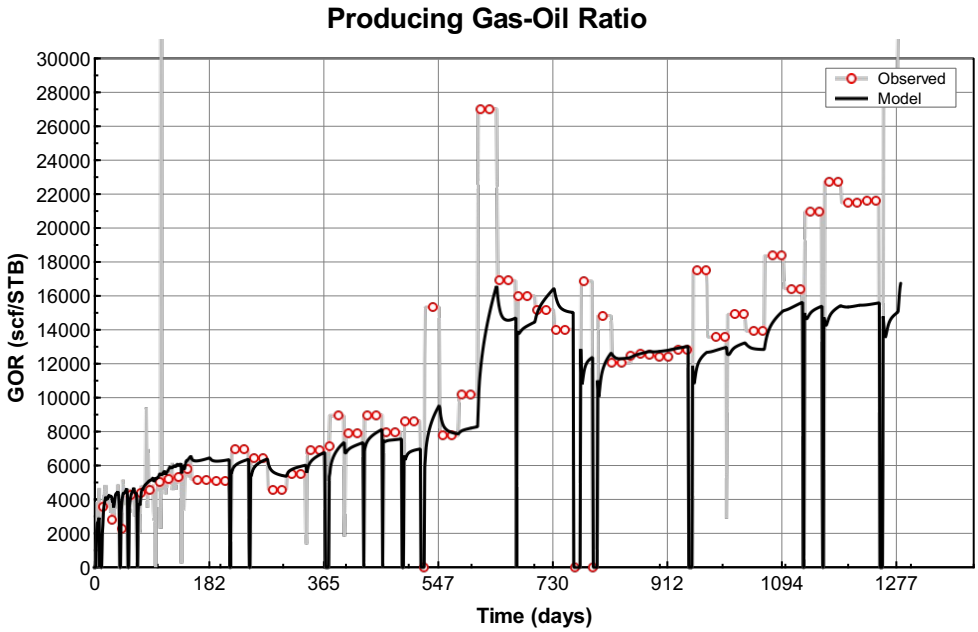

Figure 39: Calculated Producing Gas-Oil Ratio for the best history match with n_{og} = 3.5.

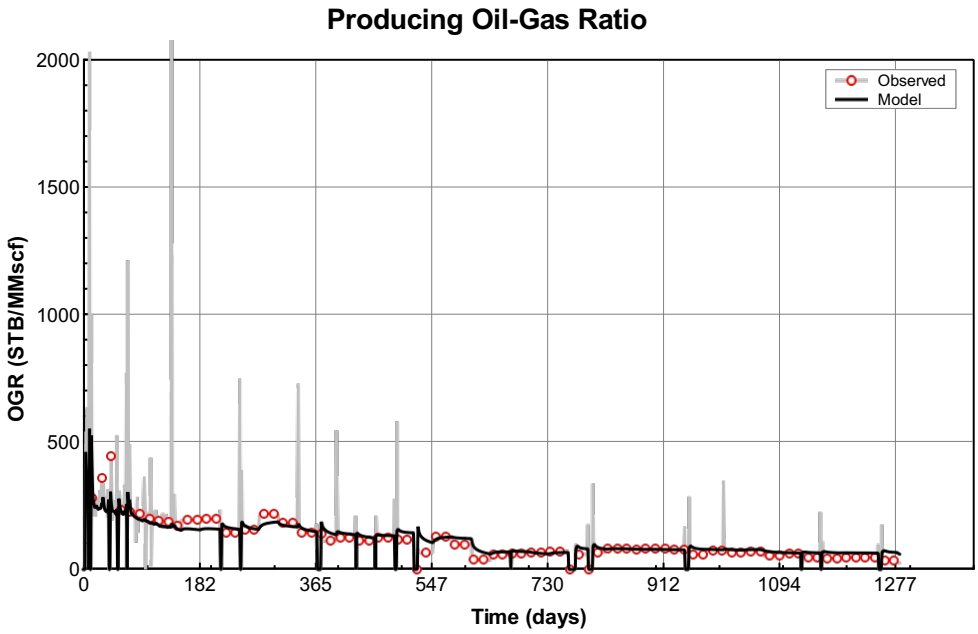

Figure 40: Calculated Producing Oil-Gas Ratio for the best history match with $n_{og} = 3.5$.

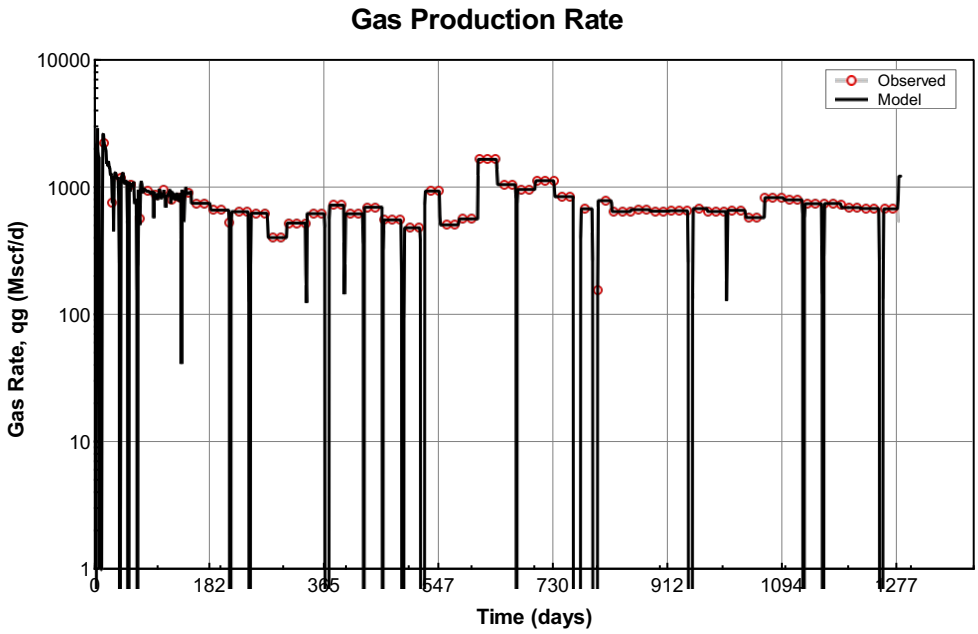

Figure 41: Measured Gas Rates. Well is run on gas rate control throughout the history match, $n_{og} = 4.5$.

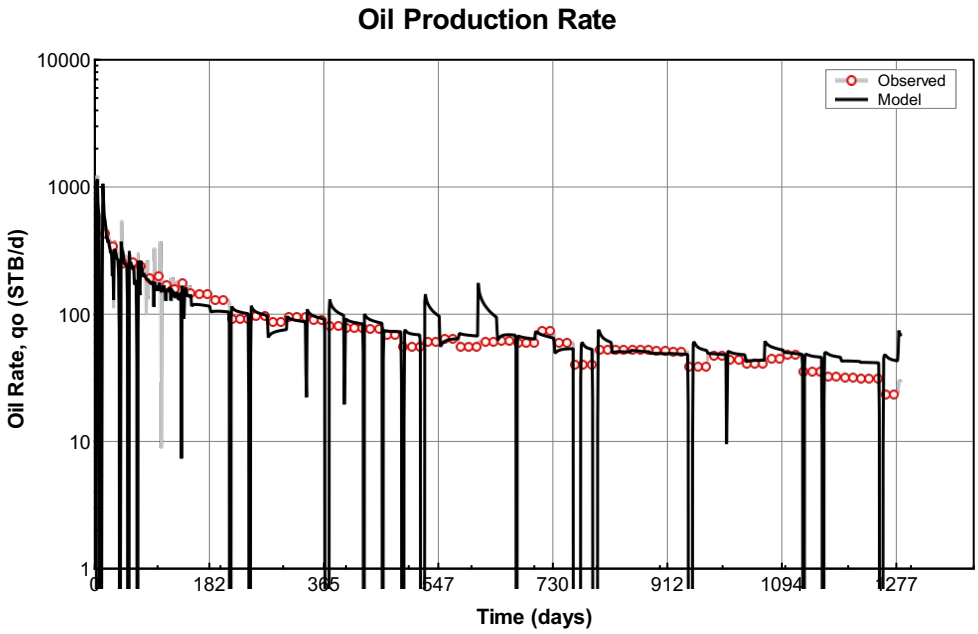

Figure 42: Calculated Oil Production Rates for the best history match with $n_{og} = 4.5$.

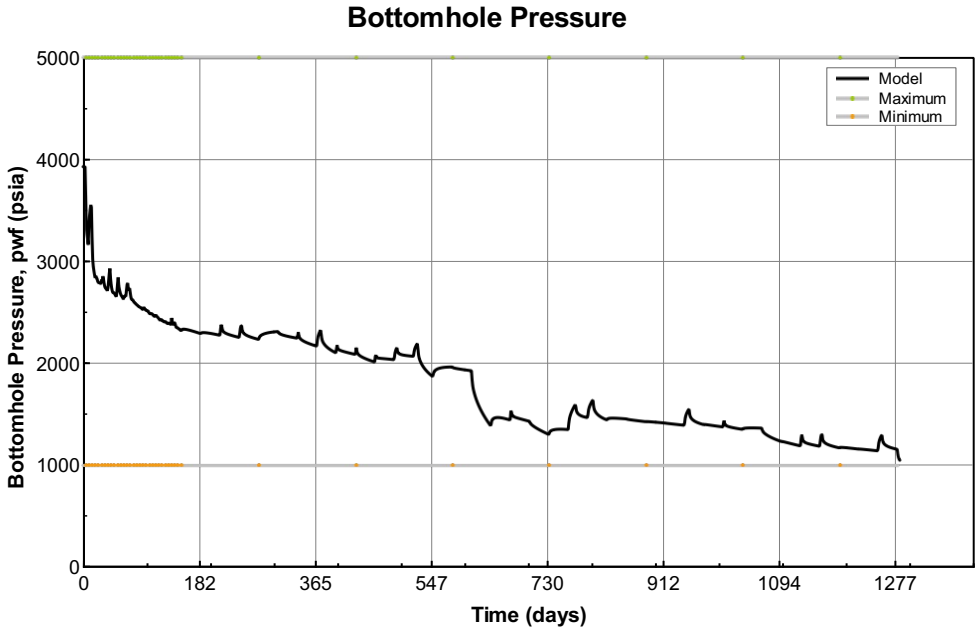

Figure 43: Calculated Flowing Bottomhole pressures for the best history match with $n_{og} = 4.5$.

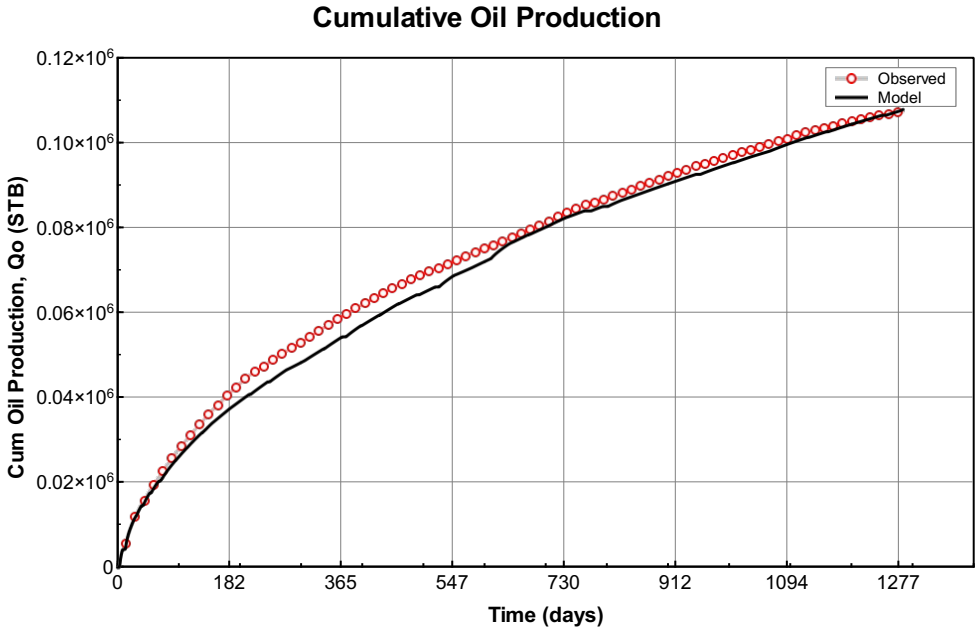

Figure 44: Calculated Cumulative Oil Production for the best history match with n_{og} = 4.5.

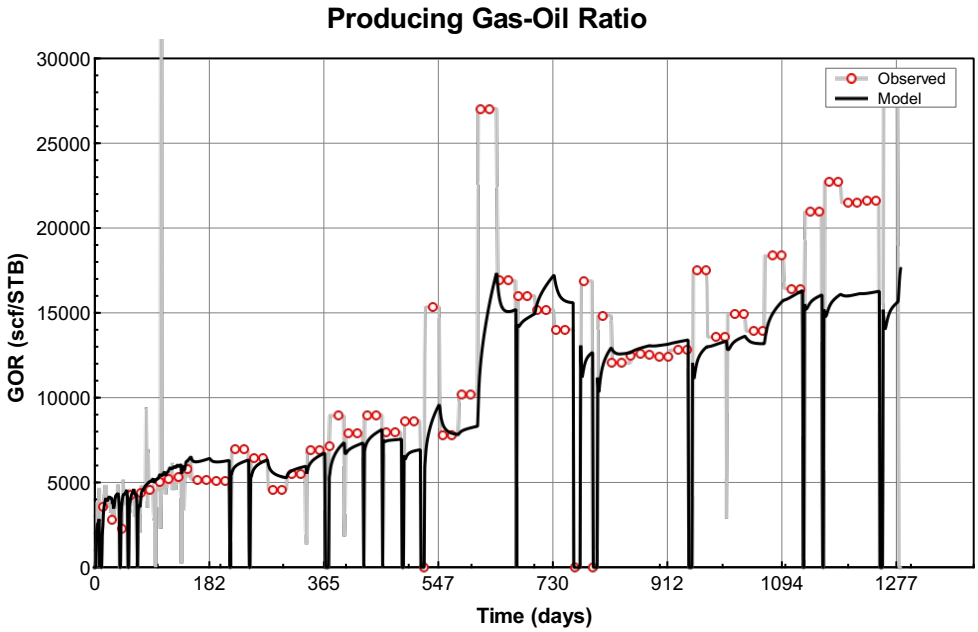

Figure 45: Calculated Producing Gas-Oil Ratio for the best history match with n_{og} = 4.5.

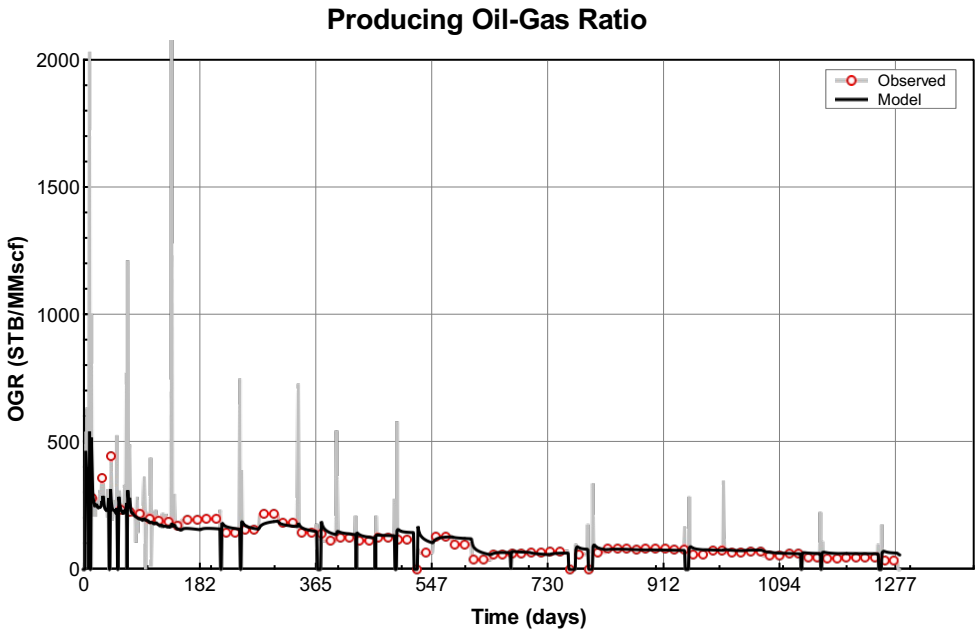

Figure 46: Calculated Producing Oil-Gas Ratio for the best history match with $n_{og} = 4.5$.

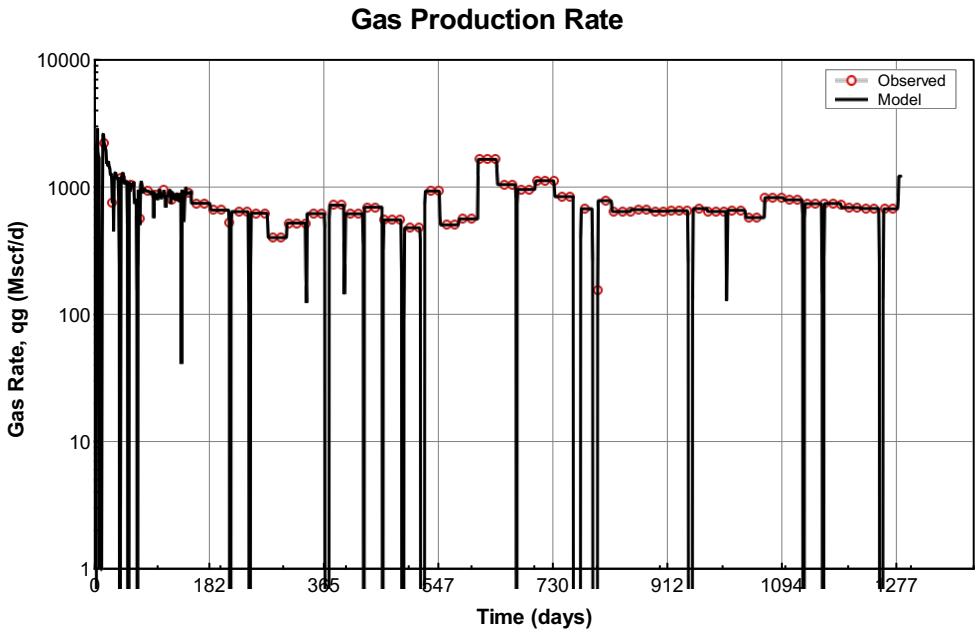

Figure 47: Measured Gas Rates. Well is run on gas rate control throughout the history match, $n_{og} = 5.5$.

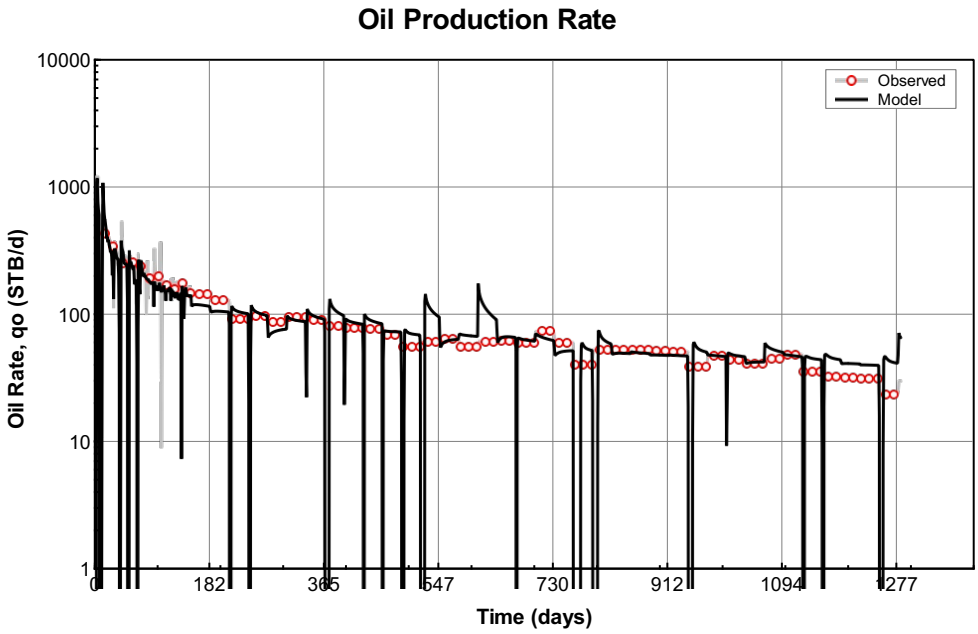

Figure 48: Calculated Oil Production Rates for the best history match with $n_{og} = 5.5$.

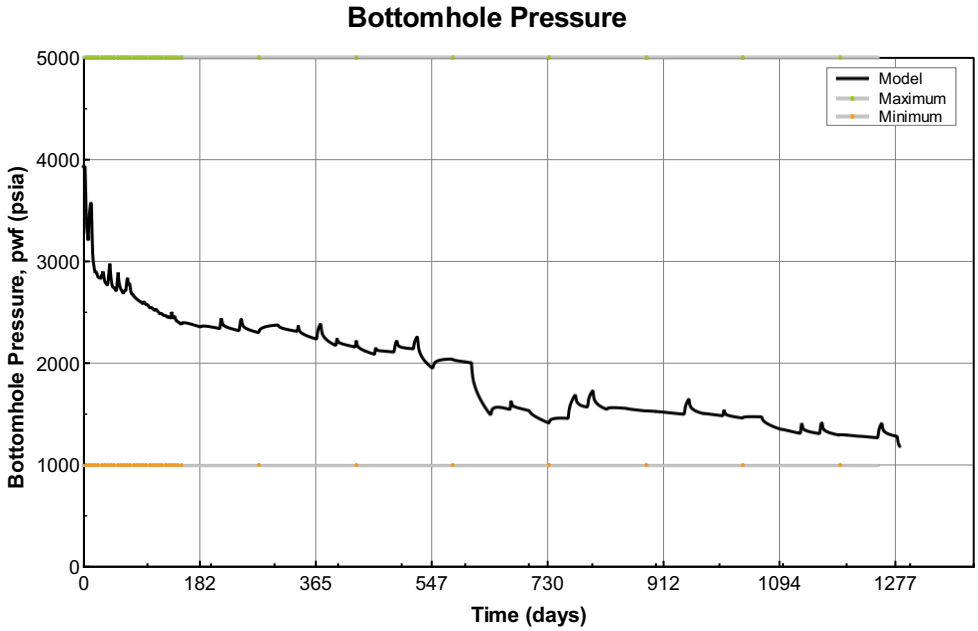

Figure 49: Calculated Flowing Bottomhole pressures for the best history match with $n_{og} = 5.5$.

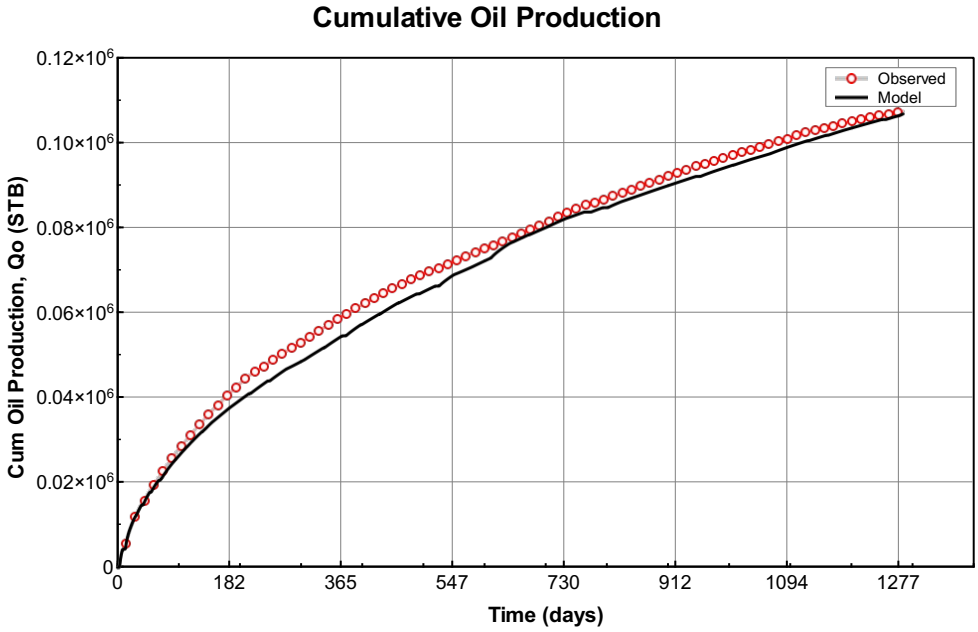

Figure 50: Calculated Cumulative Oil Production for the best history match with n_{og} = 5.5.

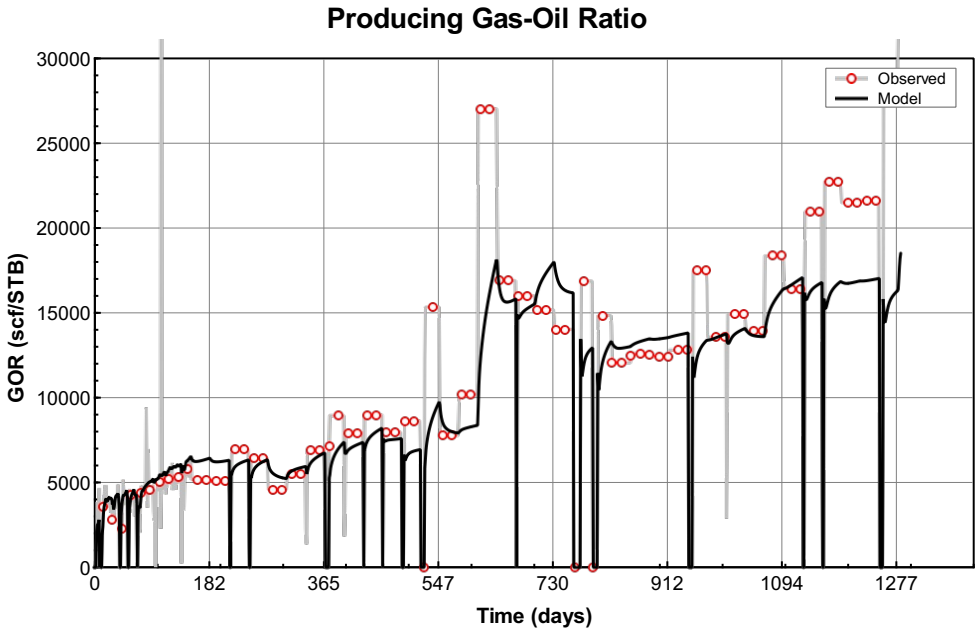

Figure 51: Calculated Producing Gas-Oil Ratio for the best history match with n_{og} = 5.5.

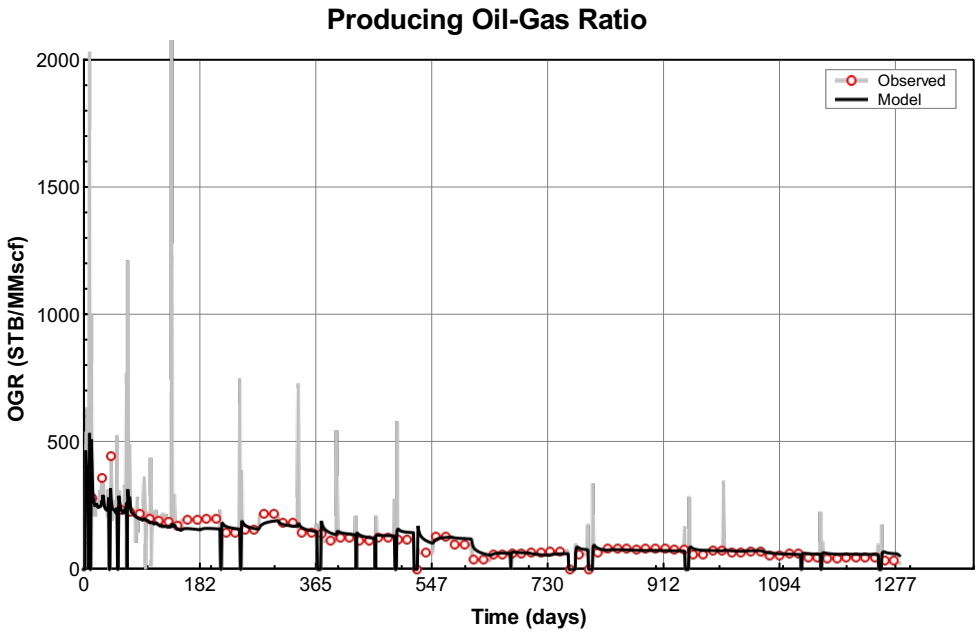

Figure 52: Calculated Producing Oil-Gas Ratio for the best history match with $n_{og} = 5.5$.

Each of the three cases yields equally good history match. The total SSQ, $SSQ_{total} = SSQ_{q_o} + SSQ_{p_{wf,bounds}}$ was around 250 for all three cases. By eyeballing it can be observed that each history match is equally good. None of the three are able to reach the high GOR (above 20,000 scf/STB) seen at the end of the history match. But oil rate and hence cumulative oil rate has a good match. The flowing bottomhole pressure is not significantly different in the three cases. This is a good indication that the three different relative permeability models are all representative for this well. The obtained matrix permeability and S_{org} for the three cases are shown below.

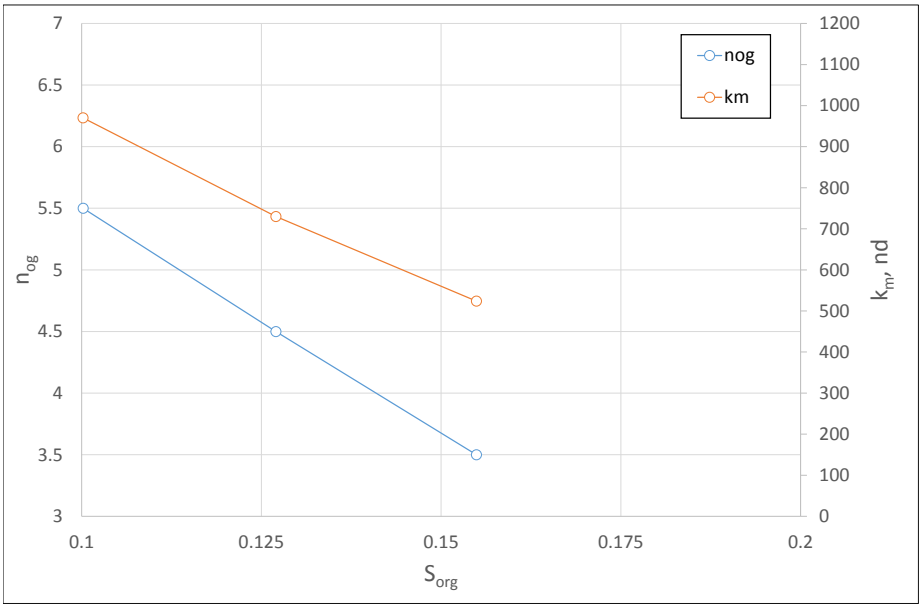

Figure 53: Plot of k_m and n_{og} versus S_{org}. Each point depicts the history match with the respective relative permeability model. Each point depicts similarly good history-match of the well.

Table 6: Matrix Permeability and Residual Oil Saturation to gas values for the best History Matches with three Relative Permeability exponents.

	$n_{og} = 3.5$	$n_{og} = 4.5$	$n_{og} = 5.5$
k_m	524 nd	730 nd	970 nd
S_{org}	0.155	0.127	0.10

Fig. 53 depicts the results of the three history matches. Three different values of n_{og} were used and kept fixed in the history match. Matrix permeability and S_{org} were used as history match parameters. The results shows that both matrix permeability and the oil-gas exponent, n_{og} are monotonically increasing for decreasing residual oil saturation to gas, S_{org}. The permeability has to be increased with decreasing oil relative permeability (increasing n_{og}) in order to be able to match oil rates and keeping the p_{wf} above 1000 psia.

7.2 Production Forecasting RHW8 Well

The three well models discussed above yielded equally good history matches. The models are based on three different relative permeability models. Three production strategies were simulated to investigate the long term effects of initializing the model with the different relative permeability models. All three strategies were simulated for all three well models. The first strategy, depicted in **Figs. 54 and 55**, produced according to best history match, followed by constant flowing bottomhole pressure of 1000 psia after end of measured data. The second strategy, depicted in **Figs. 57 and 58**, produced according to best history match, followed by constant flowing bottomhole pressure of 600 psia after end of measured data. The third strategy, depicted in **Figs. 60 and 61** produced according to best history match, followed by constant flowing bottomhole pressure equal to the flowing bottomhole pressure at end of history match for each of the individual models. The pressures used in the forecast are shown in **Tab 7**. All three models have a flowing bottomhole pressure close to 1000 psia at the end of the history match, see Tab. 7. The 600 psia case was simulated in order to yield a similar spike, with following transient, in the GOR behavior. The last case with different flowing bottomhole pressures will not have the spike in GOR at all as discussed in the preceding chapter.

7.2.1 Production Forecast with constant FBHP of 1000 psia after the end of History Match.

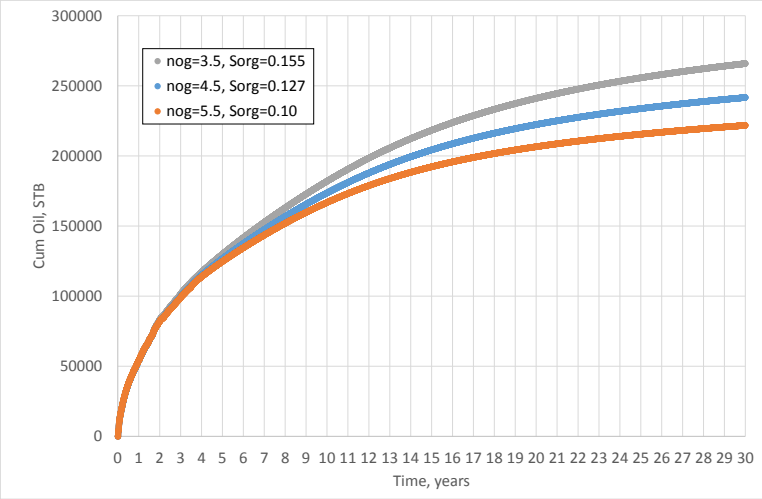

Figure 54: Cumulative Oil Production Forecast, 30 years - $P_{wf} = 1000 psia$ after end of History Match. The three lines represents the three relative permeability models.

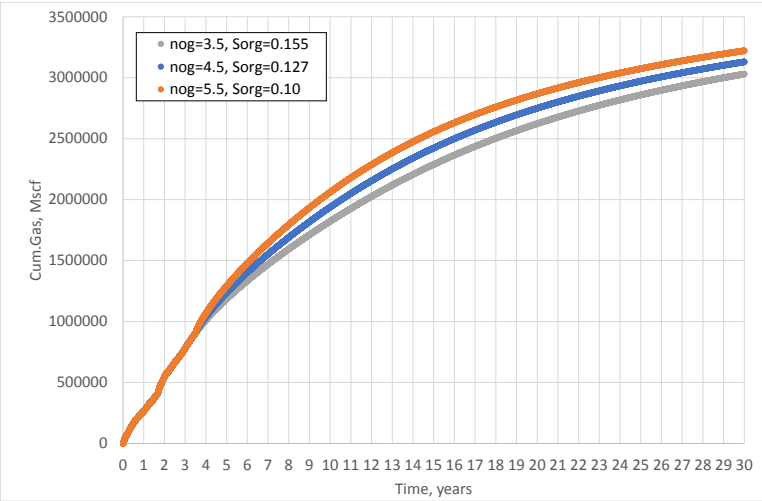

Figure 55: Cumulative Gas Production Forecast, 30 years - $P_{wf} = 1000 psia$ after end of history match. The three lines represents the three relative permeability models.

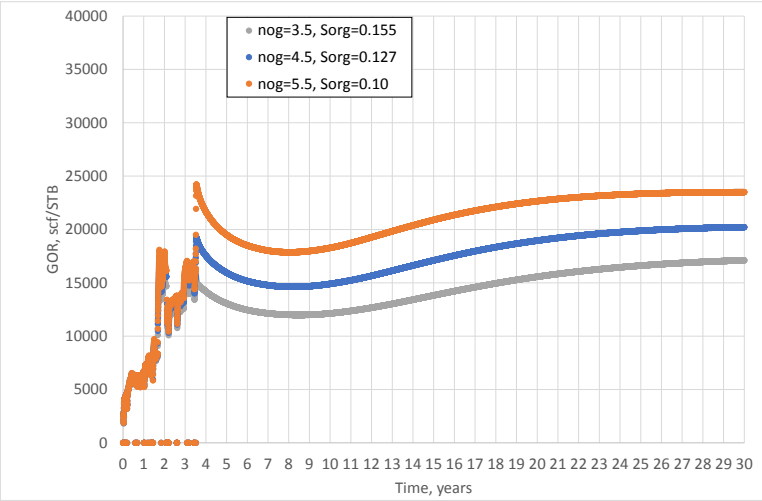

Figure 56: Producing GOR for the 30 year forecast - $P_{wf} = 1000 psia$ after end of History Match. The three lines represents the three relative permeability models.

7.2.2 Production Forecast with constant FBHP of 600 psia for all three models after History Match.

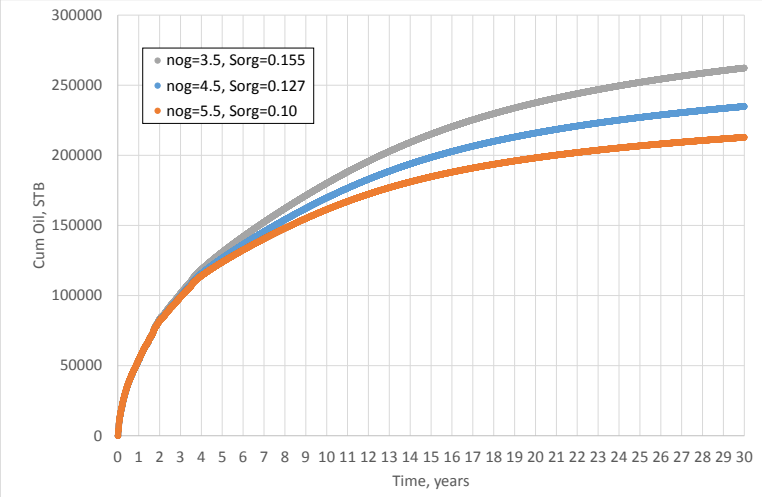

Figure 57: Cumulative Oil Production Forecast, 30 years - $P_{wf} = 600psia$ after end of History Match. The three lines represents the three relative permeability models.

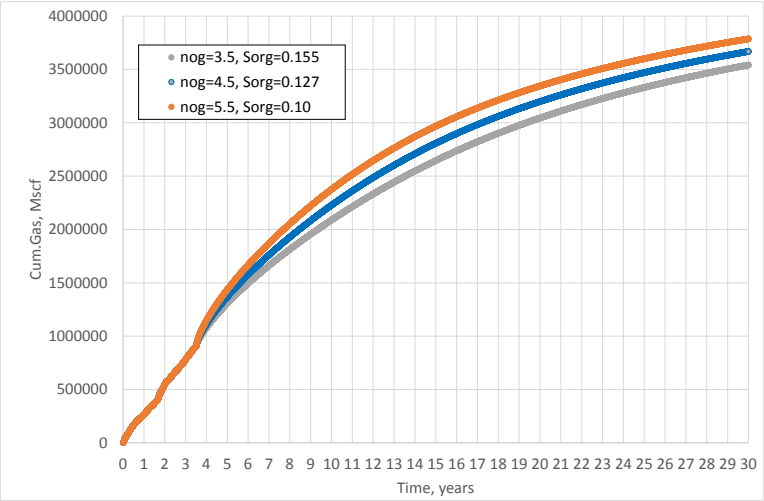

Figure 58: Cumulative Gas Production Forecast, 30 years - $P_{wf} = 600psia$ after end of History Match. The three lines represents the three relative permeability models.

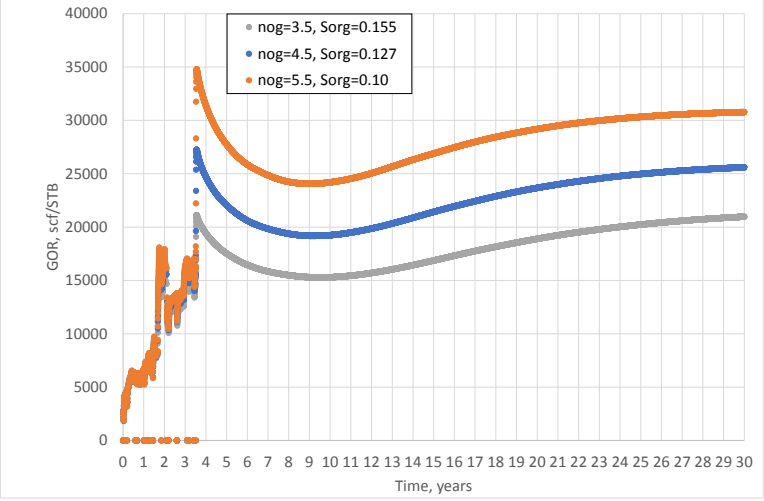

Figure 59: Producing GOR for the 30 year forecast - $P_{wf} = 600psia$ after end of History Match. The three lines represents the three relative permeability models.

7.2.3 Production Forecast with constant FBHP equal to the last flowing bottomhole pressure in the history match.

Table 7: Production forecast pressures used after the best history match of each individual model. Each pressure is equal to the last pressure calculated in the history match.

	$n_{og} = 3.5$	$n_{og} = 4.5$	$n_{og} = 5.5$
Pwf	950 psia	1040 psia	1150 psia

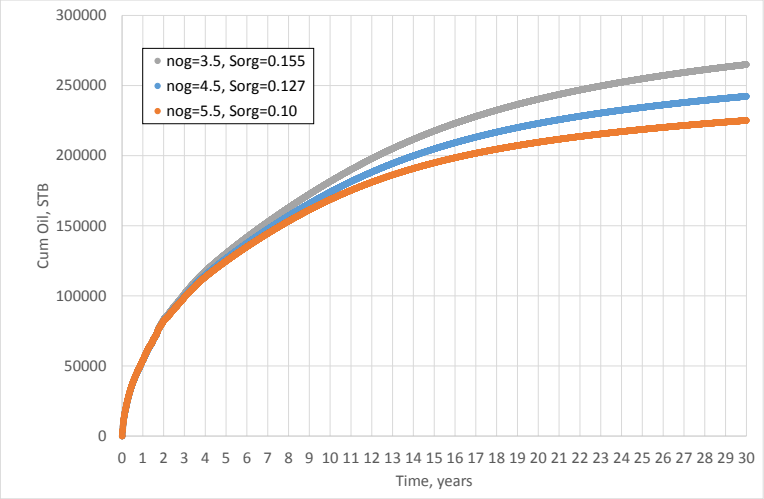

Figure 60: Cumulative Oil Production Forecast, 30 years - pressure equals pressure at the end of each individual History Match. The three lines represents the three relative permeability models.

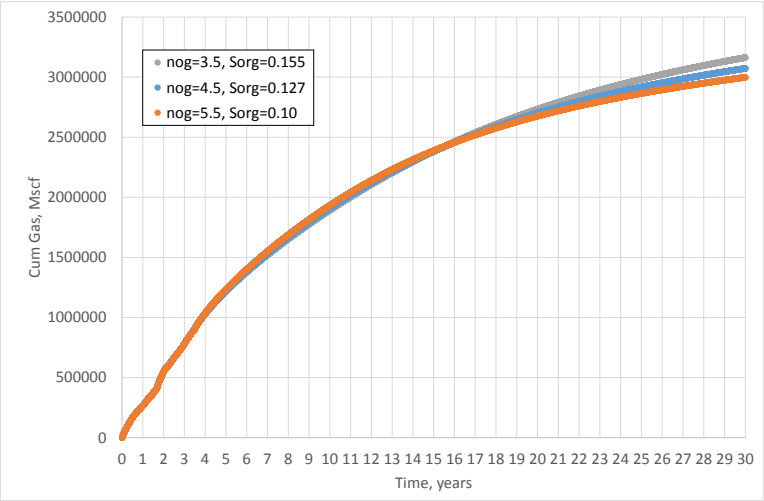

Figure 61: Cumulative Gas Production Forecast, 30 years - pressure equals pressure at end of each individual History Match. The three lines represents the three relative permeability models.

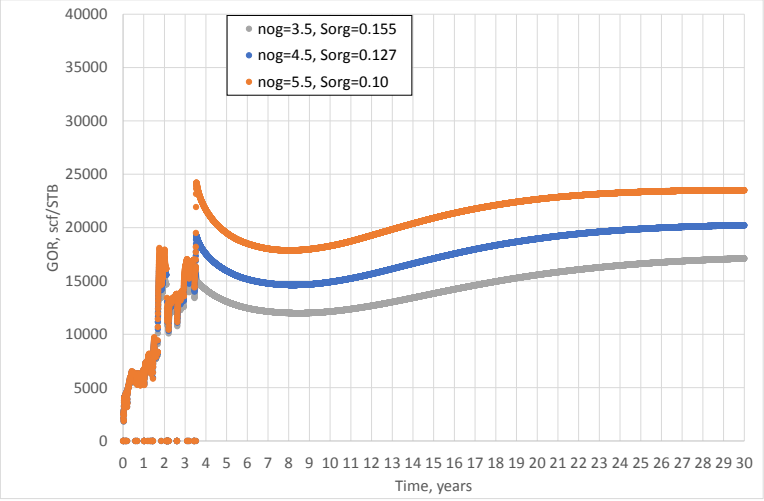

Figure 62: Producing GOR for the 30 year forecast - pressure equals pressure at end of each individual History Match. The three lines represents the three relative permeability models.

The cumulative gas production does not differ significantly for any of the three relative permeability models for any of the three thirty year forecasts, and is mostly a function of the flowing bottomhole pressure, i.e. producing GOR, where lowest flowing bottomhole pressure yields highest production. This is because the GOR is higher with lower pressure, and the well will produce at higher rates with higher drawdown.
The cumulative oil production is equal for the first ten years in all three cases. At the end of the thirty years the cumulative oil production is almost 50,000 STB higher for the case with highest oil relative permeability, n_{og} = 3.5, compared to the lowest oil relative permeability, n_{og} = 5.5. This reflects the relationship between n_{og} and p_{wf} depicted in Fig. 34. The cumulative oil production in the thirty year forecasts are almost identical for the $FBHP$ = 600 psia and $FBHP$ = 1000 psia cases. The first and the third case produce at almost equal pressures. Yielding equal behavior. However, the first and the second case produce with a difference in p_{wf} of 400 psia from 3.5 years. This pressure difference is reflected in the cumulative gas production, where the p_{wf} = 600 psia case produce significantly more gas. However, the cumulative oil production does not differ from eachother. This shows that the increased production rates obtained by decreasing p_{wf} does not overcome the effect of GOR(p_{wf}).
The relative permeability for oil and gas is a strong function of gas saturation. During the 3.5 years of history match and the following production forecast the reservoir will see a range of gas saturations. For the base case well model the saturations was plotted at one year, 3.5 years and 10 years.

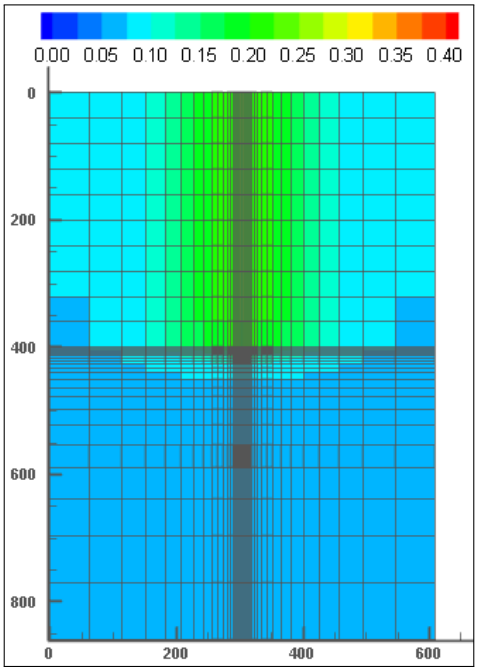

Figure 63: Contour map of the RHW8 well model with $n_{og} = 4.5$ displaying gas saturations after one year.

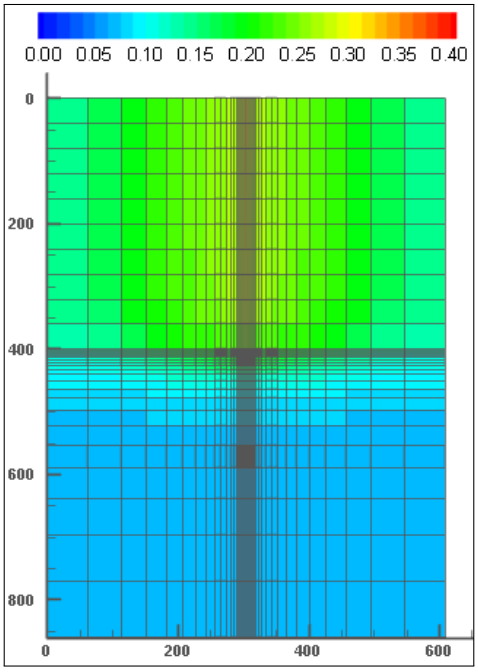

Figure 64: Contour map of the RHW8 well model with $n_{og} = 4.5$ displaying gas saturations after 1283.8 days approx. 3.5 years, end of history match.

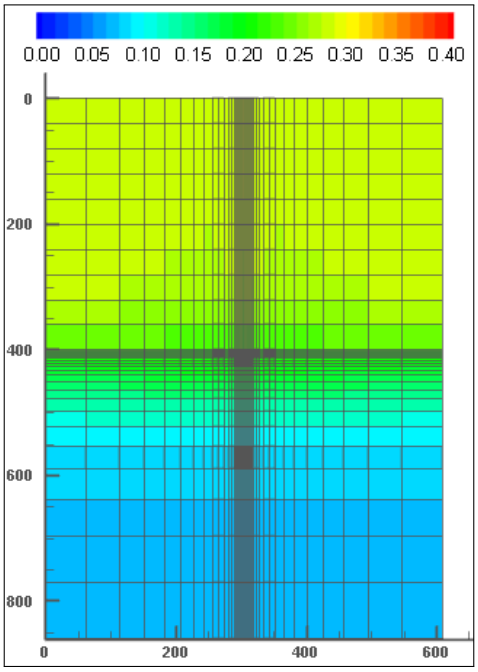

Figure 65: Contour map of the RHW8 well model with $n_{og} = 4.5$ displaying gas saturations after ten years.

Figs. 64 - 65 shows the gas saturation in the model after one year, 1283.8 (end of history match) and ten year respectively, for the history match and forecast case with $n_{og} = 4.5$. The contour maps shows that the gas saturations in the well model is in the range [0.05-0.3]. The relative permeability ratio k_{rg}/k_{ro} depicted in **Fig. 66** reflects the oil-gas mobility of the model. It is plotted for the three equally good history-matches.

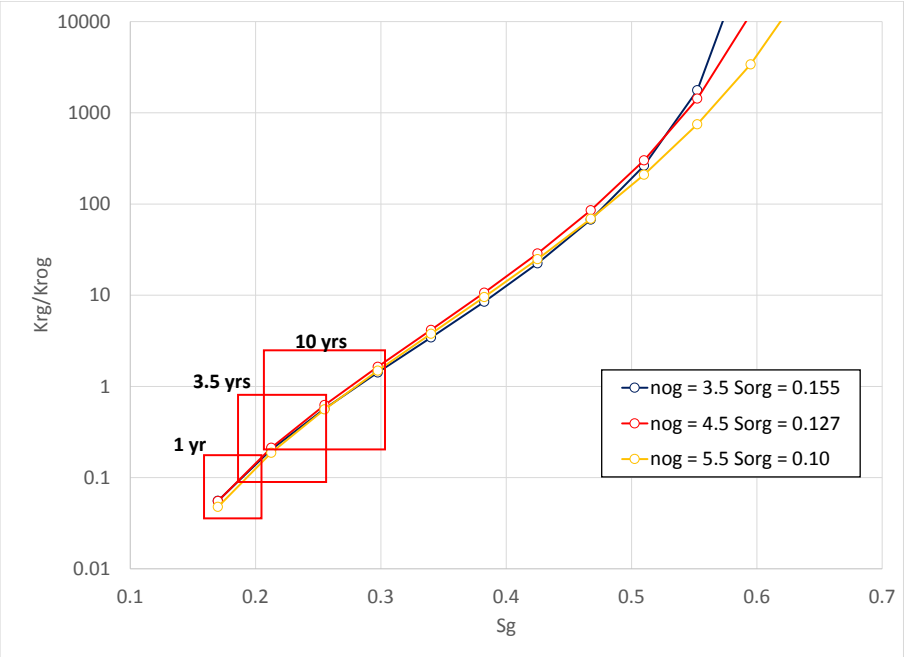

Figure 66: Plot of k_{rg}/k_{rog} versus S_g for three similarly-good History-Match runs, n_{og} fixed in each run. Matrix Permeability and S_{org} are regression variables in the History Match. Each box represents the gas saturations in the model at a given time.

As seen in Fig. 66 the saturations observed in the model the first ten years of the simulation is in the region where the three curves are almost identical. This shows that for these three models the mobility ratio of the two phases will not affect the history match or the production forecast directly.

The observed rates of this well indicate that the p_{wf} is gradually lowered the first 3.5 years. The history matched cumulative oil production with n_{og} = 4.5 was compared with the same model producing at constant p_{wf} from time = 0. **Fig. 67** depicts the cumulative oil at three different times, 1, 3.5 and 10 years. The green dots show the history matched cumulative oil production.

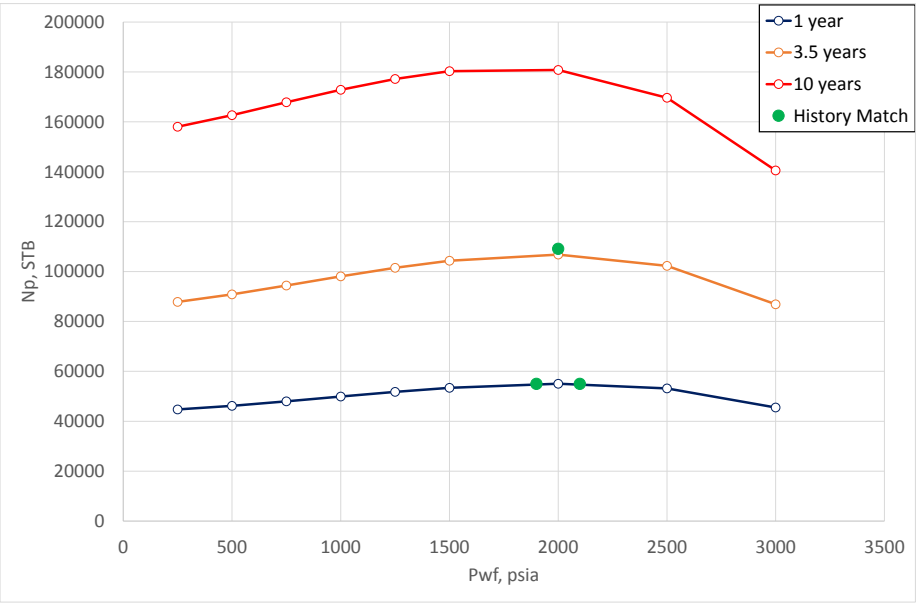

Figure 67: Cummulative oil production as a function of flowing bottomhole pressure. The three lines depict production time, 1 year, 3.5 years and 10 years. Each point is a separate simulation of the n_{og} = 4.5 case, all simulated on constant pressure control from time=0. Green dots depict history matched cum. oil production, to show what constant flowing bottomhole pressure will yield same production after 1, 3.5 and 10 years.

Fig. 67 shows that the optimal constant flowing bottomhole pressure for this well, in terms of oil production, is 2000 psia for the first ten years. After one year, there are two constant FBHP from time = 0 that would yield the same cumulative oil production as the history match of the well. It should also be noticed that the history matched cumulative oil production is higher than cumulative oil production for any constant p_{wf}, from time = 0, after 3.5 years. Indicating that gradually lowering p_{wf} will yield higher cumulative oil production for this well.

8 Conclusion

This thesis shows interesting results on GOR behavior and effects of relative permeability of two Permian Basin oil wells. The following conclusions sum up the results of this thesis:

1. Subscription based online public data from the IHS Enerdeq Browser have proven to provide data that together with some estimates will be sufficient to create a realiable FD well model.

2. Using average monthly production data for well control have proven to provide accurate simulation results after a couple of months of production. Any available daily production data should be used in the history match to improve the match of early well behavior.

3. The producing GOR (R_p) is a strong function of flowing bottomhole pressure and relative permeability.

4. Big spikes in R_p followed by long transients can not be calculated from traditional decline curve analysis. A complete, detailed FD numerical model is therefore necessary to history match the well and provide reliable production forecasts.

5. By lowering the FBHP of the well stepwise, the spikes and transients seen on the GOR will sum up, yielding a higher R_p compared to what is seen at the same constant FBHP.

6. The observed GOR for this well is significantly higher than the GOR observed in the model for low constant FBHP. The only way to achieve the high GORs seen in the observed data is by numerically simulating the well with gradually lowering the FBHP.

7. Different relative permeability models yield equally good history match of this particular well.

8. A thirty year production forecast with n_{og} = 3.5 has a cumulative oil production approximately 50,000 STB higher than the model with n_{og} = 5.5 with equally good history match after 3.5 years for the RHW8 well.

9. Different relative permeability models do not affect the production forecast significantly the first ten years.

10. Gradually lowering the FBHP will yield a higher cumulative oil production after 3.5 years compared to any constant FBHP from time = 0.

9 Limitations and Future Work

The data in this thesis is based on two permian basin oil wells. This thesis proves that a well model can be built based public data for this well. A more thorough research on a number of wells in the Permian Basin should be investigated to see if most wells can be history matched based on public data. The author recommends using public data as a first order history match if it is proved successful for more wells. It is recommended that the effects of relative permeability are further investigated on similar wells in the Permian Basin. The observed data used in this thesis does not include any pressure measurements. The p_{wf} obtained in the history match is therefore accepted based on experience of other wells in the area and no actual measurements. A history match of a well with measured p_{wf} available is recommended in order to verify the findings in this thesis.

Nomenclature

μ_g = gas viscosity, cp

μ_o = oil viscosity, cp

ϕ = matrix porosity

σ_H = largest horizontal stress, psia

σ_v = verical stress, psia

C_f = fracture conductivity, md-ft

h = net formation thickness, ft

k = permeability, md

k_m = matrix permeability, md

k_{rgcw} = relative permeability oil at $S_w = S_{wc}, S_g = 0$

k_{rgro} = relative permeability gas at $S_w = S_{wc}, S_o = S_{org}$

k_{rg} = gas relative permeability

k_{rog} = oil relative permeability to gas

k_{row} = oil relative permeability to water

k_{rwro} = relative permeability of water at $S_w = 1 - S_{orw}, S_g = 0$

k_{rw} = water relative permeability

L = distance between fractures, ft

m_{dep} = stress dependent permeability exponent in fractures

N = number of cells in the x-direction from fracture to the edge of the model

n = relative permeability exponent

N_x = number of gridcells along the wellbore

N_y = number of gridcells perpendicular to the wellbore

n_g = gas relative permeability exponent

n_{og} = oil relative permeability exponent to gas

n_{ow} = oil relative permeability exponent to water

n_w = water relative permeability exponent

p_f = pore pressure, psia

p_i = initial reservoir pressure, psia

p_w^{frac} = fracturing pressure of the well, psia

p_{wD} = dimensionless pressure

p_{wf} = flowing bottomhole pressure, psia

q_D = dimensionless flow rate
q_g = gas flow rate at standard conditions, scf/d or Mscf/d
Q_o = cumulative gas production, MMscf
Q_o = cumulative oil production, stb
q_o = oil flow rate at standard conditions, stb/d
q_w = water flow rate at standard conditions, stb/d
r_i = distance from center of fracture to the outer edge of cell i, ft
r_i = initial in-situ oil-gas ratio. STB/MMscf
R_p = producing gas-oil ratio, scf/STB
r_p = producing oil-gas ratio, STB/MMscf
R_s = solution gas-oil ratio, scf/STB
r_s = solution oil-gas ratio, STB/MMscf
S_{gc} = critical gas saturation
S_g = gas saturation
S_{org} = residual oil saturation to gas
S_{orw} = residual oil saturation to water
S_o = oil saturation
S_{wc} = connate water saturation
S_{wc} = connate water saturation
S_{wo} = initial water saturation
S_w = water saturation
T_0 = tensile strength of the formation, psia
$t_{D_{x_f}}$ = dimensionless time
W = weighting for individual SSQ
w = weighting factor for individual observed data point
w_f = fracture width, ft
x_e = distance from wellbore to outer boundary along the fracture direction, ft
x_f = fracture half-length, ft
y_e = distance from fracture to outer boundary along the wellbore direction, ft

Abbreviations

BSE	=	Back-Scattered Electrons
BO	=	Black-Oil
DCA	=	Decline Curve Analysis
EOS	=	Equation of State
FBHP	=	Flowing Bottomhole Pressure
FD	=	Finite Difference
GOR	=	Gas-Oil Ratio
LRSR	=	Liquid-Rich Shale Reservoirs
OGR	=	Oil-Gas Ratio
OOIP	=	Original Oil in Place
OGIP	=	Original Gas in Place
PVT	=	Pressure Volume and Temperature in an Equation of State
SRK	=	Soawe-Redlich-Kwong
SSQ	=	Sum of Squares

References

Abdallah, W., Buckley, J. S., Carnegie, A., Edwards, J., Herold, B., Fordham, E., Graue, A., and et. al (2007). Fundamentals of wettability. Published in *Technology Journal Volume 38* 1125-1144. Obtained from `http://www.slb.com/~/media/Files/resources/oilfield_review/ors07/sum07/p44_61.pdf` 25th of May 2015.

Baker, L. (1988). Three-phase relative permeability correlations. Presented at SPE Enhanced Oil Recovery Symposium, Oklahoma, USA, 1988.

Carrasco, A., DeGeare, J., and Hunter, J. (2014). *Achieving a More Efficient Frac Network for Horizontal Development of the Bone Spring Sandstone*. Presented at SPE Hydraulic Fracturing Technology Conference, The Woodlands, USA, 2014.

Caza Petro (2012). Retrieved from: `http://www.cazapetro.com/index.php?id=132` on 29th of April 2015.

Coats Engineering Inc. (2015). *SENSOR Manual*.

Curtis, M. E., Sondergeld, C. H., and Rai, C. S. (2013). Investigation of the microstructure of shales in the oil window. SPE-168815 presented at Unconventional Resources Technology Conference, Denver, CO, USA. August 2013.

DiCarlo, D. A., Sahni, A., and Blunt, M. J. (1998). The effect of wettability on three-phase relative permeability. SPE-49317 presented at SPE Annual Technical Conference and Exhibition, New Orleans, LA, USA. September 1998.

Fjaer, E., Holt, R. M., Horsrud, P., Raaen, A. M., and Risnes, R. (2008). *Petroleum Related Rock Mechanics 2nd Edition*. Elsevier.

IHS (2014). IHS enerdeq browser. `http://www.ihs.com/`.

Inc., C. E. (2015). SENSOR Reservoir Simulator. `www.coatsengineering.com`.

Jackson, K., Palisch, T., and Lehman, L. (2014). *Completion Optimization with Ceramics Provides Step Changes in Horizontal Performance for the* 2^{nd} *Bone Spring Formation - A southeastern New Mexico Case History*. Presented at SPE Technical Conference and Exhibition, Amsterdam, Netherlands, 2014.

Juell, A. O. and Whitson, C. H. (2013). *Optimized Well Modeling of Liquid-Rich Shale Reservoirs*. SPE-166380 presented at SPE Annual Technical Conference and Exhibition, New Orleans, LA, USA. September 2013.

Mouawad, J. (2009). Estimate places natural gas reserves 35 % higher. Published in Ny Times June 17, 2009. Retrieved from: `http://www.nytimes.com/2009/06/18/business/energy-environment/18gas.html?_r=0` on 28th of May 2015.

Petrostreamz (2012). *Pipe-It SensorGrid Documentation*.

Petrostreamz (2014). Pipe-it. `http://www.petrostreamz.com/`.

U.S. Energy Information Administration (2014a). *Outlook for U.S. shale oil and gas*. Retrieved from: `http://www.eia.gov/pressroom/presentations/sieminski_01222014.pdf` 20thMarch 2015.

U.S. Energy Information Administration (2014b). *Six formations are responsible for surge in Permian Basin crude oil production*. Retrieved from: `http://www.eia.gov/todayinenergy/detail.cfm?id=17031` on 29th of April 2015.

U.S. Energy Information Administration (2015). *Energy in Brief*. Retrieved from: `http://www.eia.gov/energy_in_brief/article/shale_in_the_united_states.cfm` on 27th of May 2015.

Wattenbarger, R. A., El-Banbi, A. H., Villegas, M. E., and Maggard, J. B. (1998). Production analysis of linear flow into fractured tight gas wells. SPE-39931 presented at SPE Rocky Mountain Regions/Low Permeability Reservoirs Symposium and Exhibition, Denver, CO, USA. April 1998.

Whitson, C. and Brule, M. R. (2000). *Phase Behavior*. SPE, 2000.

Whitson, C. and Sunjerga, S. (2012). *PVT in Liquid-Rich Shale Reservoirs*. SPE-155499 presented at SPE Annual Technical Conference and Exhibition, San Antonio, TX, USA. October 2012.

Appendices

Appendix A: RHW22 History Match and Production Forecast

Table 8: Reservoir and Well Input Data - RHW22 Well Base Case

Parameter	Value	Unit	Comment
x_f	400	feet	History Matching variable
k_m	490	nd	History Matching variable
ϕ	0.05	-	History Matching variable
GOR_i	2400	scf/STB	History Matching variable
$m_{dep_{fracs}}$	0.5	-	History Matching variable
n_g	2	-	Assumed
n_w	2.5	-	Assumed
n_{og}	4.5	-	Assumed
n_{ow}	2.5	-	Assumed
S_{wc}	0.15	-	History matching variable
S_{wi}	0.35	-	History matching variable
S_{gi}	0	-	History matching variable
S_{org}	0.107	-	History matching variable
S_{orw}	0.1	-	Assumed
P_{res_i}	4119	psia	Assumed based on the area
Reservoir Height	200	feet	Assumed based on the area
Vertical Depth	13592	feet	Found in Enerdeq Browser
Well Spacing	160	acres	Found in Enerdeq Browser
Lateral Well Length	3906	feet	Found in Enerdeq Browser
Number of Fracs	20	-	Found in Enerdeq Browser
Frac Width Physical	0.01	feet	Assumed
Frac Porosity	0.25	-	Assumed
Frac Width Model	0.08333	feet	Assumed
C_f	1000	md-feet	Assuming Infinite-Acting Fracture
Tubing Diameter	4.5	inch	Found in Enerdeq Browser
Lateral Wellbore Diameter	2.875	inch	Found in Enerdeq Browser

Best History Match with three different Relative Permeability Models

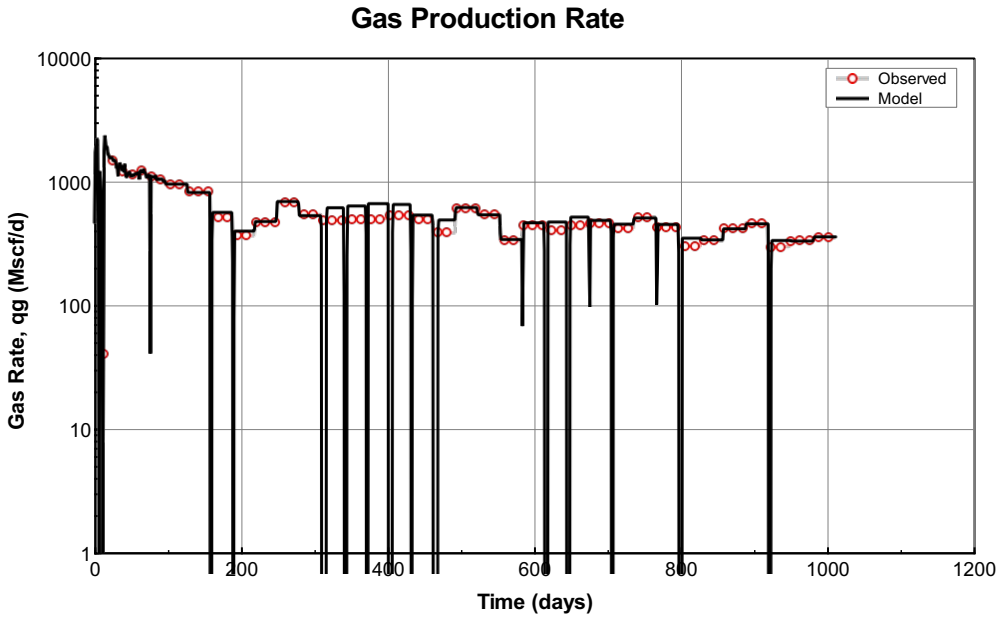

Figure 68: Measured Gas Rates. Well is run on gas rate control throughout the history match.

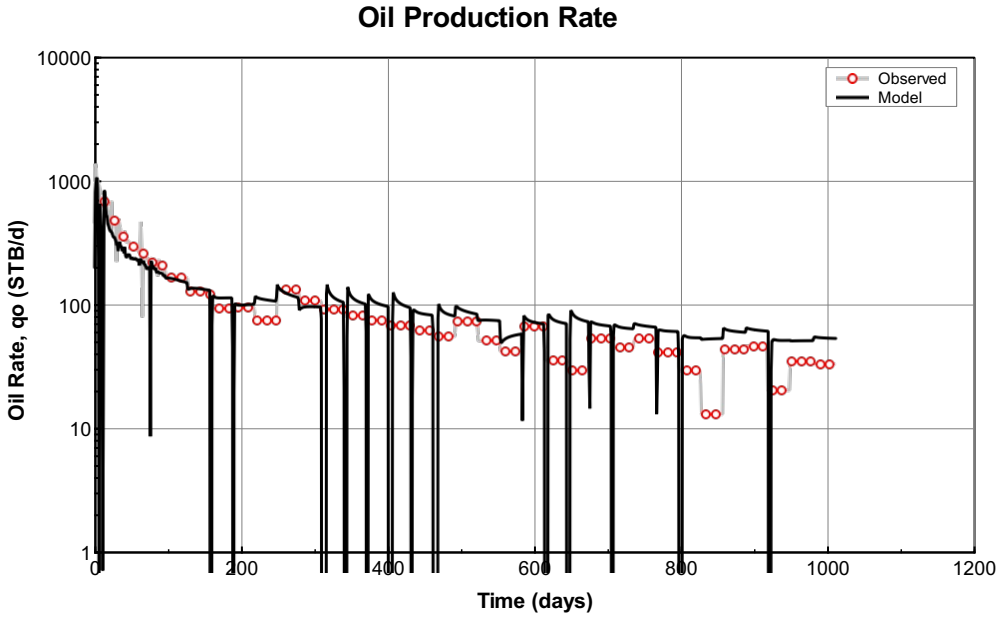

Figure 69: Calculated Oil Production Rates for the best history match with $n_{og} = 3.5$.

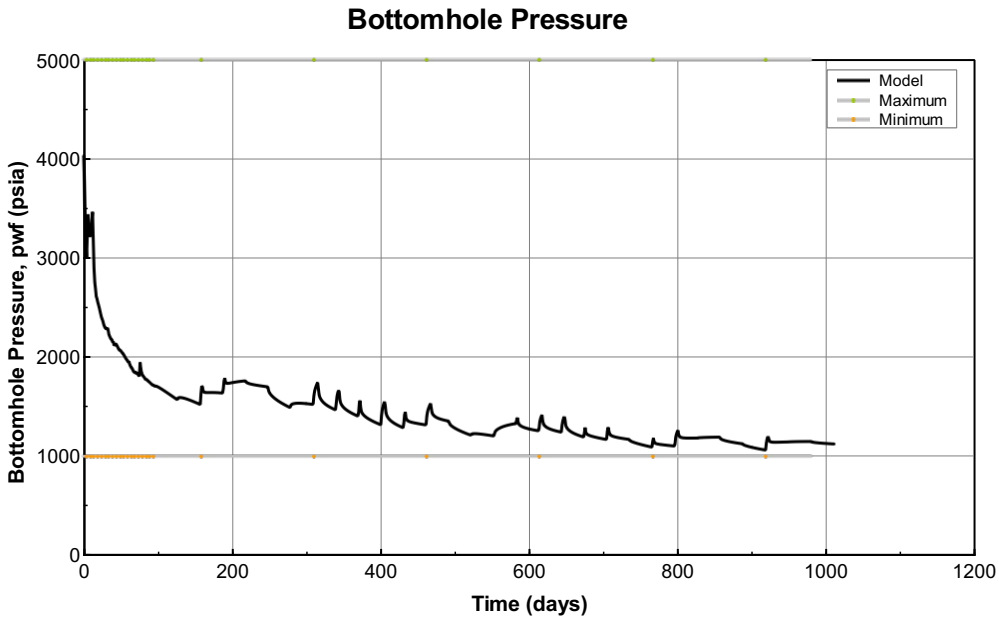

Figure 70: Calculated Flowing Bottomhole pressures for the best history match with n_{og} = 3.5.

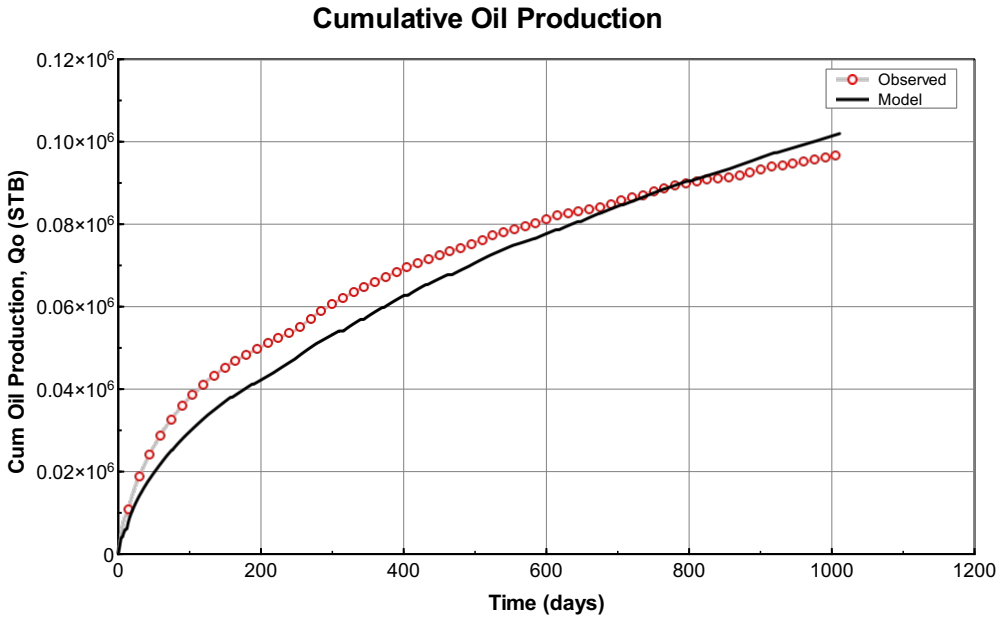

Figure 71: Calculated Cumulative Oil Production for the best history match with n_{og} = 3.5.

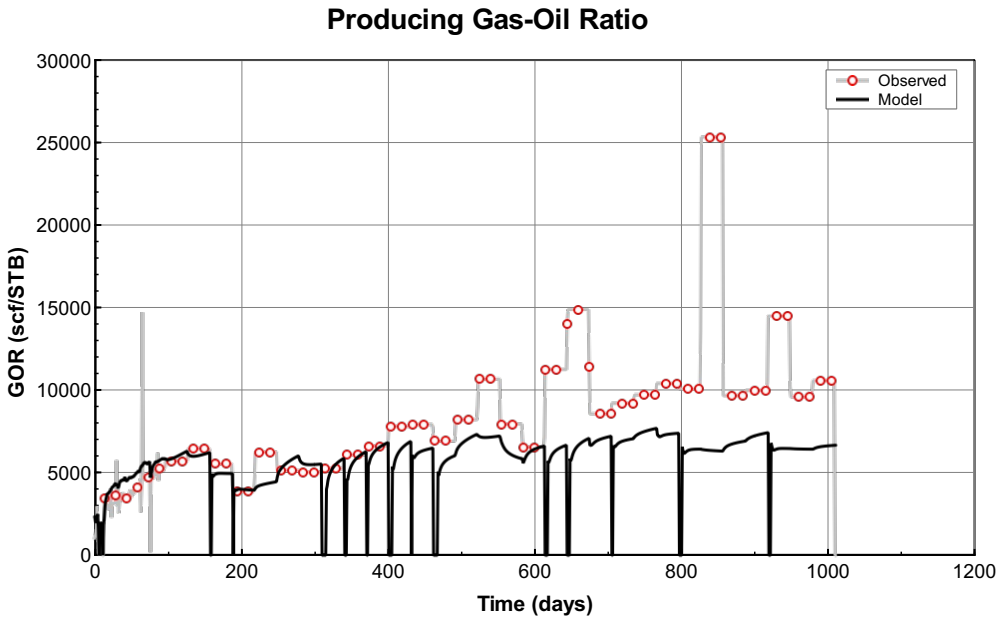

Figure 72: Calculated Producing Gas-Oil Ratio for the best history match with $n_{og} = 3.5$.

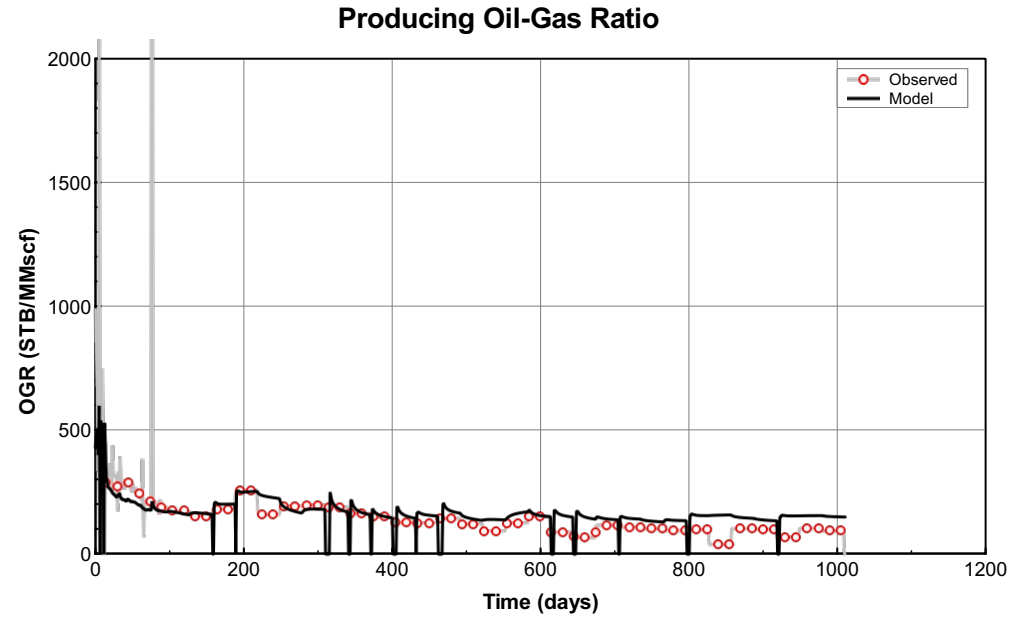

2

Figure 73: Calculated Producing Oil-Gas Ratio for the best history match with $n_{og} = 3.5$.

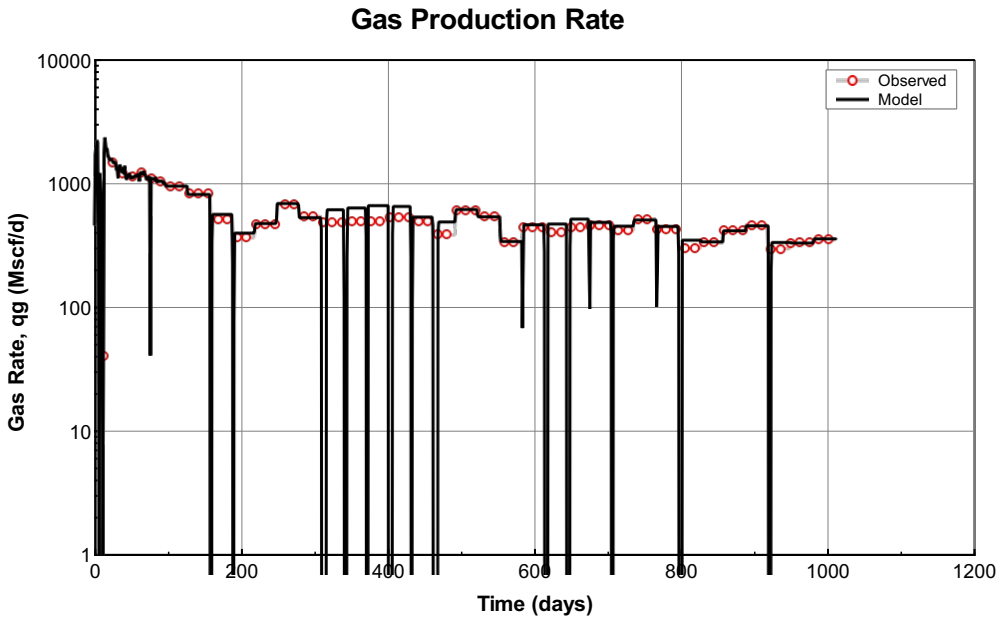

Figure 74: Measured Gas Rates. Well is run on gas rate control throughout the history match, $n_{og} = 4.5$.

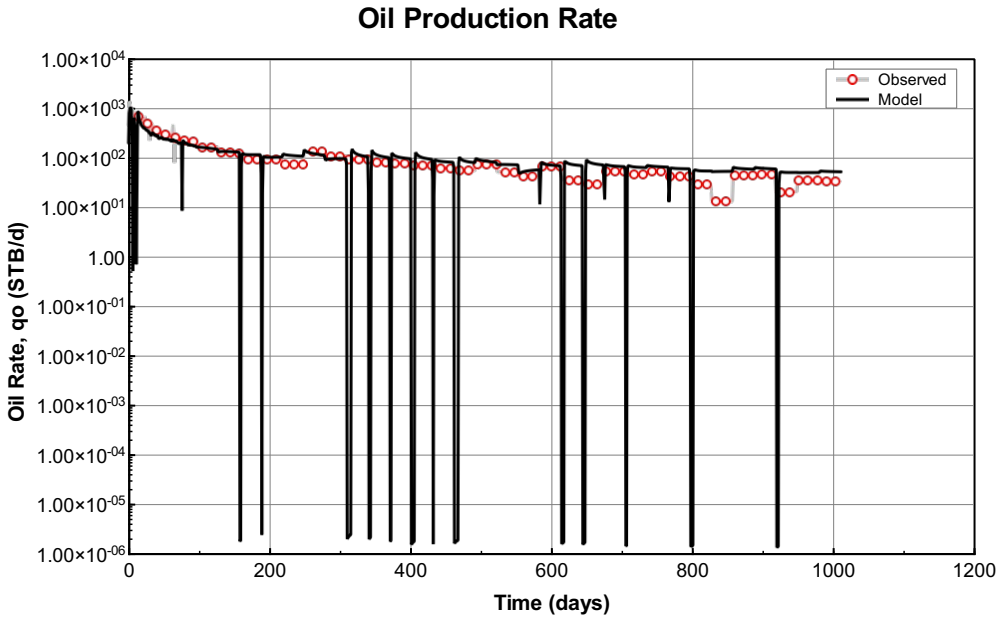

Figure 75: Calculated Oil Production Rates for the best history match with $n_{og} = 4.5$.

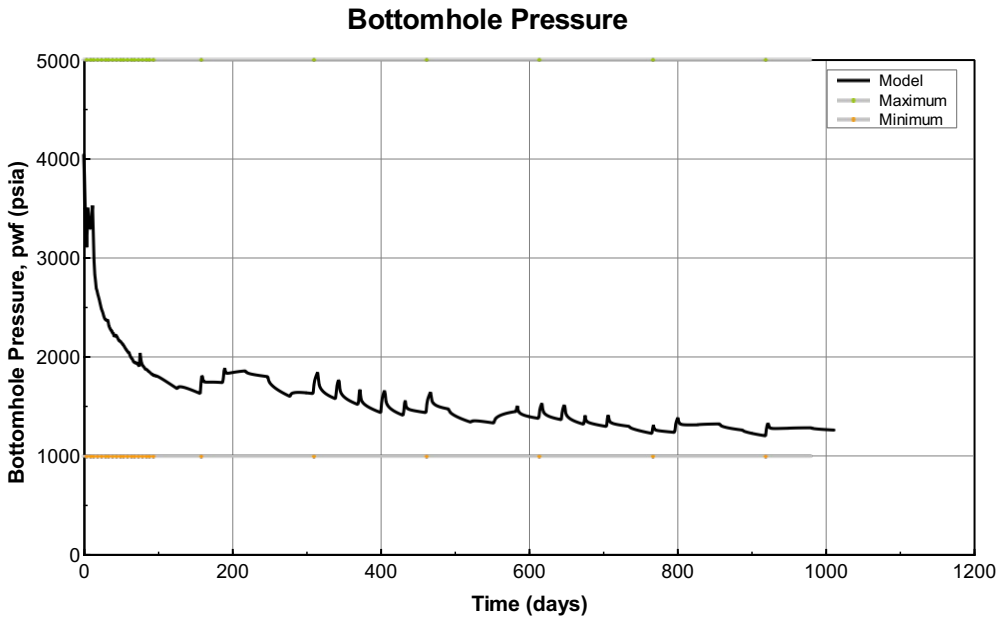

Figure 76: Calculated Flowing Bottomhole pressures for the best history match with n_{og} = 4.5.

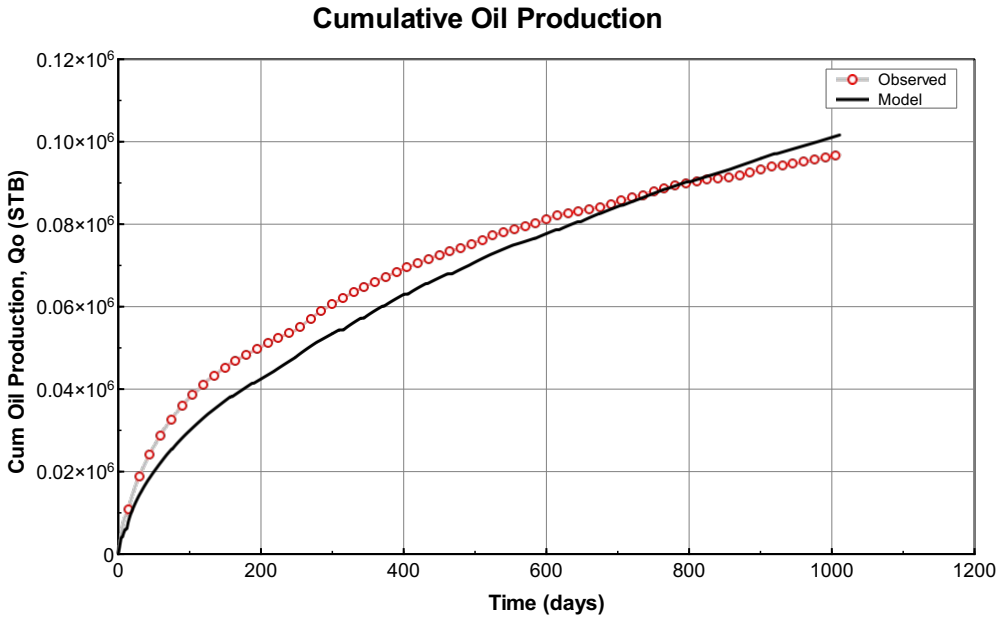

Figure 77: Calculated Cumulative Oil Production for the best history match with n_{og} = 4.5.

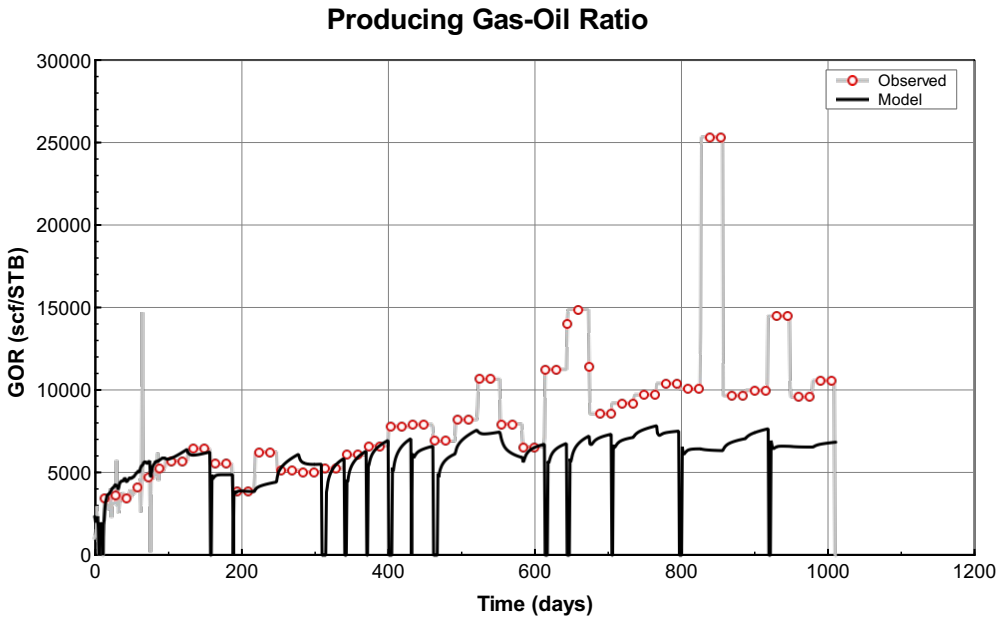

Figure 78: Calculated Producing Gas-Oil Ratio for the best history match with $n_{og} = 4.5$.

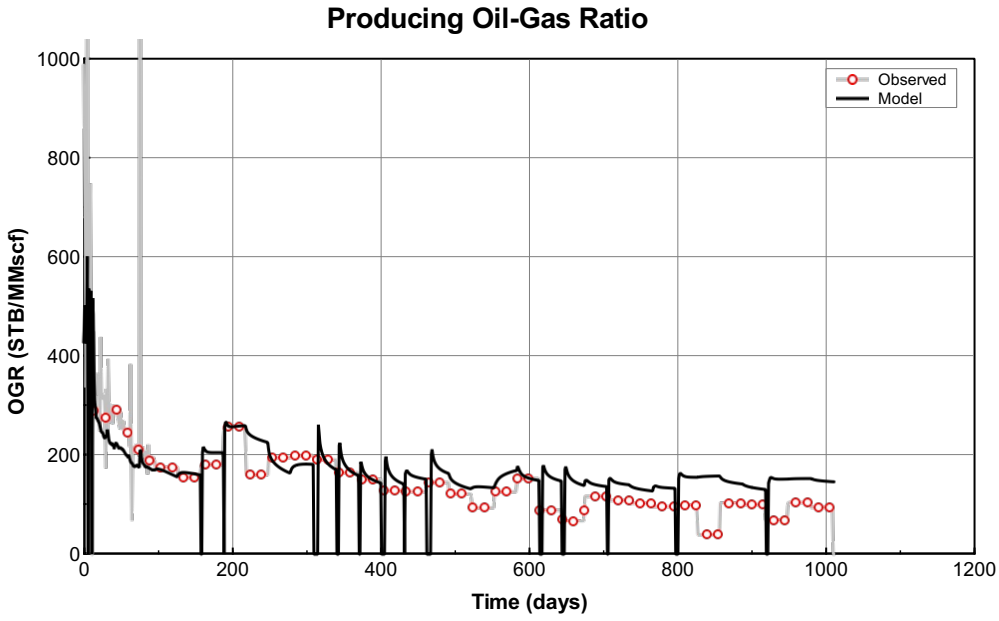

Figure 79: Calculated Producing Oil-Gas Ratio for the best history match with $n_{og} = 4.5$.

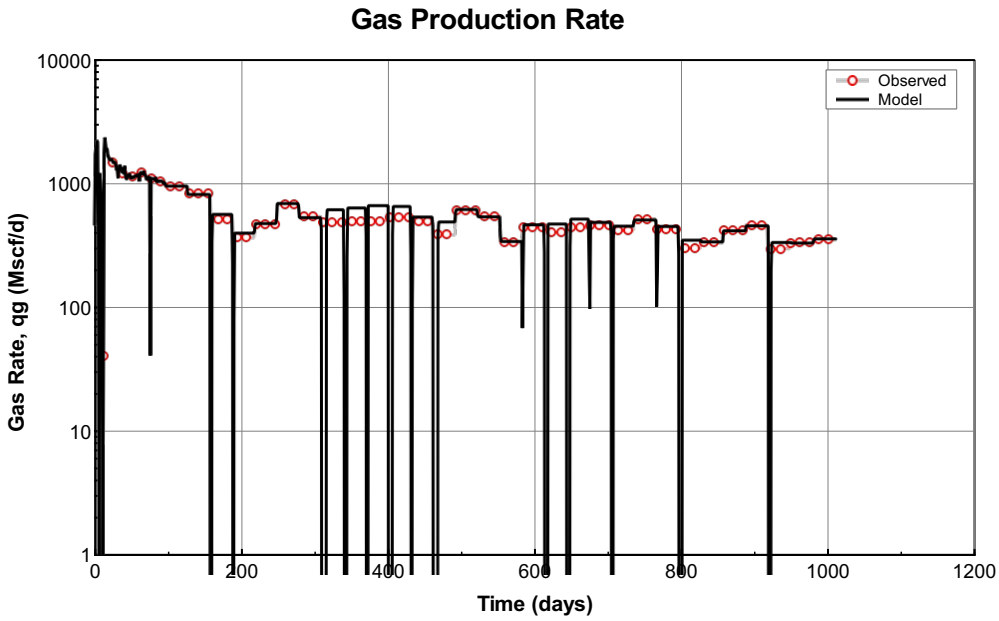

Figure 80: Measured Gas Rates. Well is run on gas rate control throughout the history match, $n_{og} = 5.5$.

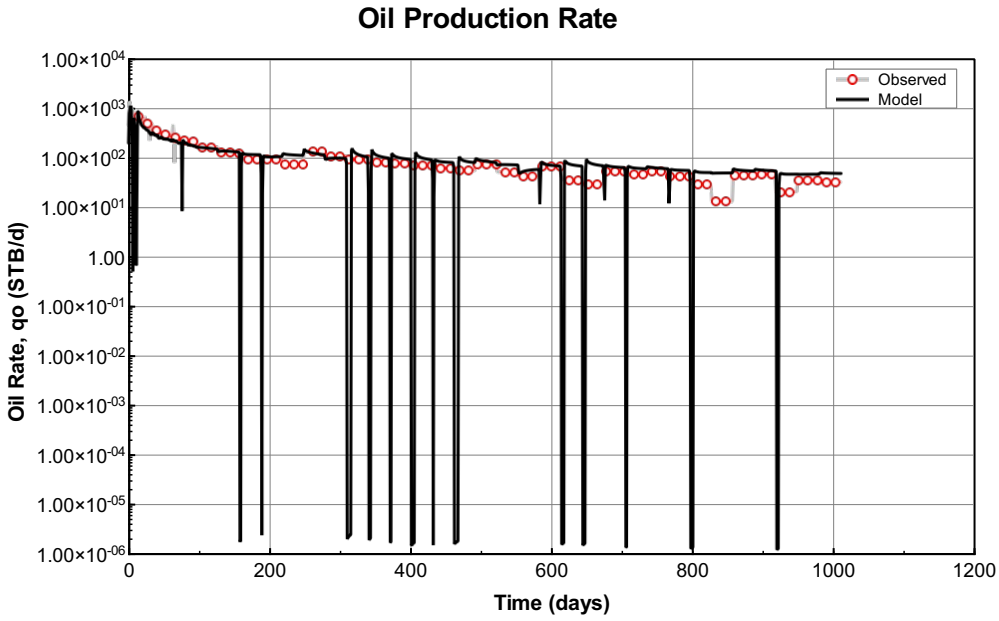

Figure 81: Calculated Oil Production Rates for the best history match with $n_{og} = 5.5$.

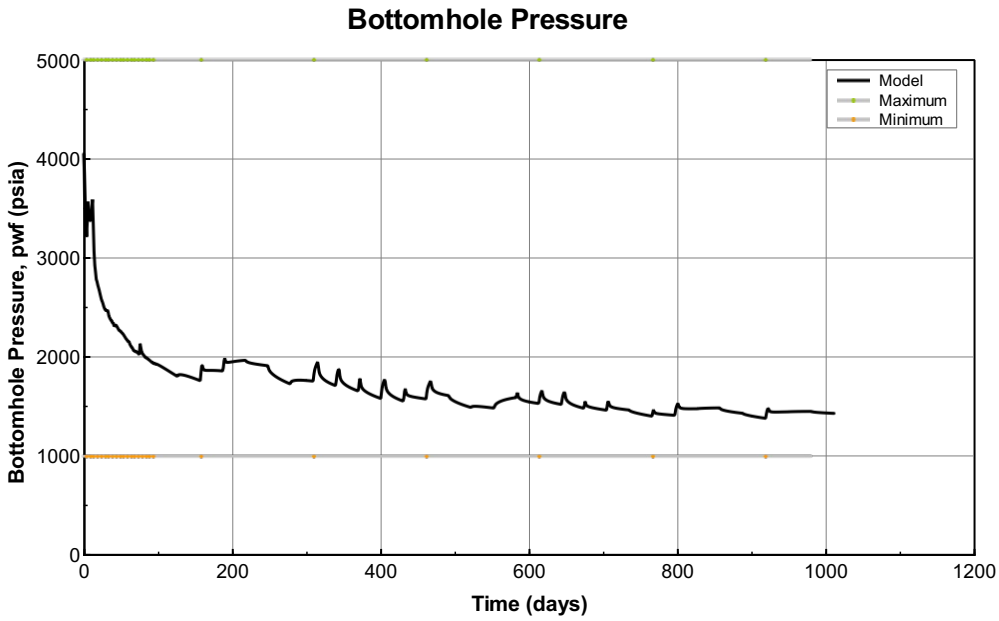

Figure 82: Calculated Flowing Bottomhole pressures for the best history match with n_{og} = 5.5.

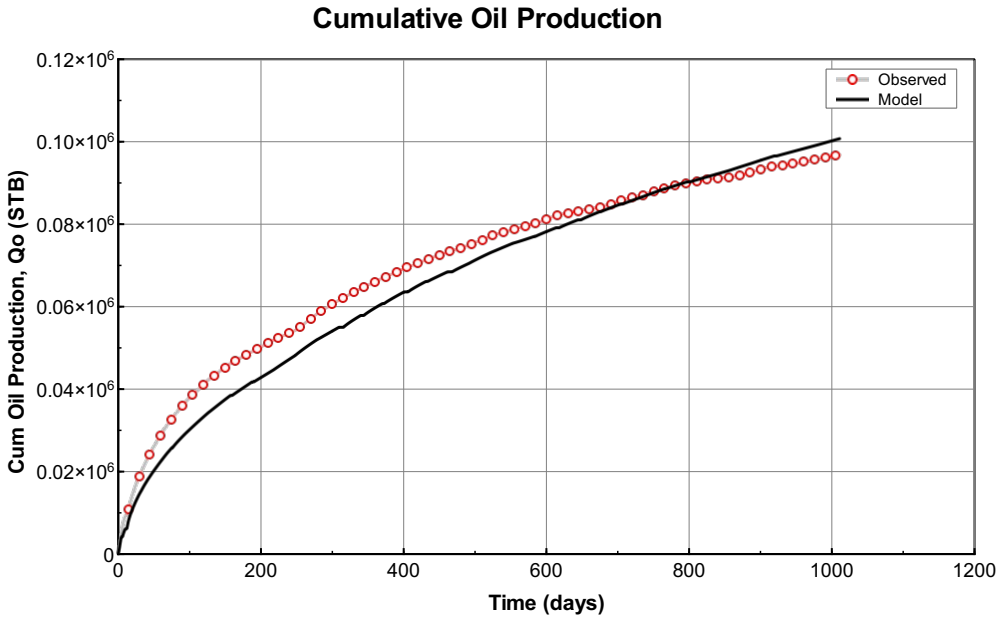

Figure 83: Calculated Cumulative Oil Production for the best history match with n_{og} = 5.5.

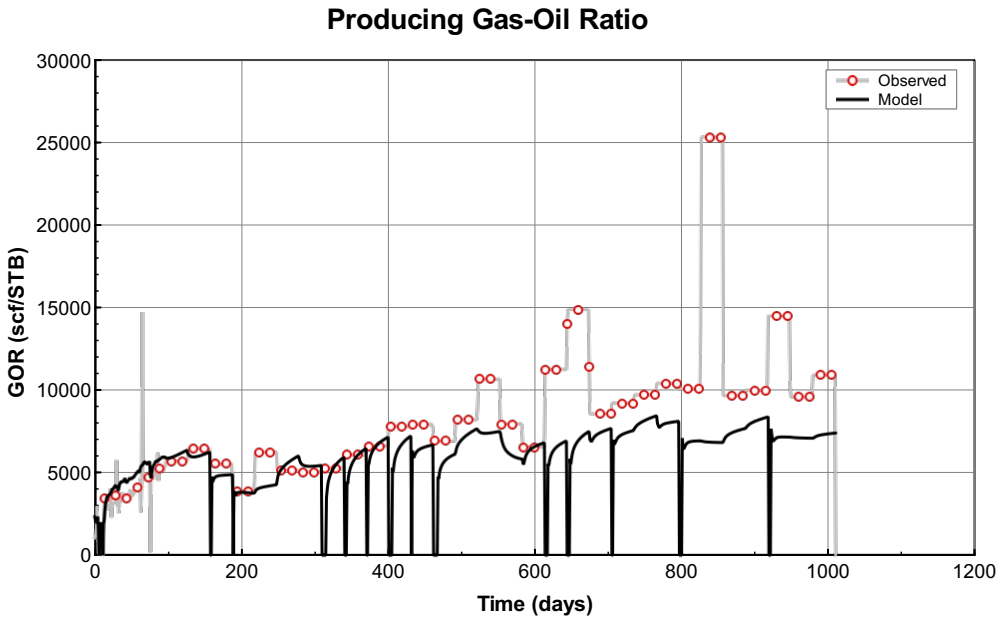

Figure 84: Calculated Producing Gas-Oil Ratio for the best history match with $n_{og} = 5.5$.

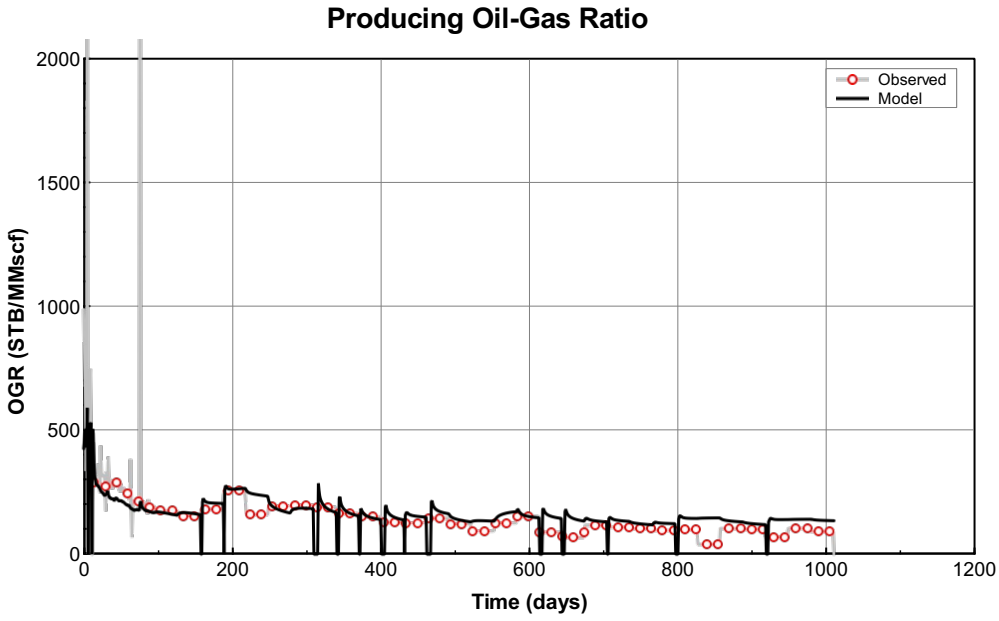

Figure 85: Calculated Producing Oil-Gas Ratio for the best history match with $n_{og} = 5.5$.

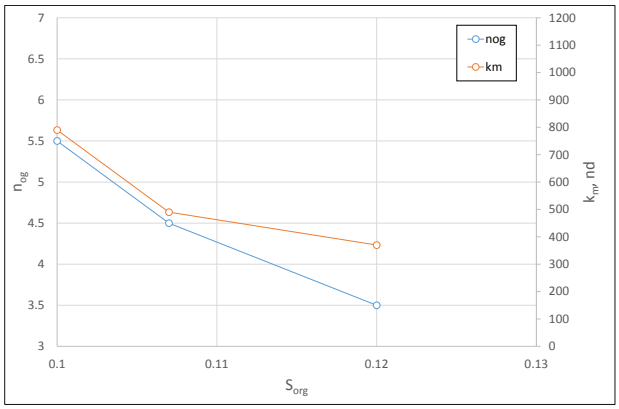

Figure 86: Plot of k_m and n_{og} versus S_{org}. Each point depicts the history match with the respective relative permeability model. Each point depicts similarly good history-match of the well.

Table 9: Matrix Permeability and Residual Oil Saturation to gas values for the best History Matches with three Relative Permeability exponents.

	$n_{og} = 3.5$	$n_{og} = 4.5$	$n_{og} = 5.5$
k_m	372 nd	490 nd	790 nd
S_{org}	0.12	0.107	0.10

Production Forecast of the three best History Matches

The results of the production forecasts of this well were similar to the RHW8 well. Below is the result of the production forecast for the three different models, all producing at a constant FBHP = 1000 psia from the end of the History Match. The big difference in cumulative oil production for the n_{og} = 5.5 case compared to the two others is explained with the FBHP at the end of the history match. A bigger difference in FBHP yield a higher spike in the producing GOR.

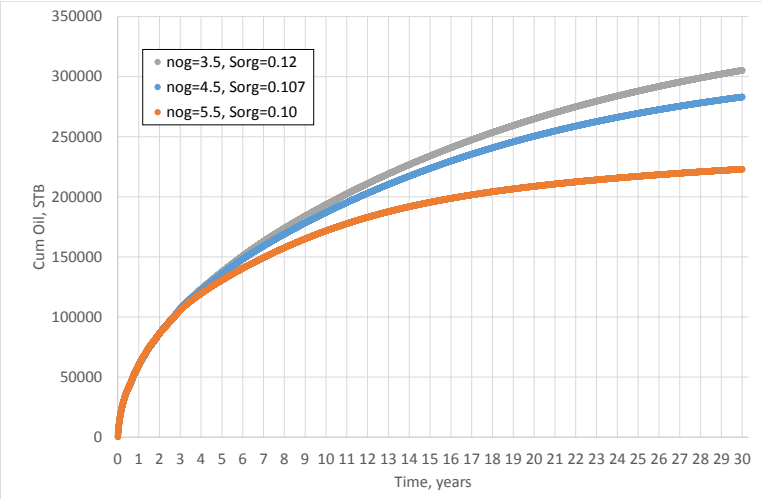

Figure 87: Cumulative Oil Production Forecast, 30 years - P_{wf} = 1000$psia$ after end of History Match. The three lines represents the three relative permeability models.

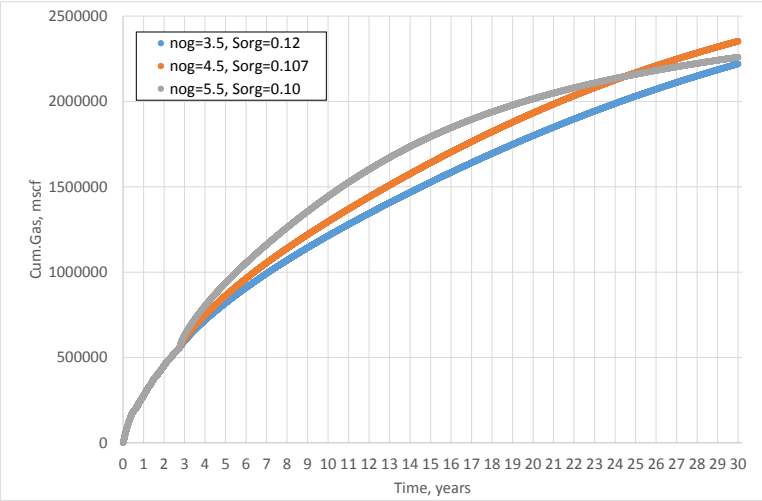

Figure 88: Cumulative Gas Production Forecast, 30 years - $P_{wf} = 1000 psia$ after end of history match. The three lines represents the three relative permeability models.

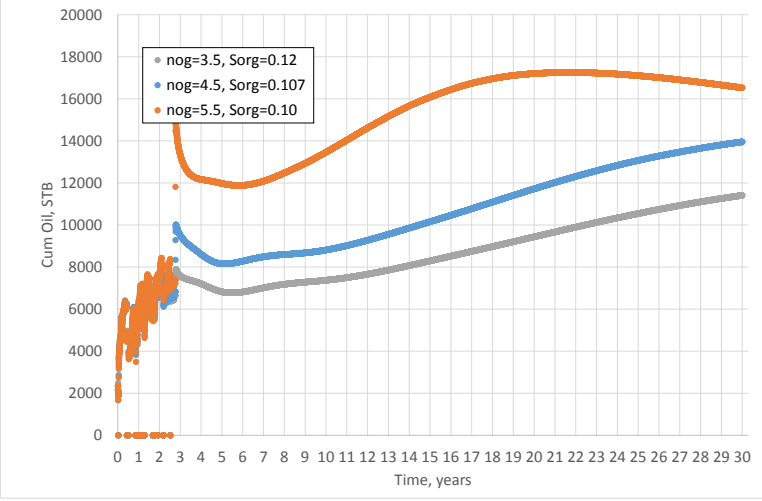

Figure 89: Producing GOR for the 30 year forecast - $P_{wf} = 1000 psia$ after end of History Match. The three lines represents the three relative permeability models.

Appendix B: Unit Conversion

Table 10: Unit Conversion Table.

	Field			SI	
Pressure	1	psia	=	6895	Pa
Flow Rate	1	Mscf/d	=	3.277E-04	m^3/d
Flow Rate	1	STB/d	=	1.80E-06	m^3/d
Length	1	ft	=	0.3048	m
Mass	1	lb	=	0.4536	kg
Temperature	1	R	=	5/9	K

Appendix C: SENSOR Data-File

```
TITLE
Black-oil run
 Liquid-Rich Shale well performance.
 Bone Spring formation - Lea County, New Mexico - RHW8 Well
ENDTITLE
GRID 69 49 1
PCMULT2 1. 0.
RUN
CPU
IMPLICIT
MAPSPRINT 1 P SG !SO SW KX
MAPSFILE P SG !SW SO SG
C    Bwi cw     denw  visw  cr      pref
MISC 1   3.0E-6 62.4  0.5   4.0E-6  6000
C ----------------------------------------------------------------------------------------
C Including grid definition created by SensorGrid
C ----------------------------------------------------------------------------------------
C I_CELLS          69
C J_CELLS          49
C K_CELLS          1
C DEPTH            8932
C GRID             PLANAR
C FRAC_AREA        80000
C ----------------------------------------------------------------------------------------
C Cell width along wellbore
C ----------------------------------------------------------------------------------------
DELX XVAR
20.7525 16.5 13.119 10.4307 8.29336 6.59395 5.24277 4.16846 3.31429 2.63515 2.09518
1.66585 1.3245 1.05309 0.8373 0.665727 0.529312 0.420849 0.334612 0.266046 0.21153
0.168185 0.133722 0.10632 0.0845341 0.067212 0.0534395 0.0424891 0.0337825 0.0268601
0.0213561 0.01698 0.0135006 0.0107342 0.0833 0.0107342 0.0135006 0.01698 0.0213561
0.0268601 0.0337825 0.0424891 0.0534395 0.067212 0.0845341 0.10632 0.133722 0.168185
0.21153 0.266046 0.334612 0.420849 0.5293120.665727 0.8373 1.05309 1.3245 1.66585
2.09518 2.63515 3.31429 4.16846 5.24277 6.59395 8.29336 10.4307 13.119 16.5 20.7525
C ----------------------------------------------------------------------------------------
C Cell width away from wellbore
C ----------------------------------------------------------------------------------------
DELY YVAR
40 40 40 40 40 40 40 40 40 40 0.0205973 0.0256903 0.0320427 0.0399657 0.0498479 0.0621737
0.0775471 0.0967219 0.120638 0.150468 0.187673 0.234079 0.291958 0.36415 0.454192
0.566499 0.706575 0.881287 1.0992 1.37099 1.71 2.13282 2.6602 3.31797 4.13845.16168 6.43799
8.02989 10.0154 12.4919 15.5807 19.4333 24.2385 30.2319 37.7072 47.0309 58.6601 73.1648 91.256
C----------------------------------------------------------------------------------------
C Porosity
C ----------------------------------------------------------------------------------------
POROS CON
 0.05
MOD
35 35 1 10 1 1 = 0.0343958
C ----------------------------------------------------------------------------------------
C Rocktype (for relperm curves)
C ----------------------------------------------------------------------------------------
ROCKTYPE CON
 1
MOD
35 35 1 10 1 1 = 2
C ----------------------------------------------------------------------------------------
C Assigning TMODTABLES (for stress dependent perm)
C ----------------------------------------------------------------------------------------
TMODTYPE CON
 1
MOD
35 35 1 10 1 1 = 2
C ----------------------------------------------------------------------------------------
C Permeability
C ----------------------------------------------------------------------------------------
KX CON
 0.00055
MOD
```

```
35 35 1 10 1 1 = 12004.8
KY EQUALS KX
KZ EQUALS KX
C -------------------------------------------------------------------------------------------
C Depth
C -------------------------------------------------------------------------------------------
DEPTH CON
 8932
C -------------------------------------------------------------------------------------------
C Thickness
C -------------------------------------------------------------------------------------------
THICKNESS CON
 200
C -------------------------------------------------------------------------------------------
C Relperm
C -------------------------------------------------------------------------------------------
KRANALYTICAL 1    ! For matrix
 0.15 0.1 0.154880676269531 0.1 ! Swc Sorw Sorg Sgc
 1 1 1            ! krw(Sorw) krg(Swc) kro(Swc)
 2.5 2.5 2 3.5  ! nw now ng nog
C 0 3480 20  PCWO        ! a1 a2 a3
C 0 3480 20 0 0  PCWOI  ! b1 b2 b3 b4 b5
 -0.941176470588235 10 1. PCGO
 KRANALYTICAL 2   ! For fractures
 0.20 0.1 0.2 0.1 ! Swc Sorw Sorg Sgc
 1 1 1            ! krw(Sorw) krg(Swc) kro(Swc)
 1 1 1 1
C 0 3480 20  PCWO        ! a1 a2 a3
C 0 3480 20 3480 2  PCWOI  ! b1 b2 b3 b4 b5
 -0.941176470588235 10 1. PCGO   ! pcgo_frac
SWINIT CON
 0.3
C -------------------------------------------------------------------------------------------
C Dry Gas Black-Oil Table
C -------------------------------------------------------------------------------------------
PVTBO
C         deno   deng  coil  cvoil
DENSITY   0.7876 0.8931   0      0
PRESSURES 27 30
14.7 200.0 400.0 600.0 800.0 1000.0 1200.0 1400.0 1600.0 1800.0 2000.0 2200.0 2400.0 2600.0 2800.0
2954.2 3200.2 3400.3 3600.2 3800.8 4000.3 4400.1 4800.9 5200.2 5600.2 6000.0 6083.2 8000.0 9000.0 10000.0
C   psia  rb/stb scf/stb     cp   stb/mmcf   rb/scf    cp   dyne/cm
    PSAT    BO      RS      VISO      SRS      BG     VISG    IFT
    14.7  1.0301     0.0   1.133   99.6149 0.224812  0.0110 17.7746
   200.0  1.0913    90.7   0.635    6.3822 0.014466  0.0120 14.3230
   400.0  1.1707   222.1   0.520    0.8819 0.006978  0.0125 12.1867
   600.0  1.2352   336.6   0.450    0.3235 0.004528  0.0129 10.4122
   800.0  1.2872   436.0   0.398    0.3019 0.003314  0.0133  8.8637
  1000.0  1.3355   531.8   0.357    0.4311 0.002592  0.0138  7.4928
  1200.0  1.3817   626.0   0.324    0.7048 0.002116  0.0144  6.2764
  1400.0  1.4270   720.0   0.296    1.1744 0.001781  0.0151  5.2016
  1600.0  1.4721   815.0   0.272    1.9112 0.001533  0.0160  4.2593
  1800.0  1.5175   911.7   0.252    2.9953 0.001345  0.0169  3.4422
  2000.0  1.5637  1010.9   0.234    4.5072 0.001198  0.0181  2.7426
  2200.0  1.6110  1113.3   0.218    6.5222 0.001082  0.0193  2.1525
  2400.0  1.6599  1219.6   0.204    9.1060 0.000989  0.0208  1.6624
  2600.0  1.7108  1330.7   0.192   12.3151 0.000914  0.0224  1.2620
  2800.0  1.7644  1447.7   0.180   16.1996 0.000853  0.0241  0.9403
  2954.2  1.8078  1542.8   0.172   19.6875 0.000813  0.0255  0.7391
  3200.2  1.8810  1703.3   0.160   26.1561 0.000762  0.0279  0.4905
  3400.3  1.9438  1841.8   0.151   32.2365 0.000729  0.0299  0.3429
  3600.2  2.0098  1987.9   0.143   39.0346 0.000703  0.0321  0.2344
  3800.8  2.0795  2143.0   0.136   46.5796 0.000682  0.0344  0.1559
  4000.3  2.1527  2306.4   0.130   54.7795 0.000665  0.0368  0.1010
  4400.1  2.3127  2665.8   0.119   73.2531 0.000643  0.0421  0.0381
  4800.9  2.4954  3078.5   0.109   94.4691 0.000633  0.0482  0.0118
  5200.2  2.7068  3558.4   0.101  118.3900 0.000631  0.0556  0.0026
  5600.2  2.9607  4135.6   0.093  145.5998 0.000637  0.0649  0.0003
  6000.0  3.2793  4858.7   0.087  177.1144 0.000651  0.0774  0.0000
  6083.2  3.3575  5035.5   0.085  198.5893 0.000667  0.0852  0.0000
C   psia   psia   rb/stb    cp     rb/scf     cp
    PSAT     P      BO     VISO      BG      VISG
```

14.7	14.7	1.0301	1.133	0.224812	0.0110
	200.0	1.0278	1.162	0.000000	0.0000
	400.0	1.0254	1.193	0.000000	0.0000
	600.0	1.0231	1.223	0.000000	0.0000
	800.0	1.0210	1.254	0.000000	0.0000
	1000.0	1.0189	1.284	0.000000	0.0000
	1200.0	1.0168	1.314	0.000000	0.0000
	1400.0	1.0149	1.344	0.000000	0.0000
	1600.0	1.0130	1.374	0.000000	0.0000
	1800.0	1.0112	1.403	0.000000	0.0000
	2000.0	1.0094	1.433	0.000000	0.0000
	2200.0	1.0077	1.462	0.000000	0.0000
	2400.0	1.0061	1.490	0.000000	0.0000
	2600.0	1.0045	1.519	0.000000	0.0000
	2800.0	1.0029	1.547	0.000000	0.0000
	2954.2	1.0018	1.569	0.000000	0.0000
	3200.2	1.0000	1.603	0.000000	0.0000
	3400.3	0.9986	1.631	0.000000	0.0000
	3600.2	0.9972	1.658	0.000000	0.0000
	3800.8	0.9959	1.686	0.000000	0.0000
	4000.3	0.9946	1.713	0.000000	0.0000
	4400.1	0.9921	1.766	0.000000	0.0000
	4800.9	0.9897	1.819	0.000000	0.0000
	5200.2	0.9875	1.870	0.000000	0.0000
	5600.2	0.9854	1.921	0.000000	0.0000
	6000.0	0.9833	1.971	0.000000	0.0000
	6083.2	0.9829	1.981	0.000000	0.0000
	8000.0	0.9745	2.209	0.000000	0.0000
	9000.0	0.9708	2.321	0.000000	0.0000
	10000.0	0.9674	2.429	0.000000	0.0000
200.0	200.0	1.0913	0.635	0.014466	0.0120
	14.7	0.0000	0.000	0.204619	0.0118
	400.0	1.0877	0.656	0.000000	0.0000
	600.0	1.0843	0.677	0.000000	0.0000
	800.0	1.0810	0.697	0.000000	0.0000
	1000.0	1.0779	0.718	0.000000	0.0000
	1200.0	1.0748	0.739	0.000000	0.0000
	1400.0	1.0720	0.759	0.000000	0.0000
	1600.0	1.0692	0.779	0.000000	0.0000
	1800.0	1.0665	0.800	0.000000	0.0000
	2000.0	1.0640	0.820	0.000000	0.0000
	2200.0	1.0615	0.840	0.000000	0.0000
	2400.0	1.0591	0.860	0.000000	0.0000
	2600.0	1.0568	0.880	0.000000	0.0000
	2800.0	1.0546	0.900	0.000000	0.0000
	2954.2	1.0529	0.915	0.000000	0.0000
	3200.2	1.0503	0.939	0.000000	0.0000
	3400.3	1.0483	0.959	0.000000	0.0000
	3600.2	1.0463	0.978	0.000000	0.0000
	3800.8	1.0444	0.998	0.000000	0.0000
	4000.3	1.0426	1.017	0.000000	0.0000
	4400.1	1.0391	1.056	0.000000	0.0000
	4800.9	1.0358	1.094	0.000000	0.0000
	5200.2	1.0326	1.131	0.000000	0.0000
	5600.2	1.0296	1.169	0.000000	0.0000
	6000.0	1.0268	1.206	0.000000	0.0000
	6083.2	1.0262	1.213	0.000000	0.0000
	8000.0	1.0145	1.385	0.000000	0.0000
	9000.0	1.0093	1.470	0.000000	0.0000
	10000.0	1.0046	1.554	0.000000	0.0000
400.0	400.0	1.1707	0.520	0.006978	0.0125
	14.7	0.0000	0.000	0.203470	0.0121
	200.0	0.0000	0.000	0.014471	0.0122
	600.0	1.1664	0.538	0.000000	0.0000
	800.0	1.1622	0.556	0.000000	0.0000
	1000.0	1.1583	0.574	0.000000	0.0000
	1200.0	1.1545	0.592	0.000000	0.0000
	1400.0	1.1509	0.610	0.000000	0.0000
	1600.0	1.1474	0.627	0.000000	0.0000
	1800.0	1.1441	0.645	0.000000	0.0000
	2000.0	1.1409	0.663	0.000000	0.0000
	2200.0	1.1378	0.681	0.000000	0.0000

```
        2400.0  1.1349   0.699 0.000000  0.0000
        2600.0  1.1320   0.716 0.000000  0.0000
        2800.0  1.1293   0.734 0.000000  0.0000
        2954.2  1.1272   0.747 0.000000  0.0000
        3200.2  1.1241   0.769 0.000000  0.0000
        3400.3  1.1216   0.786 0.000000  0.0000
        3600.2  1.1192   0.804 0.000000  0.0000
        3800.8  1.1169   0.821 0.000000  0.0000
        4000.3  1.1146   0.839 0.000000  0.0000
        4400.1  1.1103   0.873 0.000000  0.0000
        4800.9  1.1063   0.907 0.000000  0.0000
        5200.2  1.1025   0.941 0.000000  0.0000
        5600.2  1.0989   0.975 0.000000  0.0000
        6000.0  1.0954   1.009 0.000000  0.0000
        6083.2  1.0947   1.016 0.000000  0.0000
        8000.0  1.0806   1.172 0.000000  0.0000
        9000.0  1.0744   1.251 0.000000  0.0000
       10000.0  1.0688   1.329 0.000000  0.0000
600.0   600.0  1.2352   0.450 0.004528  0.0129
         14.7  0.0000   0.000 0.203393  0.0121
        200.0  0.0000   0.000 0.014506  0.0123
        400.0  0.0000   0.000 0.007018  0.0126
        800.0  1.2302   0.466 0.000000  0.0000
       1000.0  1.2255   0.482 0.000000  0.0000
       1200.0  1.2210   0.498 0.000000  0.0000
       1400.0  1.2166   0.514 0.000000  0.0000
       1600.0  1.2125   0.530 0.000000  0.0000
       1800.0  1.2086   0.546 0.000000  0.0000
       2000.0  1.2048   0.562 0.000000  0.0000
       2200.0  1.2012   0.578 0.000000  0.0000
       2400.0  1.1977   0.594 0.000000  0.0000
       2600.0  1.1943   0.610 0.000000  0.0000
       2800.0  1.1911   0.626 0.000000  0.0000
       2954.2  1.1887   0.638 0.000000  0.0000
       3200.2  1.1850   0.658 0.000000  0.0000
       3400.3  1.1821   0.674 0.000000  0.0000
       3600.2  1.1793   0.689 0.000000  0.0000
       3800.8  1.1766   0.705 0.000000  0.0000
       4000.3  1.1740   0.721 0.000000  0.0000
       4400.1  1.1690   0.753 0.000000  0.0000
       4800.9  1.1642   0.784 0.000000  0.0000
       5200.2  1.1598   0.815 0.000000  0.0000
       5600.2  1.1556   0.847 0.000000  0.0000
       6000.0  1.1517   0.877 0.000000  0.0000
       6083.2  1.1509   0.884 0.000000  0.0000
       8000.0  1.1346   1.029 0.000000  0.0000
       9000.0  1.1275   1.103 0.000000  0.0000
      10000.0  1.1211   1.176 0.000000  0.0000
800.0   800.0  1.2872   0.398 0.003314  0.0133
         14.7  0.0000   0.000 0.203411  0.0122
        200.0  0.0000   0.000 0.014529  0.0124
        400.0  0.0000   0.000 0.007043  0.0126
        600.0  0.0000   0.000 0.004553  0.0129
       1000.0  1.2817   0.412 0.002577  0.0139
       1200.0  1.2764   0.427 0.002092  0.0145
       1400.0  1.2714   0.441 0.001753  0.0153
       1600.0  1.2666   0.456 0.001506  0.0162
       1800.0  1.2620   0.471 0.001320  0.0172
       2000.0  1.2577   0.485 0.001178  0.0183
       2200.0  1.2535   0.500 0.001067  0.0195
       2400.0  1.2495   0.514 0.000980  0.0208
       2600.0  1.2456   0.529 0.000909  0.0220
       2800.0  1.2419   0.543 0.000851  0.0233
       2954.2  1.2392   0.555 0.000814  0.0242
       3200.2  1.2349   0.573 0.000764  0.0257
       3400.3  1.2316   0.587 0.000730  0.0269
       3600.2  1.2284   0.602 0.000701  0.0280
       3800.8  1.2253   0.616 0.000675  0.0291
       4000.3  1.2224   0.631 0.000653  0.0301
       4400.1  1.2167   0.660 0.000616  0.0321
       4800.9  1.2114   0.689 0.000587  0.0340
       5200.2  1.2064   0.718 0.000562  0.0358
```

```
         5600.2  1.2016   0.746 0.000542  0.0375
         6000.0  1.1972   0.775 0.000525  0.0392
         6083.2  1.1963   0.781 0.000521  0.0396
         8000.0  1.1780   0.916 0.000465  0.0471
         9000.0  1.1700   0.986 0.000445  0.0509
        10000.0  1.1628   1.054 0.000429  0.0548
1000.0   1000.0  1.3355   0.357 0.002592  0.0138
         1200.0  1.3294   0.371 0.002107  0.0145
         1400.0  1.3237   0.384 0.001768  0.0152
         1600.0  1.3182   0.397 0.001520  0.0161
         1800.0  1.3130   0.410 0.001333  0.0171
         2000.0  1.3080   0.423 0.001190  0.0181
         2200.0  1.3032   0.437 0.001078  0.0193
         2400.0  1.2987   0.450 0.000989  0.0205
         2600.0  1.2943   0.463 0.000918  0.0217
         2800.0  1.2901   0.477 0.000859  0.0229
         2954.2  1.2870   0.487 0.000821  0.0238
         3200.2  1.2822   0.503 0.000770  0.0253
         3400.3  1.2785   0.517 0.000735  0.0264
         3600.2  1.2749   0.530 0.000705  0.0275
         3800.8  1.2714   0.544 0.000680  0.0286
         4000.3  1.2681   0.557 0.000657  0.0296
         4400.1  1.2617   0.584 0.000619  0.0316
         4800.9  1.2557   0.611 0.000589  0.0335
         5200.2  1.2501   0.637 0.000564  0.0352
         5600.2  1.2448   0.664 0.000543  0.0369
         6000.0  1.2399   0.690 0.000526  0.0386
         6083.2  1.2388   0.696 0.000522  0.0389
         8000.0  1.2186   0.822 0.000465  0.0463
         9000.0  1.2097   0.887 0.000445  0.0501
        10000.0  1.2018   0.951 0.000429  0.0538
1200.0   1200.0  1.3817   0.324 0.002116  0.0144
         1400.0  1.3752   0.336 0.001776  0.0152
         1600.0  1.3689   0.348 0.001528  0.0160
         1800.0  1.3630   0.360 0.001341  0.0170
         2000.0  1.3574   0.372 0.001197  0.0180
         2200.0  1.3520   0.385 0.001085  0.0192
         2400.0  1.3469   0.397 0.000995  0.0203
         2600.0  1.3419   0.409 0.000923  0.0215
         2800.0  1.3372   0.421 0.000864  0.0227
         2954.2  1.3337   0.431 0.000825  0.0236
         3200.2  1.3284   0.446 0.000774  0.0250
         3400.3  1.3242   0.458 0.000739  0.0261
         3600.2  1.3202   0.470 0.000709  0.0272
         3800.8  1.3163   0.483 0.000682  0.0283
         4000.3  1.3125   0.495 0.000660  0.0293
         4400.1  1.3055   0.520 0.000621  0.0313
         4800.9  1.2988   0.544 0.000591  0.0331
         5200.2  1.2926   0.569 0.000566  0.0349
         5600.2  1.2867   0.594 0.000545  0.0366
         6000.0  1.2812   0.619 0.000527  0.0382
         6083.2  1.2801   0.624 0.000523  0.0385
         8000.0  1.2578   0.741 0.000465  0.0458
         9000.0  1.2480   0.802 0.000445  0.0495
        10000.0  1.2394   0.862 0.000429  0.0533
1400.0   1400.0  1.4270   0.296 0.001781  0.0151
         1600.0  1.4200   0.307 0.001532  0.0160
         1800.0  1.4133   0.318 0.001345  0.0169
         2000.0  1.4069   0.329 0.001201  0.0180
         2200.0  1.4009   0.341 0.001088  0.0191
         2400.0  1.3951   0.352 0.000998  0.0202
         2600.0  1.3896   0.363 0.000926  0.0214
         2800.0  1.3843   0.374 0.000867  0.0226
         2954.2  1.3804   0.383 0.000828  0.0235
         3200.2  1.3744   0.397 0.000776  0.0249
         3400.3  1.3698   0.408 0.000741  0.0260
         3600.2  1.3653   0.419 0.000710  0.0271
         3800.8  1.3610   0.431 0.000684  0.0282
         4000.3  1.3568   0.442 0.000661  0.0292
         4400.1  1.3490   0.465 0.000623  0.0311
         4800.9  1.3416   0.488 0.000592  0.0330
         5200.2  1.3348   0.510 0.000567  0.0347
```

```
         5600.2  1.3283   0.533 0.000546  0.0364
         6000.0  1.3223   0.556 0.000528  0.0380
         6083.2  1.3211   0.561 0.000524  0.0383
         8000.0  1.2965   0.671 0.000466  0.0456
         9000.0  1.2859   0.728 0.000446  0.0493
        10000.0  1.2764   0.784 0.000429  0.0530
1600.0   1600.0  1.4721   0.272 0.001533  0.0160
         1800.0  1.4646   0.283 0.001346  0.0169
         2000.0  1.4574   0.293 0.001202  0.0180
         2200.0  1.4507   0.303 0.001089  0.0191
         2400.0  1.4442   0.313 0.000999  0.0202
         2600.0  1.4380   0.323 0.000927  0.0214
         2800.0  1.4322   0.334 0.000868  0.0226
         2954.2  1.4278   0.342 0.000829  0.0235
         3200.2  1.4212   0.354 0.000777  0.0249
         3400.3  1.4160   0.365 0.000742  0.0260
         3600.2  1.4110   0.375 0.000712  0.0271
         3800.8  1.4063   0.386 0.000685  0.0281
         4000.3  1.4017   0.396 0.000662  0.0292
         4400.1  1.3930   0.417 0.000624  0.0311
         4800.9  1.3849   0.438 0.000593  0.0329
         5200.2  1.3774   0.460 0.000568  0.0347
         5600.2  1.3703   0.481 0.000547  0.0364
         6000.0  1.3637   0.502 0.000529  0.0380
         6083.2  1.3623   0.507 0.000525  0.0383
         8000.0  1.3355   0.609 0.000467  0.0456
         9000.0  1.3240   0.662 0.000447  0.0492
        10000.0  1.3137   0.715 0.000430  0.0529
1800.0   1800.0  1.5175   0.252 0.001345  0.0169
         2000.0  1.5095   0.261 0.001201  0.0180
         2200.0  1.5019   0.271 0.001088  0.0191
         2400.0  1.4947   0.280 0.000999  0.0203
         2600.0  1.4878   0.289 0.000927  0.0215
         2800.0  1.4813   0.299 0.000867  0.0226
         2954.2  1.4765   0.306 0.000829  0.0236
         3200.2  1.4691   0.318 0.000777  0.0250
         3400.3  1.4634   0.328 0.000742  0.0261
         3600.2  1.4579   0.337 0.000712  0.0272
         3800.8  1.4526   0.347 0.000686  0.0282
         4000.3  1.4476   0.356 0.000663  0.0292
         4400.1  1.4380   0.376 0.000625  0.0312
         4800.9  1.4291   0.395 0.000594  0.0330
         5200.2  1.4209   0.415 0.000569  0.0348
         5600.2  1.4131   0.435 0.000547  0.0364
         6000.0  1.4058   0.454 0.000529  0.0381
         6083.2  1.4044   0.459 0.000526  0.0384
         8000.0  1.3752   0.554 0.000468  0.0457
         9000.0  1.3627   0.604 0.000448  0.0494
        10000.0  1.3515   0.654 0.000431  0.0531
2000.0   2000.0  1.5637   0.234 0.001198  0.0181
         2200.0  1.5552   0.243 0.001086  0.0192
         2400.0  1.5472   0.251 0.000997  0.0204
         2600.0  1.5395   0.260 0.000925  0.0216
         2800.0  1.5322   0.269 0.000866  0.0228
         2954.2  1.5269   0.275 0.000828  0.0237
         3200.2  1.5187   0.286 0.000776  0.0251
         3400.3  1.5124   0.295 0.000742  0.0262
         3600.2  1.5063   0.304 0.000712  0.0273
         3800.8  1.5005   0.313 0.000686  0.0284
         4000.3  1.4950   0.322 0.000663  0.0294
         4400.1  1.4845   0.340 0.000625  0.0314
         4800.9  1.4747   0.358 0.000594  0.0332
         5200.2  1.4657   0.376 0.000569  0.0350
         5600.2  1.4572   0.394 0.000548  0.0367
         6000.0  1.4493   0.412 0.000531  0.0383
         6083.2  1.4477   0.416 0.000527  0.0386
         8000.0  1.4160   0.505 0.000469  0.0459
         9000.0  1.4024   0.552 0.000449  0.0497
        10000.0  1.3903   0.598 0.000433  0.0534
2200.0   2200.0  1.6110   0.218 0.001082  0.0193
         2400.0  1.6020   0.226 0.000993  0.0206
         2600.0  1.5935   0.234 0.000922  0.0218
```

```
         2800.0  1.5855   0.242 0.000864  0.0230
         2954.2  1.5795   0.248 0.000826  0.0239
         3200.2  1.5705   0.258 0.000775  0.0254
         3400.3  1.5635   0.266 0.000741  0.0265
         3600.2  1.5568   0.275 0.000711  0.0276
         3800.8  1.5504   0.283 0.000685  0.0287
         4000.3  1.5443   0.291 0.000663  0.0297
         4400.1  1.5328   0.308 0.000625  0.0317
         4800.9  1.5221   0.324 0.000595  0.0335
         5200.2  1.5122   0.341 0.000570  0.0353
         5600.2  1.5030   0.358 0.000550  0.0370
         6000.0  1.4943   0.375 0.000532  0.0386
         6083.2  1.4926   0.379 0.000528  0.0390
         8000.0  1.4582   0.461 0.000471  0.0463
         9000.0  1.4435   0.505 0.000451  0.0501
        10000.0  1.4305   0.549 0.000435  0.0539
2400.0   2400.0  1.6599   0.204 0.000989  0.0208
         2600.0  1.6504   0.211 0.000918  0.0220
         2800.0  1.6415   0.219 0.000861  0.0233
         2954.2  1.6349   0.225 0.000823  0.0242
         3200.2  1.6249   0.234 0.000773  0.0257
         3400.3  1.6172   0.241 0.000739  0.0268
         3600.2  1.6098   0.249 0.000710  0.0279
         3800.8  1.6028   0.256 0.000685  0.0290
         4000.3  1.5961   0.264 0.000663  0.0301
         4400.1  1.5834   0.279 0.000626  0.0321
         4800.9  1.5717   0.295 0.000596  0.0339
         5200.2  1.5609   0.310 0.000571  0.0357
         5600.2  1.5509   0.326 0.000551  0.0374
         6000.0  1.5415   0.342 0.000533  0.0391
         6083.2  1.5396   0.345 0.000530  0.0394
         8000.0  1.5023   0.422 0.000473  0.0469
         9000.0  1.4864   0.463 0.000453  0.0507
        10000.0  1.4723   0.503 0.000437  0.0545
2600.0   2600.0  1.7108   0.192 0.000914  0.0224
         2800.0  1.7009   0.198 0.000857  0.0236
         2954.2  1.6936   0.204 0.000820  0.0246
         3200.2  1.6825   0.212 0.000771  0.0261
         3400.3  1.6740   0.219 0.000738  0.0273
         3600.2  1.6659   0.226 0.000709  0.0284
         3800.8  1.6581   0.233 0.000684  0.0295
         4000.3  1.6508   0.240 0.000662  0.0305
         4400.1  1.6369   0.254 0.000626  0.0325
         4800.9  1.6241   0.268 0.000597  0.0344
         5200.2  1.6123   0.283 0.000573  0.0362
         5600.2  1.6013   0.297 0.000553  0.0380
         6000.0  1.5911   0.312 0.000535  0.0396
         6083.2  1.5891   0.315 0.000532  0.0400
         8000.0  1.5486   0.386 0.000476  0.0476
         9000.0  1.5314   0.424 0.000456  0.0515
        10000.0  1.5163   0.463 0.000440  0.0554
2800.0   2800.0  1.7644   0.180 0.000853  0.0241
         2954.2  1.7562   0.185 0.000816  0.0251
         3200.2  1.7440   0.193 0.000768  0.0266
         3400.3  1.7346   0.199 0.000736  0.0278
         3600.2  1.7257   0.205 0.000708  0.0289
         3800.8  1.7171   0.212 0.000683  0.0300
         4000.3  1.7090   0.218 0.000662  0.0311
         4400.1  1.6938   0.231 0.000627  0.0331
         4800.9  1.6798   0.244 0.000598  0.0350
         5200.2  1.6669   0.258 0.000574  0.0369
         5600.2  1.6549   0.271 0.000554  0.0386
         6000.0  1.6438   0.285 0.000537  0.0403
         6083.2  1.6415   0.288 0.000534  0.0407
         8000.0  1.5976   0.354 0.000479  0.0484
         9000.0  1.5791   0.389 0.000459  0.0524
        10000.0  1.5628   0.425 0.000444  0.0564
2954.2   2954.2  1.8078   0.172 0.000813  0.0255
         3200.2  1.7946   0.179 0.000766  0.0270
         3400.3  1.7844   0.185 0.000734  0.0282
         3600.2  1.7747   0.191 0.000707  0.0294
         3800.8  1.7655   0.197 0.000683  0.0305
```

	4000.3	1.7568	0.203	0.000662	0.0316
	4400.1	1.7404	0.215	0.000627	0.0337
	4800.9	1.7254	0.228	0.000599	0.0356
	5200.2	1.7115	0.240	0.000576	0.0374
	5600.2	1.6987	0.253	0.000556	0.0392
	6000.0	1.6868	0.266	0.000539	0.0410
	6083.2	1.6845	0.268	0.000536	0.0413
	8000.0	1.6377	0.331	0.000482	0.0492
	9000.0	1.6181	0.364	0.000462	0.0533
	10000.0	1.6008	0.398	0.000447	0.0574
3200.2	3200.2	1.8810	0.160	0.000762	0.0279
	3400.3	1.8694	0.165	0.000732	0.0291
	3600.2	1.8585	0.171	0.000705	0.0303
	3800.8	1.8481	0.176	0.000682	0.0314
	4000.3	1.8382	0.182	0.000662	0.0325
	4400.1	1.8198	0.193	0.000628	0.0346
	4800.9	1.8030	0.204	0.000601	0.0366
	5200.2	1.7876	0.215	0.000579	0.0385
	5600.2	1.7733	0.227	0.000560	0.0403
	6000.0	1.7600	0.238	0.000543	0.0421
	6083.2	1.7574	0.241	0.000540	0.0425
	8000.0	1.7057	0.298	0.000487	0.0506
	9000.0	1.6841	0.328	0.000468	0.0548
	10000.0	1.6651	0.359	0.000452	0.0591
3400.3	3400.3	1.9438	0.151	0.000729	0.0299
	3600.2	1.9317	0.156	0.000704	0.0311
	3800.8	1.9202	0.161	0.000682	0.0323
	4000.3	1.9093	0.166	0.000662	0.0334
	4400.1	1.8891	0.177	0.000630	0.0356
	4800.9	1.8706	0.187	0.000603	0.0376
	5200.2	1.8537	0.197	0.000581	0.0395
	5600.2	1.8381	0.208	0.000563	0.0414
	6000.0	1.8237	0.219	0.000547	0.0432
	6083.2	1.8208	0.221	0.000544	0.0436
	8000.0	1.7647	0.274	0.000491	0.0520
	9000.0	1.7413	0.302	0.000473	0.0563
	10000.0	1.7209	0.331	0.000458	0.0608
3600.2	3600.2	2.0098	0.143	0.000703	0.0321
	3800.8	1.9970	0.148	0.000682	0.0333
	4000.3	1.9851	0.153	0.000663	0.0344
	4400.1	1.9628	0.162	0.000631	0.0366
	4800.9	1.9425	0.172	0.000606	0.0387
	5200.2	1.9240	0.181	0.000585	0.0406
	5600.2	1.9069	0.191	0.000566	0.0426
	6000.0	1.8912	0.201	0.000551	0.0444
	6083.2	1.8881	0.203	0.000548	0.0448
	8000.0	1.8272	0.252	0.000497	0.0535
	9000.0	1.8019	0.279	0.000478	0.0580
	10000.0	1.7799	0.306	0.000463	0.0626
3800.8	3800.8	2.0795	0.136	0.000682	0.0344
	4000.3	2.0663	0.141	0.000664	0.0356
	4400.1	2.0417	0.149	0.000634	0.0378
	4800.9	2.0194	0.158	0.000609	0.0399
	5200.2	1.9991	0.167	0.000588	0.0419
	5600.2	1.9805	0.176	0.000571	0.0439
	6000.0	1.9633	0.185	0.000556	0.0458
	6083.2	1.9599	0.187	0.000553	0.0462
	8000.0	1.8938	0.233	0.000503	0.0552
	9000.0	1.8665	0.258	0.000485	0.0600
	10000.0	1.8427	0.283	0.000470	0.0648
4000.3	4000.3	2.1527	0.130	0.000665	0.0368
	4400.1	2.1256	0.138	0.000636	0.0391
	4800.9	2.1011	0.146	0.000612	0.0412
	5200.2	2.0789	0.155	0.000592	0.0433
	5600.2	2.0585	0.163	0.000576	0.0453
	6000.0	2.0398	0.171	0.000561	0.0473
	6083.2	2.0361	0.173	0.000558	0.0478
	8000.0	1.9643	0.216	0.000509	0.0572
	9000.0	1.9348	0.238	0.000491	0.0621
	10000.0	1.9091	0.262	0.000477	0.0671
4400.1	4400.1	2.3127	0.119	0.000643	0.0421
	4800.9	2.2831	0.126	0.000621	0.0444

```
          5200.2  2.2563   0.133 0.000603  0.0466
          5600.2  2.2319   0.140 0.000587  0.0488
          6000.0  2.2095   0.147 0.000573  0.0509
          6083.2  2.2051   0.149 0.000570  0.0514
          8000.0  2.1203   0.186 0.000524  0.0617
          9000.0  2.0857   0.205 0.000507  0.0672
         10000.0  2.0559   0.226 0.000493  0.0728
  4800.9  4800.9  2.4954   0.109 0.000633  0.0482
          5200.2  2.4630   0.115 0.000615  0.0506
          5600.2  2.4336   0.122 0.000601  0.0530
          6000.0  2.4068   0.128 0.000588  0.0554
          6083.2  2.4015   0.129 0.000585  0.0559
          8000.0  2.3009   0.161 0.000541  0.0674
          9000.0  2.2603   0.178 0.000525  0.0735
         10000.0  2.2254   0.196 0.000511  0.0798
  5200.2  5200.2  2.7068   0.101 0.000631  0.0556
          5600.2  2.6712   0.106 0.000617  0.0582
          6000.0  2.6389   0.112 0.000605  0.0609
          6083.2  2.6325   0.113 0.000603  0.0615
          8000.0  2.5125   0.140 0.000561  0.0745
          9000.0  2.4646   0.155 0.000545  0.0815
         10000.0  2.4236   0.171 0.000532  0.0887
  5600.2  5600.2  2.9607   0.093 0.000637  0.0649
          6000.0  2.9213   0.098 0.000626  0.0680
          6083.2  2.9136   0.099 0.000624  0.0686
          8000.0  2.7691   0.123 0.000584  0.0836
          9000.0  2.7120   0.136 0.000569  0.0918
         10000.0  2.6633   0.149 0.000556  0.1002
  6000.0  6000.0  3.2793   0.087 0.000651  0.0774
          6083.2  3.2698   0.087 0.000649  0.0782
          8000.0  3.0929   0.108 0.000611  0.0960
          9000.0  3.0238   0.119 0.000596  0.1057
         10000.0  2.9653   0.131 0.000584  0.1158
  6083.2  6083.2  3.3575   0.085 0.000667  0.0852
          8000.0  3.1724   0.105 0.000630  0.1051
          9000.0  3.1004   0.116 0.000616  0.1160
         10000.0  3.0394   0.127 0.000604  0.1273
C ---------------------------------------------------------------------------------------
C Stress dependent trans.
C ---------------------------------------------------------------------------------------
 C Model: k/ko=10^(-m*(stress/ref pres))
 C  Fro matrix
  TMODTABLE 1
  3930 0
 C stress TXMOD TYMOD TZMOD
  -6570 1000000 1000000 1000000
  -6351 1000000 1000000 1000000
  -6132 1000000 1000000 1000000
  -5913 1000000 1000000 1000000
  -5694 1000000 1000000 1000000
  -5475 1000000 1000000 1000000
  -5256 1000000 1000000 1000000
  -5037 1000000 1000000 1000000
  -4818 1000000 1000000 1000000
  -4599 560725.103794971 560725.103794971 560725.103794971
  -4380 298538.261891796 298538.261891796 298538.261891796
  -4161 158946.145286128 158946.145286128 158946.145286128
  -3942 84625.256880727 84625.256880727 84625.256880727
  -3723 45055.72682645 45055.72682645 45055.72682645
  -3504 23988.3291901949 23988.3291901949 23988.3291901949
  -3285 12771.7379758115 12771.7379758115 12771.7379758115
  -3066 6799.86045003323 6799.86045003323 6799.86045003323
  -2847 3620.34534591118 3620.34534591118 3620.34534591118
  -2628 1927.52491319094 1927.52491319094 1927.52491319094
  -2409 1026.24250892745 1026.24250892745 1026.24250892745
  -2190 546.386549881855 546.386549881855 546.386549881855
  -1971 290.904205677276 290.904205677276 290.904205677276
  -1752 154.881661891248 154.881661891248 154.881661891248
  -1533 82.4612663620516 82.4612663620516 82.4612663620516
  -1314 43.9035865640945 43.9035865640945 43.9035865640945
  -1095 23.3749128315349 23.3749128315349 23.3749128315349
  -876 12.4451461177139 12.4451461177139 12.4451461177139
```

```
 -657 6.62597815904146 6.62597815904146 6.62597815904146
 -438 3.52776786618874 3.52776786618874 3.52776786618874
 -219 1.87823530639501 1.87823530639501 1.87823530639501
 0 1 1 1
 196.5 1 1 1
 393 1 1 1
 589.5 1 1 1
 786 1 1 1
 982.5 1 1 1
 1179 1 1 1
 1375.5 1 1 1
 1572 1 1 1
 1768.5 1 1 1
 1965 1 1 1
 2161.5 1 1 1
 2358 1 1 1
 2554.5 1 1 1
 2751 1 1 1
 2947.5 1 1 1
 3144 1 1 1
 3340.5 1 1 1
 3537 1 1 1
 3733.5 1 1 1
 3930 1 1 1
C  For fractures
 TMODTABLE 2
 3930 0
C stress TXMOD TYMOD TZMOD
 -6570 1000000 1000000 1000000
 -6351 1000000 1000000 1000000
 -6132 1000000 1000000 1000000
 -5913 1000000 1000000 1000000
 -5694 1000000 1000000 1000000
 -5475 1000000 1000000 1000000
 -5256 1000000 1000000 1000000
 -5037 1000000 1000000 1000000
 -4818 1000000 1000000 1000000
 -4599 560725.103794971 560725.103794971 560725.103794971
 -4380 298538.261891796 298538.261891796 298538.261891796
 -4161 158946.145286128 158946.145286128 158946.145286128
 -3942 84625.256880727 84625.256880727 84625.256880727
 -3723 45055.72682645 45055.72682645 45055.72682645
 -3504 23988.3291901949 23988.3291901949 23988.3291901949
 -3285 12771.7379758115 12771.7379758115 12771.7379758115
 -3066 6799.86045003323 6799.86045003323 6799.86045003323
 -2847 3620.34534591118 3620.34534591118 3620.34534591118
 -2628 1927.52491319094 1927.52491319094 1927.52491319094
 -2409 1026.24250892745 1026.24250892745 1026.24250892745
 -2190 546.386549881855 546.386549881855 546.386549881855
 -1971 290.904205677276 290.904205677276 290.904205677276
 -1752 154.881661891248 154.881661891248 154.881661891248
 -1533 82.4612663620516 82.4612663620516 82.4612663620516
 -1314 43.9035865640945 43.9035865640945 43.9035865640945
 -1095 23.3749128315349 23.3749128315349 23.3749128315349
 -876 12.4451461177139 12.4451461177139 12.4451461177139
 -657 6.62597815904146 6.62597815904146 6.62597815904146
 -438 3.52776786618874 3.52776786618874 3.52776786618874
 -219 1.87823530639501 1.87823530639501 1.87823530639501
 0 1 1 1
 196.5 0.797535456790016 0.797535456790016 0.797535456790016
 393 0.63606280483726 0.63606280483726 0.63606280483726
 589.5 0.507282639603023 0.507282639603023 0.507282639603023
 786 0.404575891697443 0.404575891697443 0.404575891697443
 982.5 0.322663618591148 0.322663618591148 0.322663618591148
 1179 0.257335676442611 0.257335676442611 0.257335676442611
 1375.5 0.205234326260026 0.205234326260026 0.205234326260026
 1572 0.163681652142781 0.163681652142781 0.163681652142781
 1768.5 0.130541921209837 0.130541921209837 0.130541921209837
 1965 0.104111810762334 0.104111810762334 0.104111810762334
 2161.5 0.0830328605535737 0.0830328605535737 0.0830328605535737
 2358 0.0662216503701762 0.0662216503701762 0.0662216503701762
 2554.5 0.0528141141773672 0.0528141141773672 0.0528141141773672
```

```
  2751 0.0421211286754067 0.0421211286754067 0.0421211286754067
  2947.5 0.0335930935986515 0.0335930935986515 0.0335930935986515
  3144 0.0267916832481903 0.0267916832481903 0.0267916832481903
  3340.5 0.0213673173375189 0.0213673173375189 0.0213673173375189
  3537 0.0170411931931554 0.0170411931931554 0.0170411931931554
  3733.5 0.0135909557975501 0.0135909557975501 0.0135909557975501
  3930 0.010839269140212 0.010839269140212 0.010839269140212
C ------------------------------------------------------------------------------------------
C Initialize
C ------------------------------------------------------------------------------------------
INITREG CON
 1
INITIAL 1
DEPTH GOR
9032 2400
GOC 9032
PINIT 3930
ENDINIT
C ------------------------------------------------------------------------------------------
C Define wells
C ------------------------------------------------------------------------------------------
C Include recurrent data generated by SensorGrid (perforations and TZ modifiers)
C ------------------------------------------------------------------------------------------
C ---------------------------------
C Trans. modification to fractures
C ---------------------------------
MODIFY TX 1.0
 34 34 10 10 1 1 * 1
 35 35 10 10 1 1 * 1
C ---------------------------------
C Define Wells
C ---------------------------------
WELL
        I J  K  PI
 PROD   35 1 1    100
 INJ    35 1 1    100
BHP
 PROD 500
 INJ  10000
SKIP
THP
 PROD 100 -2
SKIPEND
WELLTYPE
 PROD MCF
 INJ  STBWATINJ
PSM
MAPSFREQ 1
MAPSFILEFREQ 1
DTMAX 1
C ------------------------------------------------------------------------------------------
C Define rate schedules.
C ------------------------------------------------------------------------------------------
WELL PROD
INJ_PERIOD 0
INJ_RATE 0
SHUTIN_PERIOD 0
SYM_ELEMENTS 40
TEST_TIME 6
! User supplied data:
SCHEDULE
TIME RATE Q_TYPE PRESSURE P_TYPE THP_TABLE
1 0.000001 GAS 14.7 BHP
2 0.000001 14.7
3 0.000001 14.7
4 0.000001 14.7
5 2238 14.7
6 2886 14.7
7 1916 14.7
8 1738 14.7
9 1698 14.7
10 1 14.7
```

```
11 96 14.7
12 1 14.7
13 1 14.7
14 365 14.7
15 2586 14.7
16 2615 14.7
17 2225 14.7
18 2100 14.7
19 2043 14.7
20 1917 14.7
21 1524 14.7
22 1603 14.7
23 1459 14.7
24 1588 14.7
25 1435 14.7
26 1408 14.7
27 1239 14.7
28 1280 14.7
29 1165 14.7
30 751 14.7
31 1213 14.7
32 452 14.7
33 1115 14.7
34 1289 14.7
35 1298 14.7
36 1262 14.7
37 1190 14.7
38 1164 14.7
39 1197 14.7
40 830 14.7
41 255 14.7
42 0.000001 14.7
43 3 14.7
44 1188 14.7
45 1218 14.7
46 1273 14.7
47 1297 14.7
48 1201 14.7
49 1056 14.7
50 1076 14.7
51 1089 14.7
52 1111 14.7
53 1114 14.7
54 528 14.7
55 0.000001 14.7
56 0.000001 14.7
57 1102 14.7
58 923 14.7
59 1033 14.7
60 1066 14.7
61 1043 14.7
62 1022 14.7
63 1001 14.7
64 1103 14.7
65 786 14.7
66 738 14.7
67 786 14.7
68 801 14.7
69 158 14.7
70 0.000001 14.7
71 246 14.7
72 953 14.7
73 564 14.7
74 505 14.7
75 1033 14.7
76 1111 14.7
77 1050 14.7
78 943 14.7
79 898 14.7
80 975 14.7
81 966 14.7
82 939 14.7
```

```
83 948 14.7
84 932 14.7
85 922 14.7
86 934 14.7
87 926 14.7
88 931 14.7
89 908 14.7
90 903 14.7
91 890 14.7
92 883 14.7
93 898 14.7
94 931 14.7
95 915 14.7
96 572 14.7
97 910 14.7
98 843 14.7
99 866 14.7
100 845 14.7
101 870 14.7
102 792 14.7
103 890 14.7
104 881 14.7
105 962 14.7
106 906 14.7
107 847 14.7
108 807 14.7
109 842 14.7
110 842 14.7
111 888 14.7
112 947 14.7
113 861 14.7
114 834 14.7
115 693 14.7
116 850 14.7
117 846 14.7
118 859 14.7
119 890 14.7
120 914 14.7
121 942 14.7
122 953 14.7
123 743 14.7
124 927 14.7
125 793 14.7
126 887 14.7
127 890 14.7
128 878 14.7
129 835 14.7
130 790 14.7
131 830 14.7
132 868 14.7
133 898 14.7
134 856 14.7
135 780 14.7
136 784 14.7
137 822 14.7
138 820 14.7
139 902 14.7
140 41 14.7
141 945 14.7
142 906 14.7
143 891 14.7
144 534 14.7
145 791 14.7
146 900 14.7
147 1002 14.7
148 925 14.7
149 869 14.7
150 892 14.7
151 894 14.7
152 901 14.7
153 893 14.7
154 899 14.7
```

```
155 935 14.7
185.4 745.2631579 14.7
215.8 659.2105263 14.7
218.2 0.000001 14.7
246.2 640.6428571 14.7
249.6 0.000001 14.7
276.6 623.0740741 14.7
307 401.1184211 14.7
337.4 521.3486842 14.7
338.8 0.000001 14.7
367.8 618.3448276 14.7
374.2 0.000001 14.7
398.2 721.0833333 14.7
399.6 0.000001 14.7
428.6 616.6206897 14.7
430 0.000001 14.7
459 693.6896552 14.7
460.4 0.000001 14.7
489.4 552.4137931 14.7
493.8 0.000001 14.7
519.8 479.0769231 14.7
526.2 0.000001 14.7
550.2 930.1666667 14.7
580.6 504.8684211 14.7
611 562.4671053 14.7
641.4 1649.802632 14.7
671.8 1044.375 14.7
673.2 0.000001 14.7
702.2 956.8965517 14.7
732.6 1121.414474 14.7
763 840.3947368 14.7
774.4 0.000001 14.7
793.4 674.8421053 14.7
801.8 0.000001 14.7
823.8 781.6818182 14.7
854.2 641.7105263 14.7
884.6 664.6710526 14.7
915 645.9868421 14.7
945.4 651.8421053 14.7
952.8 0.000001 14.7
975.8 677.4347826 14.7
1006.2 642.7631579 14.7
1007.6 0.000001 14.7
1036.6 656.5172414 14.7
1067 576.0197368 14.7
1097.4 825.6907895 14.7
1127.8 793.4210526 14.7
1130.2 0.000001 14.7
1158.2 740.1428571 14.7
1161.6 0.000001 14.7
1188.6 742.7407407 14.7
1219 690.0328947 14.7
1249.4 678.3881579 14.7
1255.8 0.000001 14.7
1279.8 674.625 14.7
1283.8 1216.5 14.7
END
```

Appendix D: Pipe-It Graphical Interface

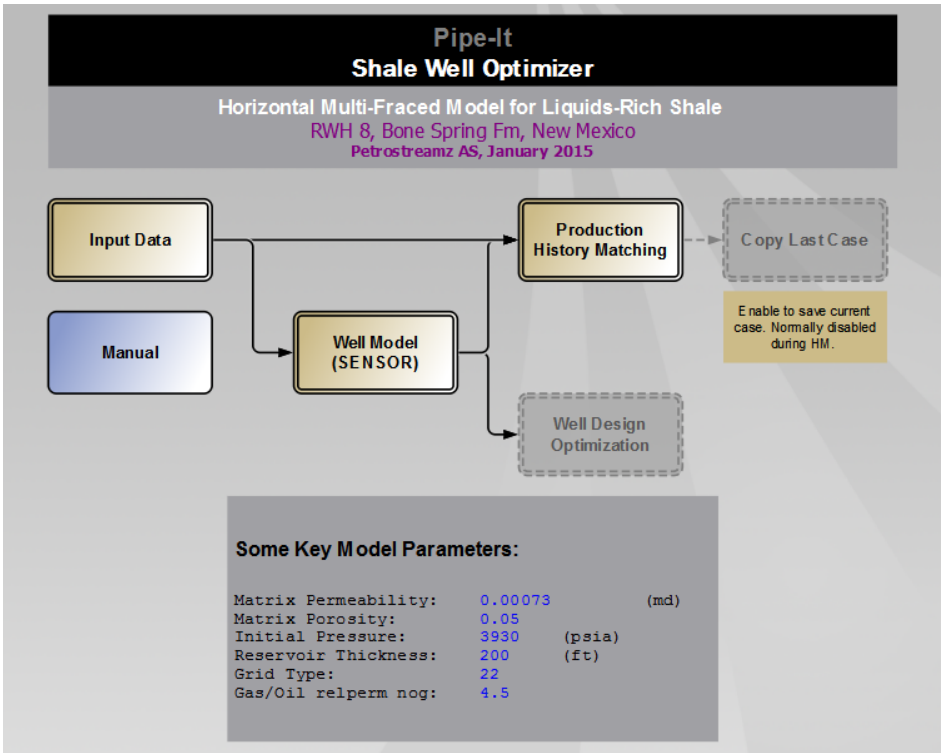

Figure 90: Main view of Pipe-It Shale Well Template.

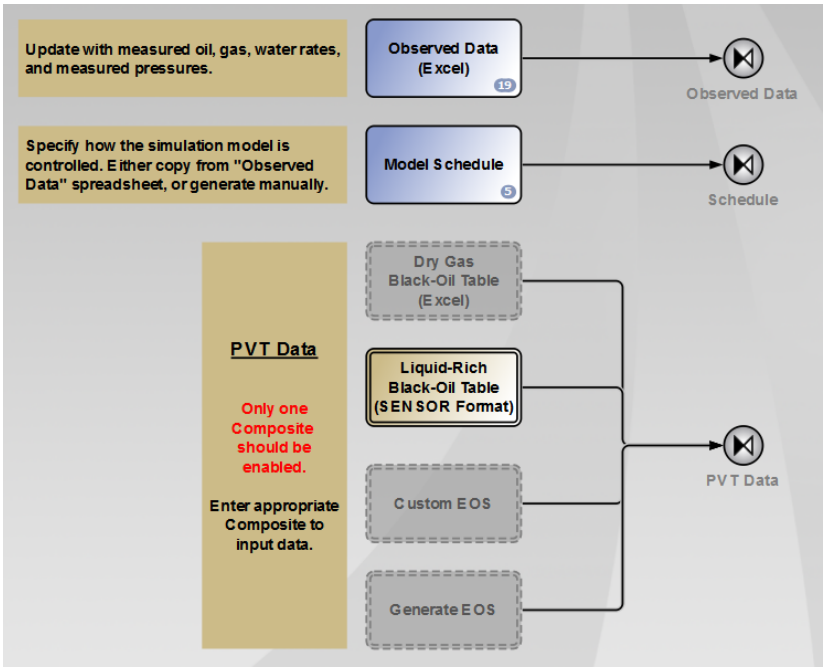

Figure 91: View of Pipe-It Shale Well Template. This is where schedule file, observed data and BO-table is included.

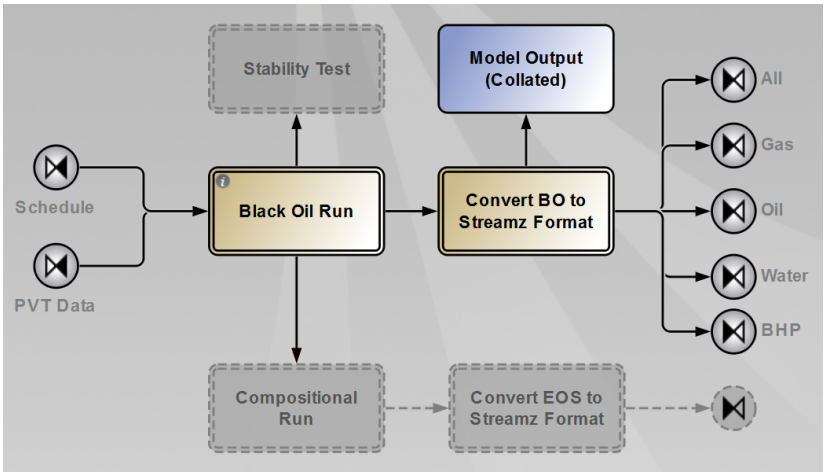

Figure 92: View of Pipe-It Shale Well Template. User have the choice to run BO or Compositional.

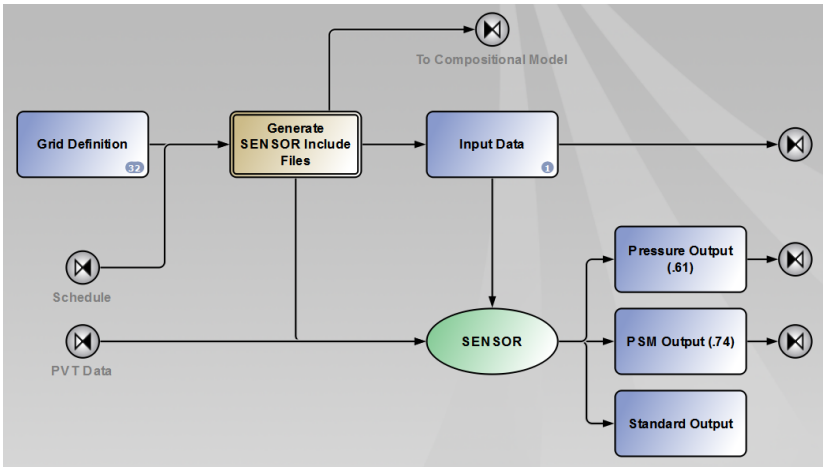

Figure 93: View of Black Oil Pipe-It Shale Well Template. Sensor is run here, data file with other inputs are found here as well.

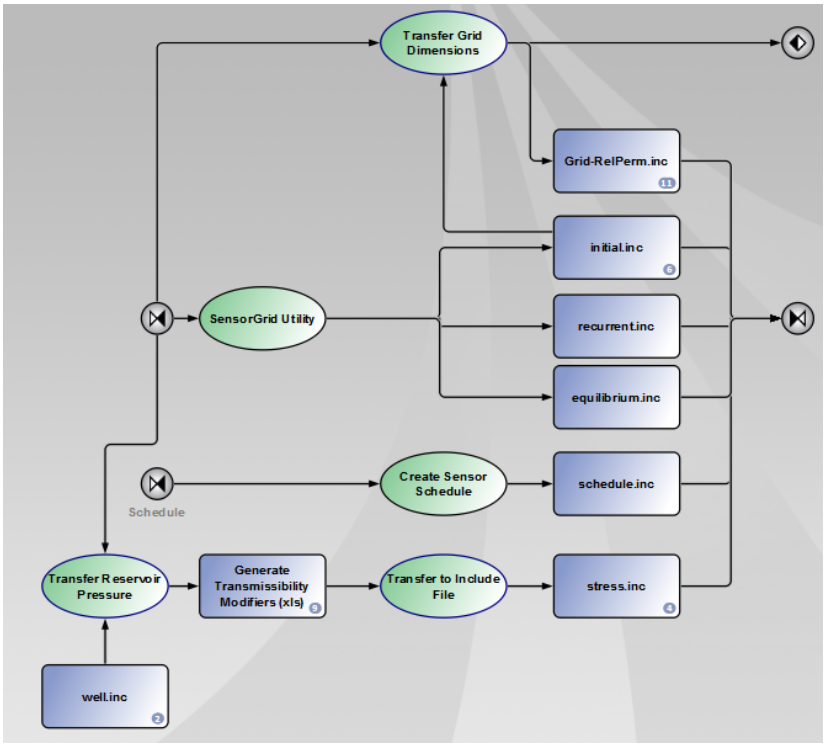

Figure 94: Overview of the creation of the SENSOR data-file Pipe-It Shale Well Template.

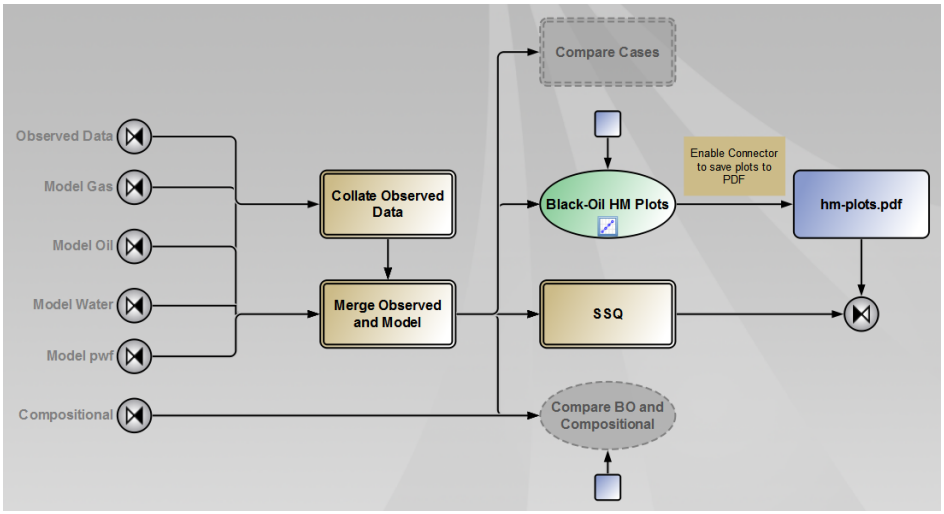

Figure 95: View of the History Matching part of Pipe-It Shale Well Template. SSQs are calculated here. The results are plotted and saved to a PDF.

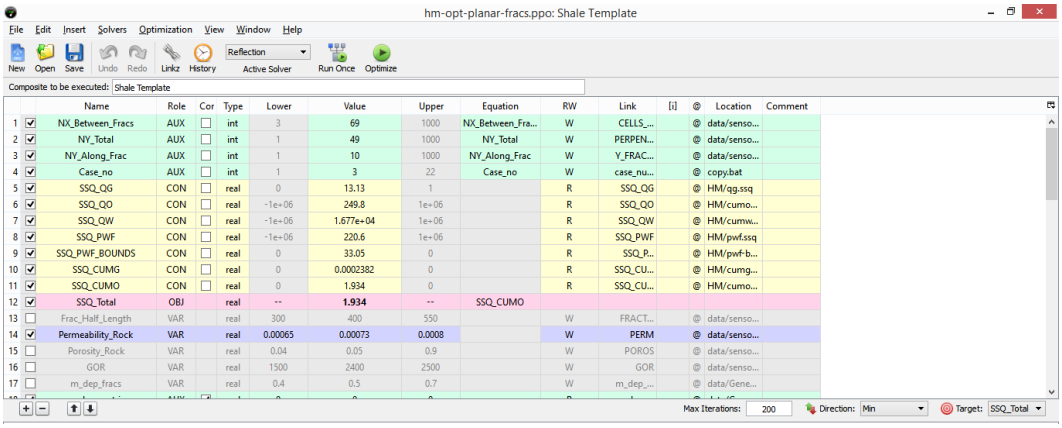

Figure 96: View of the Optimizer in Pipe-It. Most parameters are linked to the datafile here. This is where the history match is performed.